

A NEW ROBUST SCENARIO APPROACH TO SUPPLY
CHAIN OPTIMIZATION
UNDER BOUNDED UNCERTAINTY

by

NIAZ BAHAR CHOWDHURY

A thesis submitted to the
Department of Chemical Engineering
in conformity with the requirements for
the degree of Master of Applied Science

Queen's University
Kingston, Ontario, Canada

November 2015

Copyright © Niaz Bahar Chowdhury, 2015

Abstract

Supply Chain Optimization (SCO) problem under uncertainty can be modeled as two-stage optimization problem where first-stage decisions are associated with design and development of facilities and second-stage decisions are associated with operation of the supply chain network. Recently, a robust scenario approach combining the traditional scenario or robust approach has been developed to better address uncertainties in SCO problems, and it can ensure solution feasibility and better expected objective value. But this approach can only address uncertainties bounded with the infinity-norm.

This thesis proposes a modified robust scenario approach, which can be used to address uncertainty region bounded with the p -norm in SCO. In this case, after the normalization of the uncertainty region, the smallest box uncertainty region, that covers the normalized uncertainty region, can be partitioned into a number of box uncertainty subregions. Following some screening criteria, two subsets of the subregions that over-estimates and under-estimates the original uncertainty region can be selected. When the number of scenarios increases, the optimal objective values of the two robust scenario formulations converge to a constant, which is a good estimate of the true optimal value. This new robust scenario approach is then extended for any bounded uncertainty regions, in the context of robust optimization.

In many industrial problem, the historical realizations of uncertain parameters are known. This thesis gives a preliminary discussion on a data driven robust scenario approach, where the available data are normalized and a reference box that covers the data with a certain confidence is constructed. Then, the reference box is partitioned into box-shaped uncertainty subregions.

The benefits of the proposed robust scenario approach are demonstrated through some simple examples as well as an industrial SCO problem. The approach requires the solution of large-scale optimization problems when the number of scenarios is large, and these large-scale problems have a decomposable structure that can be exploited for efficient solution via decomposition-based optimization. A computational study demonstrates that, when the large-scale optimization problem is a second-order cone programming problem, generalized Benders decomposition is much faster than a state-of-the-art optimization solver.

Acknowledgments

I would like to express my sincere gratitude to my supervisor Dr. Xiang Li for continuous support and guidance in research; for his enthusiasm, patience, motivation and great efforts to explain research topics simply and clearly. His guidance helped me immensely while doing research and writing the thesis. Besides my supervisor, I would like to thank my fellow lab-mates and my friends in Queen's University for their continuous support. Also, I would like to acknowledge the funding agency for supporting the research. Last but not the least, I would like to thank my family: my parents and brother, for supporting me all-through my life.

Contents

Abstract	i
Acknowledgments	iii
Contents	iv
List of Tables	vii
List of Figures	viii
Chapter 1: Introduction	1
1.1 Supply Chain Optimization and Uncertainties	1
1.2 Illustrative Example: Farm Planning Problem	7
1.3 Two-Stage Stochastic Programming Formulations for SCO Under Uncertainty	15
1.4 Generalized Benders Decomposition	18
1.5 Goal of the Thesis	20
1.6 Organization of Thesis	20
Chapter 2: A Robust Scenario Approach for Uncertainty Regions Bounded With the p-Norm	22
2.1 Reformulation of the Robust Scenario Formulation When the Uncertainty Subregions are Bounded With a Norm	22
2.2 Systematic Partitioning of Uncertainty Regions Bounded with the p -Norm	25
2.2.1 Partitioning of Uncertainty Regions Bounded with the Infinity-Norm	25
2.2.2 Normalization of Uncertainty Regions Bounded with the p -Norm and the Reference Box	28
2.2.3 Subregions Generated by Partitioning of the Reference Box	34
2.2.4 Illustrative Example: Normalization and Partitioning	35
2.3 Linear Programming Reformulations for the 1-Norm Constraints	40

2.4	Case Study	44
2.4.1	An Industrial Chemical Supply Chain from DuPont	44
2.4.2	Demand Uncertainty	46
2.4.3	Case Study Results	49
Chapter 3:	Robust Scenario Approaches for Robust Optimization and Data Driven Stochastic Programming	55
3.1	A Robust Scenario Approach for Robust Optimization	56
3.1.1	An Illustrative Example	59
3.1.2	A Different Way to Partition the Original Uncertainty Region	64
3.1.3	Benefit of Rotation of the Uncertainty Region	65
3.2	A Robust Scenario Approach for Data Driven Stochastic Programming	67
3.2.1	Normalization and Partitioning Process for Data Driven Stochastic Programming	68
3.2.2	Case Study Results	70
Chapter 4:	Nonlinear Robust Constraints and Decomposition Based Optimization	76
4.1	Non-linear Robust Constraints	77
4.2	Generalized Benders Decomposition Algorithm	79
4.3	Computational Study	84
Chapter 5:	Summary and Conclusions	88
	Bibliography	93
Appendix A:	DuPont Industrial Chemical Supply Chain	100
A.1	Nomenclature and Symbols for DuPont Supply Chain network	100
A.2	Deterministic Model for DuPont Supply Chain Network	104
A.3	Robust Scenario Formulation Model for DuPont Supply Chain Network	109
Appendix B:	The Robust Scenario Formulation for Problem (1) in Chapter 3	118
Appendix C:	Generalized Benders Decomposition Sub-Problems for simplified DuPont Industrial Chemical Supply Chain Optimization Problem	121
C.1	Original Problem (P)	121
C.2	Primal Problem (PP_{ω}^k)	127
C.3	Feasibility Problem (FP_{ω}^k)	129
C.4	Relaxed Master Problem (RMP^k)	129

C.5 Feasibility Relaxed Master Problem ($FRMP^k$)	131
---	-----

List of Tables

1.1	List of variables for farm planning case	8
1.2	List of variables and parameters for the general formulation of two-stage stochastic programming	21
3.1	Computational Results for the data driven robust scenario formulation with different numbers of available samples	72
4.1	Comparison of computational times for different numbers of scenarios	85
4.2	Other computational results	87

List of Figures

1.1	Two-stage decision making procedure	10
1.2	Decomposable structure of Formulation (RS)	19
2.1	(a) Partitioning of uncertainty region bounded with the infinity-norm (with 9 partition) (b) Partitioning of uncertainty region bounded with the 2-norm into box-shaped uncertainty sub-regions is not simple . . .	25
2.2	An uncertainty region bounded with the infinity-norm with 9 partitions	27
2.3	Normalization of different 2-norm bounded original uncertainty regions into an unit circular uncertainty region centered at origin	28
2.4	Normalization process of original uncertainty region	30
2.5	Normalized uncertainty regions bounded with different p-norms . . .	32
2.6	Division of the reference box into box-shaped sub-regions	34
2.7	Over-estimation of the normalized uncertainty region	36
2.8	Under-estimation of the normalized uncertainty region	36
2.9	Approximation of the normalized uncertainty region with many scenarios	37
2.10	Original uncertainty region bounded with $(\xi_1 - 2)^2 + (\xi_2 - 3)^2 \leq 4$. . .	38
2.11	Normalization process of original uncertainty region bounded with $(\xi_1 - 2)^2 + (\xi_2 - 3)^2 \leq 4$	39

2.12 (a) Reference uncertainty region with 25 partition (b) Overestimation of normalized uncertainty region (c) Underestimation of normalized uncertainty region	40
2.13 DuPont industrial chemical supply chain network	45
2.14 Normalized uncertainty region with 16 sub-regions	48
2.15 Convergence of RSF-OE and RSF-UE	51
2.16 Optimality test for DuPont Industrial Chemical Supply Chain Problem	53
2.17 Feasibility test for DuPont Industrial Chemical Supply Chain Problem	54
3.1 An asymmetric and nonconvex bounded uncertainty region	56
3.2 Normalization process for a bounded uncertainty region	58
3.3 Uncertainty region, Ξ of Problem (1)	60
3.4 Normalization process for Ξ	62
3.5 (a) Reference uncertainty region with 25 scenarios (b) Overestimation of normalized uncertainty region (c) Underestimation of normalized uncertainty region	63
3.6 Uncertainty region rotation and normalization	65
3.7 (a) Reference uncertainty region with 25 scenarios (b) Overestimation of uncertainty region (c) Underestimation of uncertainty region	66
3.8 Convergence of RSF-OE and RSF-UE, Scenario 9-900	67
3.9 Convergence of RSF-OE and RSF-UE, Scenario 2500-22500	68
3.10 Representation of uncertain parameters using a data set	69
3.11 Normalization of original uncertainty region described as data set and partitioning of reference box	71
3.12 100 samples and the corresponding reference uncertainty box	73

3.13	500 samples and the corresponding reference uncertainty box	74
3.14	1000 samples and the corresponding reference uncertainty box	75
4.1	(a) Uncertainty sub-regions are bounded with the infinity-norm (b) Uncertainty sub-regions are bounded with the 2-norm	78
4.2	Comparison of computational times	86

Chapter 1

Introduction

1.1 Supply Chain Optimization and Uncertainties

A supply chain is a group of organizations (including design, procurement, manufacturing and distribution) that work together to profitably provide the right product or service to the right customer at the right time [2]. Supply Chain Optimization (SCO) is the study of strategies and methodologies that enables these organizations to meet their objectives efficiently. SCO is a key research area in the field of Process System Engineering (PSE). In PSE, SCO has been extensively applied to oil, gas and petrochemical supply chains [3, 4, 5, 6, 7], agro supply chains [8, 9], pharmaceutical supply chains [10, 11, 12, 13], bio-refinery and bio-energy supply chains [14, 15, 16, 17, 18]. SCO has also been applied to more recent applications like carbon dioxide emission control [19], wind farm diversification [20], disaster management [21], project planning [22], environmental planning [23] and sustainable chemical process development [24, 25] etc. Papageorgiou [26] gave a brief discussion on the advances and opportunities of supply chain optimization for different processing industries.

SCO problems can be categorized into three different types of problems, which are strategic, tactical and operational problem. Each of the different types of SCO problems are associated with different kinds of decision making regarding design, long-term/mid-term planning and short-term operations [27]. At any decision making stage in SCO, it is very common to have some parameters that are not known exactly but might have significant effect on the supply chain network. These parameters can be found in the form of final product demand, final product price, raw material price, transportation cost, fuel cost, labor cost etc. [28, 29]. Failing to address uncertain parameters in SCO problems may lead to poor operational decisions hence resulting in poor economic performance.

There are different ways to address uncertainties in SCO [30], but a common way to do that in SCO is to use stochastic programming with recourse. Stochastic programs with recourse are solved over a number of stages. In each stage, there are some decisions to be made. The decisions in the first-stage are made without the realization of uncertainties. After that, between each stage, some uncertainties are realized and the decision maker must choose an corrective action that optimizes the current objective plus the expectation of the future objectives [27]. The ability to take corrective action after uncertainty realization has taken place is known as *recourse*. Although multi-stage stochastic programming with more than two stages has been applied in PSE [31] [32], the most common stochastic programs, used in PSE, are two-stage models in which first-stage decisions (e.g. capacity of manufacturing plant) are made before the realization of all uncertainties and second-stage decisions (e.g. operational decisions of manufacturing plant) are those which can be made after the

realization of all uncertainties.

In PSE, two-stage stochastic programming has been extensively studied for oil, gas and petrochemical industry. Ribas et al. [3] proposed the development of a two-stage stochastic programming model with a finite number of uncertainty realizations for an integrated oil supply chain in Brazil. Three sources of uncertainties, crude oil production, demand for refined products and market prices, were considered in the model. The main contribution of the proposed study was to develop a strategic planning model using a two-stage stochastic model, including 17 refineries, three petrochemical plants and a complex logistic network, that account for uncertainties and to apply the model in a real life case. From the study it was found that, two-stage stochastic model had significant impact on the decision making, resulting in increasing capacity of separation units. Lababidi et al. [4] proposed a two-stage stochastic formulation with a finite number of uncertainty realizations to address the uncertain operating and economic conditions in a petrochemical industry. The optimization model was tested on a typical petrochemical company, manufacturing different grades of polyethylene, operating at a single site and using two reactors. The uncertain parameters were demands, market prices, raw material costs, and production yields. The main conclusion of that study was, uncertainties had a significant effect on the planning decisions of the petrochemical supply chain. The most important uncertain parameter was market demand, showing a strong impact on the production decisions, followed by the production yields. Wafa et al. [5] proposed a two-stage stochastic formulation, with finite number of uncertainty realizations. The proposed stochastic programming approach proved to be effective in developing resilient production plans in presence

of high degree of demands and prices uncertainty for petrochemical industries.

Agro-industry is another area where SCO has been applied intensively. Barker et al. [9] proposed a two-stage stochastic programming with recourse model for determining optimal planting plans for a vegetable crop. In many arising systems in horticulture, uncertainty caused by natural factors, such as weather on yields, has a significant influence. Typical linear programming models, which are usually unsatisfactory in dealing with the uncertainties, produce solutions that are involved with high degree of risk. The first-stage of the model was, to find a planting plan, common to all scenarios. In the second-stage, a harvesting schedule was developed for each scenario. Solutions were obtained for a range of risk aversion factors that not only resulted in greater expected profit compared to the corresponding deterministic model, but also were more robust. The major element of uncertainty on that case study was the effect of weather on yields.

SCO is widely applied in the pharmaceutical industry also. Shah [10] discussed the key sources of uncertainties in pharmaceutical supply chain, which are, the demands for existing drugs and uncertainty in the pipeline of new drugs, in particular, which ones will be successful in trials, and what sort of dosage and treatment regime will be optimal. Papageorgiou et al. [13] developed a two-stage stochastic programming based optimization approach to select both a product development and introduction strategy and a capacity planning and investment strategy. The problem was formulated as a mixed-integer linear programming (MILP) model, taking consideration of

both the important features of pharmaceutical industries, active ingredient manufacturing and the global trading structures. The major sources of uncertainties were, the uncertainties on the outcome of the clinical trials of all candidate products.

Bio-refinery and bio-energy is another field where SCO is implemented. A two-stage stochastic mixed-integer linear programming model to address the optimal design of hydrocarbon bio-refinery supply chains under supply and demand uncertainties was presented by Akgul et al [14]. The multiple conversion technologies, feedstock seasonality and fluctuation, geographical diversity, biomass degradation, demand variation, government incentives, and risk management was accounted for the model. The objective of the model was to minimize the expected annualized cost and the financial risk associated with the industry management, measured by conditional value-at-risk and downside risk, simultaneously. Chen [16] proposed a mixed integer two-stage stochastic programming model to support strategic planning of bio-energy supply chain systems and optimal feedstock resource allocation under different kinds of uncertainties. The two-stage stochastic programming model, along with a Lagrangian relaxation based decomposition solution algorithm, was implemented in a California based real-world case study to explore the scopes of waste based bio-ethanol production. The results showed that, for the future, bio-waste based ethanol can be an important part of the sustainable energy solution. Dal-mas et al. [18] presented a two-stage MILP modeling approach, to help decision-makers and potential investors, assessing economic performances and risk associated with investment on the biomass based ethanol supply chain network. A case study, concerned with the corn-to-ethanol production supply chain in Northern Italy, was used to effectively demonstrate the

ideas of determining economic performances and risk associated with investment. The uncertain parameters in the model were, biomass production cost and product selling price.

SCO has also been applied to more recent applications like carbon dioxide emission control. Chen et al. [19] developed a two-stage inexact-stochastic programming model for planning carbon dioxide emission where the uncertain parameter was green house gas (GHG) emission. The decisions obtained from the two-stage inexact-stochastic programming were effectively used for generating decision alternatives and to help decision makers in identifying desired GHG abatement policies under different economic and system-reliability conditions. Wind farm diversification proposed by Liu et al. [20] is another example of most recent application of SCO where the production of wind power was the uncertain parameter. SCO can be applied to disaster management problems also. Dal-mas et al. [21] proposed a two-stage stochastic programming approach regarding the storage and distribution problem of medical supplies. These medical supplies can be used for disaster management under a wide varieties of possible disaster types and magnitudes. Project planning is an important application of SCO [22] where the problem of setting target finish times for project activities with random durations can be determined by two-stage mixed integer linear stochastic programming. Target times were determined in the first-stage and detailed project planning schedules were developed in the second-stage.

This thesis only considers two-stage stochastic programming which can be used to model most SCO problems, and the results of the thesis work can also be extended for

multi-stage stochastic programming. In the following section, an illustrative example will be used to explain how a two-stage stochastic programming is formulated and how it is solved via different existing approaches.

1.2 Illustrative Example: Farm Planning Problem

This section discusses a farm planning problem, modified from a classical farm planning problem in the operations research literature [33]. In this problem, a farmer needs to plan the allocation of his land area for raising two crops; wheat and corn. The goal of the planning is to achieve the best overall profit while reserving a certain amount of wheat and corn for cattle feeding. If the harvested wheat or corn is not enough for cattle feeding, then both can be purchased from the market at a relatively high price.

Total land area for planting wheat and corn is 500 acres. Yield of wheat and corn is, 2.5 t/acre and 3 t/acre respectively. Planting cost for wheat and corn is, 150 \$/acre and 230 \$/acre respectively. Purchasing cost of wheat and corn from the market is, 238 \$/t and 210 \$/t respectively. The selling price of wheat and corn from the market is, 170 \$/t and 150 \$/t respectively. Amount of wheat and corn reserved for feeding cattle is at least, 300 t and 340 t respectively.

The deterministic formulation for the farm planning problem is described below,

and the list of variables used in the formulation can be found in Table 1.1.

$$\min 150x_{wh} + 230x_c + 238y_{wh} + 210y_c - 170z_{wh} - 150w_c \quad (1.1)$$

$$s.t. \quad x_{wh} + x_c \leq 500, \quad (1.2)$$

$$2.5x_{wh} + y_{wh} - z_{wh} \geq 300, \quad (1.3)$$

$$3x_c + y_c - z_c \geq 340, \quad (1.4)$$

$$x_{wh}, x_c, y_{wh}, y_c, z_{wh}, z_c \geq 0. \quad (1.5)$$

Now assume that the amount of wheat needed for feeding cattle is not exactly known when the farmer is planning the land allocation, but will be known before the farmer needs to determine the sell and purchase of wheat and corn. Let's represent this uncertain amount by F , which ranges from 270 t to 330 t. In this case, the overall profit is dependent on the realization of F ; naturally, we can choose the expected overall profit (over the range of possible values of F) to be the objective function, and the optimization problem can be written as:

Table 1.1: List of variables for farm planning case

x_{wh}	Land allocation for wheat, acre
x_c	Land allocation for corn, acre
y_{wh}	Amount of wheat purchased from the market, t
y_c	Amount of corn purchased from the market, t
z_{wh}	Amount of wheat sold in the market, t
z_c	Amount of corn sold in the market, t

Formulation (SP) for the Farm Planning Problem

$$\min 150x_{wh} + 230x_c + E_{F_\omega \in \Xi} \{Q(x_{wh}, x_c, F_\omega)\} \quad (1.6)$$

$$s.t. \quad x_{wh} + x_c \leq 500, \quad (1.7)$$

$$x_{wh}, x_c \geq 0 \quad (1.8)$$

Here, $Q(x_{wh}, x_c, F_\omega)$ represents the net purchase/sell cost associated with a particular planning decision x_{wh} , x_c , and a particular realization of F , F_ω . $E_{F_\omega \in \Xi} \{\cdot\}$ represents expected value over uncertainty realization $F_\omega \in \Xi$, and $\Xi = [270, 330]$. Since the farmer can determine the wheat purchase and sell optimally after knowing F , so

$$Q(x_{wh}, x_c, F_\omega) = \min 238y_{wh,\omega} + 210y_{c,\omega} - 170z_{wh,\omega} - 150z_{c,\omega}, \quad (1.9)$$

$$s.t. \quad 2.5x_{wh} + y_{wh,\omega} - z_{wh,\omega} \geq F_\omega, \quad (1.10)$$

$$3x_c + y_{c,\omega} - z_{c,\omega} \geq 340, \quad (1.11)$$

$$y_{wh,\omega}, y_{c,\omega}, z_{wh,\omega}, z_{c,\omega} \geq 0 \quad (1.12)$$

The above optimization problem is called a recourse problem, which needs to be solved for all realizations of F in order to solve Problem (SP). Problem (SP), together with all the recourse problems, is called a two-stage stochastic programming problem with recourse. Here, x_{wh} and x_c represent first-stage decision variables that need to be determined before the realization of uncertainty, F , and $y_{wh,\omega}$, $y_{c,\omega}$, $z_{wh,\omega}$ and $z_{c,\omega}$ are called second-stage decision variables for uncertainty realization F_ω . The two-stage decision making procedure described by the two-stage stochastic programming

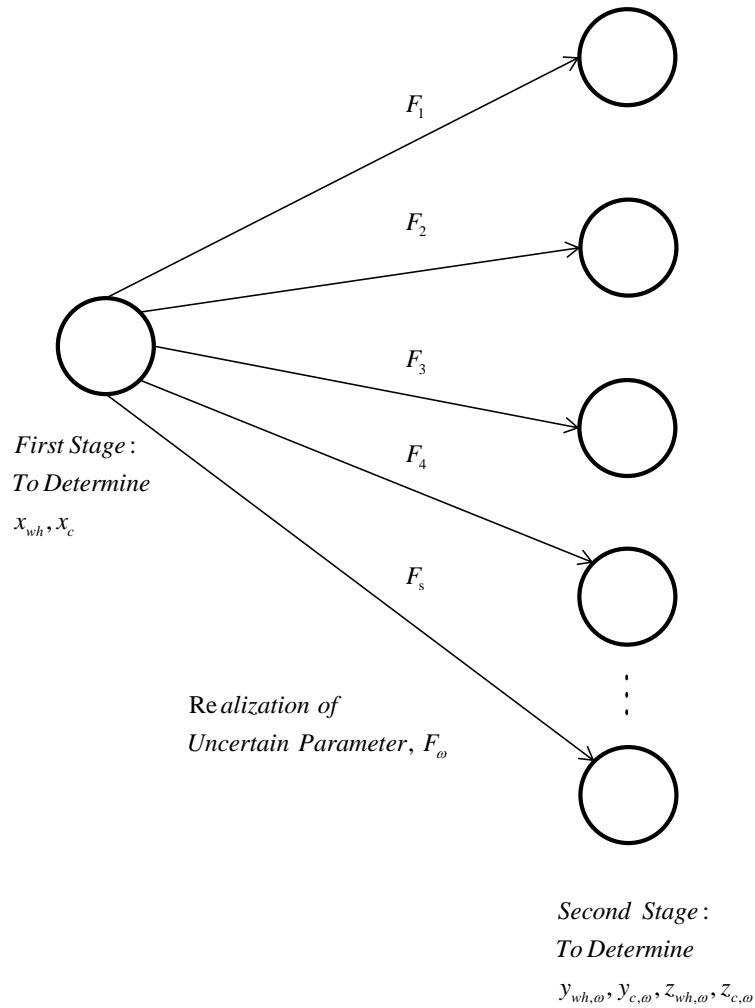


Figure 1.1: Two-stage decision making procedure

formulation is illustrated through Figure 1.1.

In order to rigorously solve Formulation (SP), we need to solve an infinite number of recourse problems (for every possible values of F within $[270, 330]$), which is apparently not realistic. A practical way to solve Formulation (SP) is to consider only a finite subset of uncertainty realizations of F , and each considered uncertainty

realization is called a *scenario*. The resulting formulation can be written as a single-level optimization problem, and it is also called a scenario formulation [33]. When S scenarios are considered, the scenario problem for the farm planning problem is:

Formulation (S) for the Farm Planning Problem

$$\min 150x_{wh} + 230x_c + \sum_{\omega=1}^s P_{\omega}(238y_{wh,\omega} + 210y_{c,\omega} - 170z_{wh,\omega} - 150z_{c,\omega}) \quad (1.13)$$

$$s.t. \quad x_{wh} + x_c \leq 500, \quad (1.14)$$

$$2.5x_{wh} + y_{wh,\omega} - z_{wh,\omega} \geq F_{\omega}, \quad \omega = 1, \dots, s, \quad (1.15)$$

$$3x_c + y_{c,\omega} - z_{c,\omega} \geq 340, \quad \omega = 1, \dots, s, \quad (1.16)$$

$$x_{wh}, x_c \geq 0, \quad (1.17)$$

$$y_{wh,\omega}, y_{c,\omega}, z_{wh,\omega}, z_{c,\omega} \geq 0, \quad \omega = 1, \dots, s, \quad (1.18)$$

Here, P_{ω} is the probability of uncertainty realization ω . When a large number of uncertainty realizations of F is considered, the objective function of Formulation (S) is close to that of Formulation (SP), but the optimal solution of Formulation (S) is not guaranteed to be feasible for Formulation (SP).

In order to ensure feasibility of solution, a conservative version of Formulation (SP) can be considered, where the "worst" realization of F is considered in the constraints. This formulation is called a robust formulation [34] [35]. Here worst realization means the realization that can most violate the constraints, which is usually modeled indirectly within the robust formulation and unknown before the solution is obtained. The robust formulation for the farm planning problem is:

Formulation (R) for the Farm Planning Problem

$$\min 150x_{wh} + 230x_c + 238y_{wh} + 210y_c - 170z_{wh} - 150z_c \quad (1.19)$$

$$s.t. \quad x_{wh} + x_c \leq 500, \quad (1.20)$$

$$2.5x_{wh} + y_{wh} - w_{wh} \geq \max_{F_\omega \in \Xi} \{F_\omega\}, \quad (1.21)$$

$$3x_{wh} + y_{wh} - w_{wh} \geq 340, \quad (1.22)$$

$$x_{wh}, x_c, y_{wh}, y_c, z_{wh}, z_c \geq 0. \quad (1.23)$$

It is not difficult to find that, the solution of Formulation (R) is always feasible for Formulation (SP), but it may be overly conservative and far less optimal than the solution of Formulation (SP). McLean and Li [36] recently proposed to solve a hybrid formulation for better solution of Formulation (SP). This formulation is called a robust scenario formulation, which combines the ideas of classical scenario and robust formulations. In the robust scenario formulation, we partition uncertainty region Ξ into s subregions Ξ_ω (rather than selecting s points in Ξ), and each Ξ_ω is called a scenario. For each uncertainty subregion Ξ_ω , the worst-case scenario is addressed for constraint satisfaction in a robust approach. This idea leads to the

following problem formulation:

$$\min 150x_{wh} + 230x_c + \sum_{\omega=1}^s P_{\omega}(238y_{wh,\omega} + 210y_{c,\omega} - 170z_{wh,\omega} - 150z_{c,\omega}) \quad (1.24)$$

$$s.t. \quad x_{wh} + x_c \leq 500, \quad (1.25)$$

$$2.5x_{wh} + y_{wh,\omega} - z_{wh,\omega} \geq \max_{F_{\omega} \in \Xi_{\omega}} \{F_{\omega}\}, \quad \omega = 1, \dots, s, \quad (1.26)$$

$$3x_c + y_{c,\omega} - z_{c,\omega} \geq 340, \quad \omega = 1, \dots, s, \quad (1.27)$$

$$x_{wh}, x_c \geq 0, \quad (1.28)$$

$$y_{wh,\omega}, y_{c,\omega}, z_{wh,\omega}, z_{c,\omega} \geq 0, \quad \omega = 1, \dots, s. \quad (1.29)$$

Here P_{ω} is the total probability for all uncertainty realizations in Ξ_{ω} . Note that the above formulation can be very conservative, because it enforces the same second-stage decisions for different uncertainty realizations with an uncertainty subregion, while in reality the decision maker can have different second-stage decisions for different uncertainty realizations. In order to reduce the conservativeness, we can assume that the second-stage decision variables vary linearly (or more precisely, affinely) with respect to the uncertainty realizations within an uncertainty subregion. This affine approximation strategy has been widely used in classical robust optimization [34]. With this strategy, the second-stage decision variable $y_{wh,\omega}$ is replaced by $U_{y_{wh,\omega}}F_{\omega} + v_{y_{wh,\omega}}$, where $U_{y_{wh}}$ and $v_{y_{wh,\omega}}$ are new decision variables to be determined in optimization. Similarly, $y_{c,\omega}$ is replaced by $U_{y_{c,\omega}}F_{\omega} + v_{y_{c,\omega}}$, $z_{wh,\omega}$ by $U_{z_{wh,\omega}}F_{\omega} + v_{z_{wh,\omega}}$, and $z_{c,\omega}$ by $U_{z_{c,\omega}}F_{\omega} + v_{z_{c,\omega}}$. The resulting formulation is:

Formulation (RS) for the Farm Planning Problem

$$\begin{aligned} \min \quad & 150x_{wh} + 230x_c + \sum_{\omega=1}^s P_\omega [238(U_{y_{wh},\omega} \bar{F}_\omega + v_{y_{wh},\omega}) + 210(U_{y_c,\omega} \bar{F}_\omega + v_{y_c,\omega}) \\ & - 170(U_{z_{wh},\omega} \bar{F}_\omega + v_{z_{wh},\omega}) - 150(U_{z_c,\omega} \bar{F}_\omega + v_{z_c,\omega})] \end{aligned} \quad (1.30)$$

$$s.t. \quad x_{wh} + x_c \leq 500, \quad (1.31)$$

$$\begin{aligned} 2.5x_{wh} + \min_{F_\omega \in \Xi_\omega} \{F_\omega U_{y_{wh},\omega} + v_{y_{wh},\omega} - (F_\omega U_{z_{wh},\omega} + v_{z_{wh},\omega}) - F_\omega\} \geq 0, \\ \omega = 1, \dots, s, \end{aligned} \quad (1.32)$$

$$3x_c + y_{c,\omega} - z_{c,\omega} \geq 340, \quad \omega = 1, \dots, s, \quad (1.33)$$

$$x_{wh}, x_c \geq 0, \quad (1.34)$$

$$\min_{F_\omega \in \Xi_\omega} \{F_\omega U_{y_{wh},\omega} + v_{y_{wh},\omega}\} \geq 0, \quad \omega = 1, \dots, s, \quad (1.35)$$

$$\min_{F_\omega \in \Xi_\omega} \{F_\omega U_{y_c,\omega} + v_{y_c,\omega}\} \geq 0, \quad \omega = 1, \dots, s, \quad (1.36)$$

$$\min_{F_\omega \in \Xi_\omega} \{F_\omega U_{z_{wh},\omega} + v_{z_{wh},\omega}\} \geq 0, \quad \omega = 1, \dots, s, \quad (1.37)$$

$$\min_{F_\omega \in \Xi_\omega} \{F_\omega U_{z_c,\omega} + v_{z_c,\omega}\} \geq 0, \quad \omega = 1, \dots, s. \quad (1.38)$$

Here, \bar{F}_ω is the expected value of F_ω for scenario ω .

The formulations discussed in this section will be generalized in the next section for SCO problems under uncertainty.

1.3 Two-Stage Stochastic Programming Formulations for SCO Under Uncertainty

The general formulation of two-stage stochastic programming with recourse [33] can be described as below. All the symbols, used in this section, are also summarized in Table 1.2 at the end of this Chapter.

Formulation (SP)

$$\min_{x \in X} c^T x + E_{\xi \in \Xi} \{Q(x, \xi)\} \quad (1.39)$$

$$s.t. \quad Ax \leq b. \quad (1.40)$$

Here $x \in X \subset \mathbb{R}^{n_x}$ represents first-stage decision variables that can be either continuous or integer. $\xi \in \Xi$ represents uncertain parameters, each of which is independent on other uncertain parameters. Most of the times, first-stage decision variables in SCO problems are related to design variables of the supply chain network, e.g. capacity of processing plants. In Formulation (SP), $c \in \mathbb{R}^{n_x}$ is the cost related to the first-stage decision variables. The second-stage decision variables are $y \in \mathbb{R}^{n_y}$, and costs related to the second-stage decisions variables are the optimal objective value of the recourse problem, i.e.,

$$Q(x, \xi) = \min q(\xi)^T y \quad (1.41)$$

$$s.t. \quad t_i(\xi)^T x + w_i^T y \leq 0, \quad i = 1, \dots, m, \quad (1.42)$$

where $q(\xi) \in \mathbb{R}^{n_y}$, $t_i(\xi) \in \mathbb{R}^{n_x}$, $w_i \in \mathbb{R}^{n_y}$ are parameters that are dependent on the uncertain parameters. Note that any constraint with an uncertain parameter in the

right-hand-side can be reformulated with a zero right-hand-side in form of (1.42), and it is explained in [36]. In order to solve Formulation (SP), the expected cost of second-stage decisions over different realizations of uncertain parameter, $E_{\xi \in \Xi}[Q(x, \xi)]$, needs to be calculated by solving an infinite number of recourse problems, which is usually unrealistic. In order to solve Formulation (SP) practically, the classical scenario or robust formulation can be used. The classical scenario formulation with s scenarios can be written as

Formulation (S)

$$\min_{\substack{x \in X, \\ y_1, \dots, y_s}} c^T x + \sum_{\omega=1}^s P_\omega \cdot q(\xi_\omega)^T y_\omega \quad (1.43)$$

$$s.t. \quad Ax \leq b, \quad (1.44)$$

$$t_i(\xi_\omega)^T x + w_i^T y_\omega \leq 0, \quad i = 1, \dots, m, \quad \omega = 1, \dots, s, \quad (1.45)$$

and the classical robust formulation is:

Formulation (R)

$$\min_{\substack{x \in X, \\ y}} c^T x + \bar{q}^T y \quad (1.46)$$

$$s.t. \quad Ax \leq b, \quad (1.47)$$

$$\max_{\xi \in \Xi} \{t_i^T(\xi)x + w_i^T y\} \leq 0, \quad i = 1, \dots, m. \quad (1.48)$$

Here \bar{q} represents the nominal cost for second-stage decisions, but it can also represent the worst-case cost if that is more appropriate for a SCO problem. Formulation (R) is a bi-level optimization problem, which can be reformulated into single level

linear and quadratic programming problems with the assumption of polyhedral and ellipsoidal uncertainty [34, 37, 38, 39, 40]. The various uncertainty regions assumed in the literature have been thoroughly discussed by Li et al. [41], from both the geometrical point of view and the computational point of view. To reduce the conservativeness of the robust formulation, an iterative strategy was proposed by Li et al. [42]. In their method, a tight posterior probability bounds were used to improve the robust solution within an iterative framework. Compared to the single-step classical robust optimization method, the quality of the robust solution were improved after applying the iterative strategy.

The Robust Scenario Formulation is another approach to reduce the conservativeness of a robust formulation. In this formulation, a scenario is associated with an uncertainty subregion Ξ_ω rather than a single uncertainty realization. When s uncertainty subregions are used and $\bigcup_{\omega=1}^s \Xi_\omega \supset \Xi$, then the solution of the robust scenario formulation is guaranteed to be feasible for Formulation (SP). For convenience of discussion, q and t_i are assumed to be affine functions of ξ_ω , i.e., $q_\omega = \alpha_q \xi_\omega + \beta_q$ and $t_{i,\omega} = \alpha_{t,i} \xi_\omega + \beta_{t,i}$, where $\alpha_q \in \mathbb{R}^{n_y \times n_\xi}$, $\beta_q \in \mathbb{R}^{n_y}$, $\alpha_{t,i} \in \mathbb{R}^{n_x \times n_\xi}$, $\beta_{t,i} \in \mathbb{R}^{n_x}$. Here, n_ξ is the number of uncertain parameters. As a result, the robust scenario formulation can be written as:

Formulation (RS)

$$\min_{\substack{x \in X \\ U_1, \dots, U_s \\ v_1, \dots, v_s}} c^T x + \sum_{\omega=1}^s P_{\omega}(\alpha_q \bar{\xi}_{\omega} + \beta_q)^T (U_{\omega} \bar{\xi}_{\omega} + v_{\omega}) \quad (1.49)$$

$$s.t. \quad Ax \leq b, \quad (1.50)$$

$$\max_{\xi_{\omega} \in \Xi_{\omega}} \{(\alpha_{t,i} \xi_{\omega} + \beta_{t,i})^T x + w_i^T (U_{\omega} \xi_{\omega} + v_{\omega})\} \leq 0, \quad i = 1, \dots, m, \quad \omega = 1, \dots, s. \quad (1.51)$$

Here, $\bar{\xi}_{\omega}$ denotes the expected value of ξ_{ω} for scenario ω . As explained in the previous section, the robust scenario formulation approximates second-stage decisions, y_{ω} , as an affine function of ξ_{ω} i.e. $y_{\omega} = U_{\omega} \xi_{\omega} + v_{\omega}$. As a result, the second-stage decision variables are allowed to vary affinely with respect to uncertainty realizations within a scenario, and it is less conservative than forcing the second-stage decisions to be constant for a scenario. Formulation (RS) is a bi-level optimization problem, and it has been shown that, if the uncertainty region Ξ is bounded with the infinity-norm, then this bi-level optimization problem can be equivalently transformed into a single level LP problem [36].

1.4 Generalized Benders Decomposition

Formulation (RS) is better than either Formulation (S) or Formulation (R), because its solution is guaranteed to be feasible and usually close to be optimal for the original formulation (SP). However, Formulation (RS) can be large scale optimization problem when the number of scenarios, s , is large, especially the formulation includes both integer variables and nonlinear functions. On the other hand, the optimization problem does have a special structure, commonly known as L-shaped structure, which

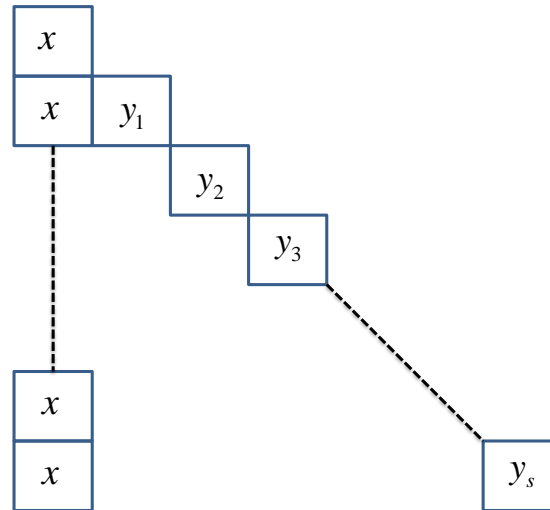


Figure 1.2: Decomposable structure of Formulation (RS)

can be exploited by decomposition algorithms for efficient solution [33].

Figure 1.2 illustrates the L-shaped decomposable structure. The first row of Figure 1.2 indicates the constraints that only contain first-stage decision variables (i.e., Equation (1.50)). The subsequent rows denote those constraints which contain both first-stage decision variables (x) and second-stage decision variables (y_ω) for different scenarios (i.e., Equation (1.51)). For example, the third row indicates the constraint for scenario 2 and it only involves variables x and y_2 . From Figure 1.2, it can be seen that, when x is known, the problem can be decomposed into s sub-problems which are much easier to solve. This leads to the idea of Benders decomposition [43] (applicable to LPs and MILPs) and generalized Benders decomposition [44] that is an extension of Benders decomposition to nonlinear and mixed-integer nonlinear programming problems.

1.5 Goal of the Thesis

One of the main objectives of the thesis is to develop a new robust scenario approach to solve two-stage supply chain optimization problems under uncertainty, where the uncertainty region is bounded with the general p -norm. After that, the new approach will be extended for any bounded uncertainty region.

For problems where the uncertainty region is characterized by a group of data points instead of a bounded region, a different approach will be developed to construct the bounded uncertainty region and formulate the robust scenario formulation.

Furthermore, some preliminary studies are conducted to demonstrate the computational advantages of generalized Benders decomposition for solving robust scenario formulations with nonlinear functions, in comparison to the use of the state-of-the-art commercial solvers, such as MOSEK [1] and CPLEX [45].

1.6 Organization of Thesis

In this thesis, Chapter 2 presents a new robust scenario formulation approach to solve two-stage supply chain optimization problems where the uncertainty region is bounded with the general p -norm. In Chapter 3, a robust scenario formulation approach for more general bounded uncertainty regions, and the data driven robust scenario approach, will be discussed. In Chapter 4, application of the generalized Benders decomposition to solving a robust scenario problem that arises from an industrial chemical supply chain problem will be discussed. Finally, in Chapter 5, the conclusions and possible future research directions will be presented.

Table 1.2: List of variables and parameters for the general formulation of two-stage stochastic programming

Symbol	Meaning
c	Cost associated with first-stage decisions
$E\{\cdot\}$	Expected value operator
P_ω	Probabilities of corresponding uncertainty realizations
\bar{q}	Nominal cost for second-stage decisions
$Q(x, \xi)$	Total cost associated with second-stage decisions
$q(\xi)$	Second-stage cost (that depends on uncertainty realizations)
s	Number of scenarios
$t_i(\xi)$	Coefficient depending on uncertainty realization
U_ω	Second-stage decisions for affine approximation of y_ω
v_ω	Second-stage decisions for affine approximation of y_ω
$w_i(\xi)$	Coefficient depending on uncertainty realization
x	First-stage decision variables
y	Second-stage decision variables
y_ω	Second-stage decision variables for different uncertainty realizations
$\alpha_{t,i}$	Coefficient of linear dependency of $t_{i,\omega}$ on ξ_ω
α_q	Coefficient of linear dependency of q_ω on ξ_ω
$\beta_{t,i}$	Coefficient of linear dependency of $t_{i,\omega}$ on ξ_ω
β_q	Coefficient of linear dependency of q_ω on ξ_ω
Ξ	Uncertainty region
Ξ_ω	Uncertainty sub-regions
ξ	Uncertain parameters
ξ_ω	Uncertainty realization in a scenario
ω	Index of uncertainty realizations for uncertain parameter

Chapter 2

A Robust Scenario Approach for Uncertainty Regions Bounded With the p -Norm

2.1 Reformulation of the Robust Scenario Formulation When the Uncertainty Subregions are Bounded With a Norm

For convenience of discussion, the robust scenario formulation, Formulation (RS), described in Chapter 1, is given here again:

Formulation (RS)

$$\min_{\substack{x \in X \\ U_1, \dots, U_s \\ v_1, \dots, v_s}} c^T x + \sum_{\omega=1}^s P_{\omega} (\alpha_q \bar{\xi}_{\omega} + \beta_q)^T (U_{\omega} \bar{\xi}_{\omega} + v_{\omega}) \quad (2.1)$$

$$s.t. \quad Ax \leq b, \quad (2.2)$$

$$\max_{\xi_{\omega} \in \bar{\Xi}_{\omega}} \{(\alpha_{t,i} \xi_{\omega} + \beta_{t,i})^T x + w_i^T (U_{\omega} \xi_{\omega} + v_{\omega})\} \leq 0, \quad i = 1, \dots, m, \quad \omega = 1, \dots, s. \quad (2.3)$$

Formulation (RS) is a bi-level optimization problem which in general is not easy to solve, but it can be transformed into a single-level optimization problem if each

uncertainty subregion, Ξ_ω , is bounded with a norm. For convenience, let

$$\Xi_\omega = \{\xi_\omega : \|M(\xi_\omega - \bar{\xi}_\omega)\| \leq \delta_\omega\},$$

where M is related to the shape of Ξ_ω and δ_ω is related to the size of Ξ_ω . In this case, the left-hand side of Equation (2.3) can be re-written as below:

$$\begin{aligned} & \max_{\xi \in \Xi_\omega} \{(\alpha_{t,i}\xi_\omega + \beta_{t,i})^T x + w_i^T (U_\omega \xi_\omega + v_\omega)\} \\ &= \beta_{t,i}^T x + w_i^T v_\omega + \max_{\xi \in \Xi_\omega} \{(x^T \alpha_{t,i} + w_i^T U_\omega) \xi_\omega\}, \\ &= \beta_{t,i}^T x + w_i^T v_\omega + (x^T \alpha_{t,i} + w_i^T U_\omega) \bar{\xi}_\omega + \max_{\xi \in \Xi_\omega} \{(x^T \alpha_{t,i} + w_i^T U_\omega) (\xi_\omega - \bar{\xi}_\omega)\}. \end{aligned}$$

According to the result given in [46],

$$\max_{\xi \in \Xi_\omega} \{(x^T \alpha_{t,i} + w_i^T U_\omega) (\xi_\omega - \bar{\xi}_\omega)\} = \delta_\omega \|(x^T \alpha_{t,i} + W_i^T U_\omega) M^{-1}\|_*, \quad (2.4)$$

Here, $\|\cdot\|_*$ indicates the dual norm [47] of the norm used to bound the uncertainty subregions. In some cases, the explicit form of the dual norm is known. For example, if the norm used to bound the uncertainty subregion is a p -norm, then its dual norm is a q -norm and the relationship between p and q is: $q = 1 + \frac{1}{p-1}$ [46]. Note that the p -norm of a vector $x \in \mathbb{R}^n$ is $\|x\|_p = (\sum_{i=1}^n |x_i|^p)^{1/p}$.

According to the above discussion, Problem (RS) can be transformed into the following form:

Formulation (RS-norm)

$$\min_{\substack{x \in X \\ U_1, \dots, U_s \\ v_1, \dots, v_s}} c^T x + \sum_{\omega=1}^s P_{\omega} (\alpha_q \bar{\xi}_{\omega} + \beta_q)^T (U_{\omega} \bar{\xi}_{\omega} + v_{\omega}) \quad (2.5)$$

$$s.t. \quad Ax \leq b, \quad (2.6)$$

$$\beta_{t,i}^T x + w_i^T v_{\omega} + (x^T \alpha_{t,i} + w_i^T U_{\omega}) \bar{\xi}_{\omega} + \delta_{\omega} \|(x^T \alpha_{t,i} + w_i^T U_{\omega}) M^{-1}\|_* \leq 0, \quad (2.7)$$

$$i = 1, \dots, m, \quad \omega = 1, \dots, s.$$

Note that this reformulation is done with the assumption that the uncertainty subregions Ξ_{ω} can be constructed such that $\bigcup_{\omega=1}^s \Xi_{\omega} \supset \Xi$, which is essential to ensure feasibility of the optimization problem as mentioned in Chapter 1, but how to partition the uncertainty region Ξ to generate uncertainty subregions Ξ_{ω} is not trivial. For example, when Ξ is bounded with the infinity-norm, say, $\Xi = \{\xi : \|M(\xi - \bar{\xi})\|_{\infty} \leq 1\}$, the uncertainty region is box shaped and it can be easily partitioned into a number of box subregions that can also be expressed with the infinity-norm. This is illustrated in Figure 2.1(a). However, when Ξ is bounded with the 2-norm, then the uncertainty region is an ellipse, as shown in Figure 2.1(b), which cannot be easily partitioned into uncertainty subregions that can also be expressed with the 2-norm. The next subsection will discuss how to systematically partition an uncertainty region Ξ when it is bounded with a p -norm, such that the reformulation of Formulation (RS) into Formulation (RS-norm) is possible.

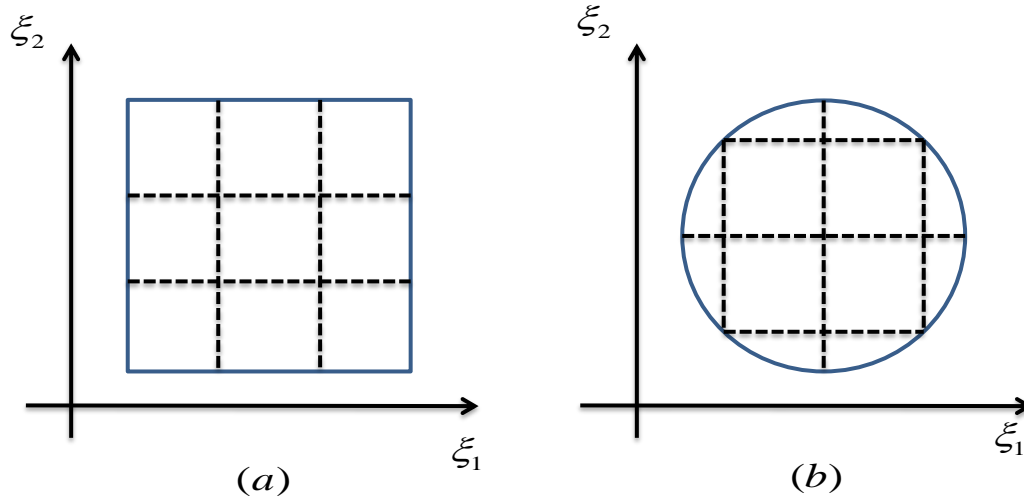


Figure 2.1: (a) Partitioning of uncertainty region bounded with the infinity-norm (with 9 partition) (b) Partitioning of uncertainty region bounded with the 2-norm into box-shaped uncertainty sub-regions is not simple

2.2 Systematic Partitioning of Uncertainty Regions Bounded with the p -Norm

2.2.1 Partitioning of Uncertainty Regions Bounded with the Infinity-Norm

In order to develop a general approach for partitioning the p -norm bounded uncertainty region, we start with an easy case where the uncertainty region is bounded with the infinity-norm. In this case, the region is box shaped and generation of box-shaped subregions is explained via a simple example.

Assume there are two uncertain parameters. The first uncertain parameter, ξ_1 , has a range $[0.6 \quad 1.4]$ and second uncertain parameter, ξ_2 , has a range $[0.7 \quad 1.3]$.

Then, the box-shaped uncertainty region can be expressed as follows:

$$\begin{bmatrix} 0.6 \\ 0.7 \end{bmatrix} \leq \begin{bmatrix} \xi_1 \\ \xi_2 \end{bmatrix} \leq \begin{bmatrix} 1.4 \\ 1.3 \end{bmatrix} \quad (2.8)$$

Let the middle value for the uncertain parameters be $\bar{\xi}_1 = 1$ and $\bar{\xi}_2 = 1$, then

$$\begin{bmatrix} -0.4 \\ -0.3 \end{bmatrix} \leq \begin{bmatrix} \xi_1 - \bar{\xi}_1 \\ \xi_2 - \bar{\xi}_2 \end{bmatrix} \leq \begin{bmatrix} 0.4 \\ 0.3 \end{bmatrix} \quad (2.9)$$

, and

$$\begin{bmatrix} -1 \\ -1 \end{bmatrix} \leq \begin{bmatrix} 0.4^{-1} & 0 \\ 0 & 0.3^{-1} \end{bmatrix} \begin{bmatrix} \xi_1 - \bar{\xi}_1 \\ \xi_2 - \bar{\xi}_2 \end{bmatrix} \leq \begin{bmatrix} 1 \\ 1 \end{bmatrix}. \quad (2.10)$$

Equation (2.10) can also be written with the infinity-norm as

$$\|M(\xi - \bar{\xi})\|_{\infty} \leq \delta$$

, where

$$M = \begin{bmatrix} 0.4^{-1} & 0 \\ 0 & 0.3^{-1} \end{bmatrix}, \quad \delta = \begin{bmatrix} 1 \\ 1 \end{bmatrix}$$

In order to construct the robust scenario formulation, we can partition Ξ into 9

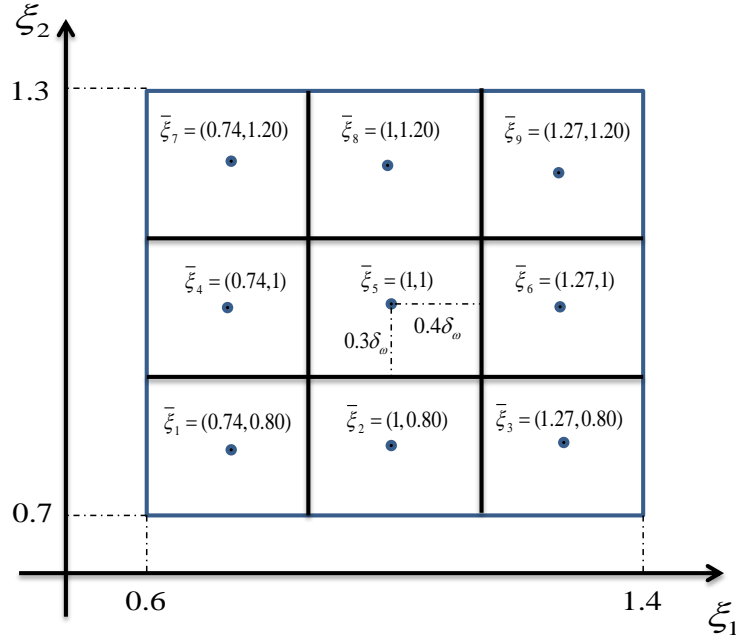


Figure 2.2: An uncertainty region bounded with the infinity-norm with 9 partitions

identical subregions, each mathematically expressed as:

$$\|M(\xi_\omega - \bar{\xi}_\omega)\|_\infty \leq \delta_\omega,$$

where $\delta_\omega = \frac{1}{3}$ for all ω , and $\bar{\xi}_\omega$ denotes the mid point for scenario/subregion ω .

The partitioning of this uncertainty region is illustrated in Figure 2.2.

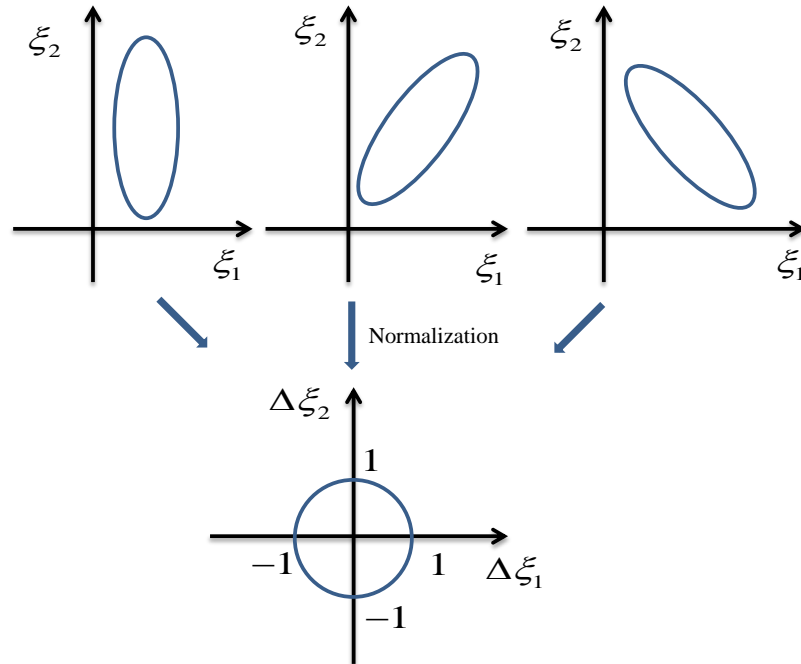


Figure 2.3: Normalization of different 2-norm bounded original uncertainty regions into an unit circular uncertainty region centered at origin

2.2.2 Normalization of Uncertainty Regions Bounded with the p -Norm and the Reference Box

In the example of the previous section, the ranges of uncertain parameters are different and they may vary from problem to problem. For convenience of analysis, we can normalize the ranges of all uncertain parameters in a problem to $[-1 \ 1]$, which is a common idea in different statistical analysis [48]. For example, when a uncertainty region is bounded with the 2-norm, then, it can have different ellipsoidal shapes at different locations of the parameter space, as illustrated by Figure 2.3. But after normalization, all regions will become a unit circle centered at the origin.

In the remaining part of this thesis, two terms, "original uncertainty region" and "normalized uncertainty region" will be used frequently. "Original uncertainty region" refers to the uncertainty region of the parameters in the original problem. "Normalized uncertainty region" refers to the uncertainty region of the transformed uncertain parameters after the normalization process, and the transformed uncertain parameters is called "normalized uncertain parameters".

To normalize the original uncertainty region, bounded with a p -norm, there are several steps involved. The first step is to find the ranges of the original uncertain parameters, ξ_{max} and ξ_{min} , and then shift the center of the original uncertainty region to the origin, by introducing new uncertain parameters $\hat{\xi} = \xi - \bar{\xi}$, where $\bar{\xi}$ is the mid values of the original uncertain parameters, $\bar{\xi} = \frac{\xi_{max} + \xi_{min}}{2}$.

The second step is to rotate the shifted uncertainty region around the origin, by introducing new uncertain parameters $\hat{\xi}^r = M^\theta \hat{\xi}$, where the rotation matrix [49]

$$M^\theta = \begin{bmatrix} \cos\theta & -\sin\theta \\ \sin\theta & \cos\theta \end{bmatrix},$$

and θ is the rotation angle around the origin and possess positive sign for counter clockwise rotation.

The third step is to resize the shifted and rotated uncertainty region by introducing normalized uncertain parameters $\Delta\xi = M^R \hat{\xi}^r$, such that the normalized uncertain

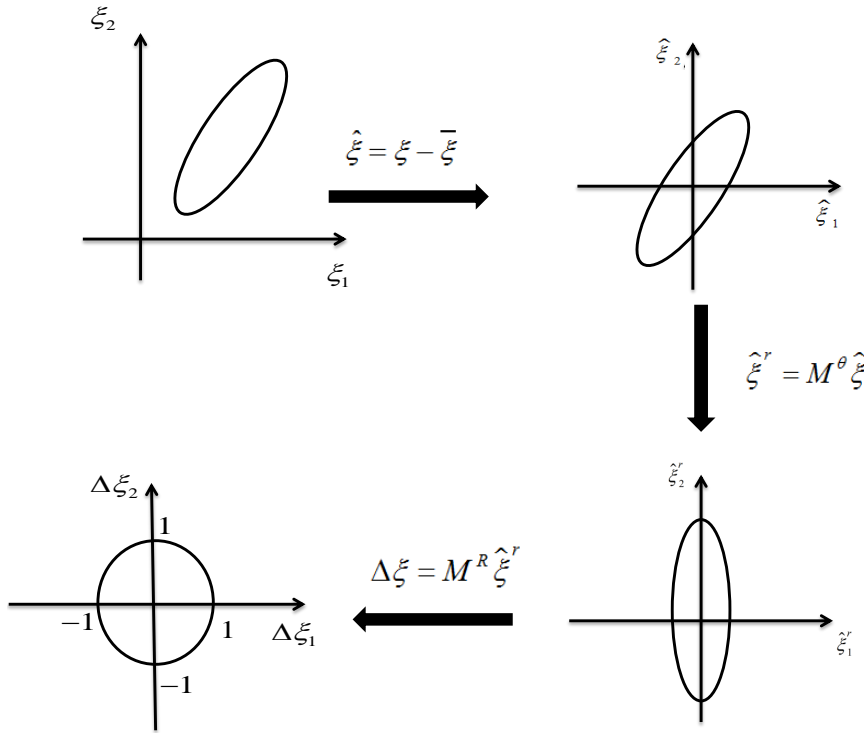


Figure 2.4: Normalization process of original uncertainty region

parameters all range from -1 to 1 . The resizing matrix M^R is a diagonal matrix adjusting the size of the uncertainty region along different dimensions.

Figure 2.4 illustrates the three steps for the normalization process. If, as shown in the figure, the original uncertainty regions is an ellipse, then after the normalization process, the normalized uncertainty region for the normalized uncertain parameters can be expressed with the 2-norm as $\Xi_{\Delta} = \{\Delta\xi \in \mathbb{R}^2 : \|\Delta\xi\|_2 \leq 1\}$. The original uncertainty region can then be expressed as $\Xi = \{\xi \in \mathbb{R}^2 : \xi = \bar{\xi} + M^{-1}\Delta\xi, \|\Delta\xi\|_2 \leq 1\}$, where $M = M^R M^{\theta}$.

When the original uncertainty region is bounded with a p -norm, as

$$\Xi_p = \{\xi : \|M(\xi - \bar{\xi})\|_p \leq 1\},$$

it can be readily normalized and the normalized uncertainty region can always be expressed as

$$\Xi_{\Delta,p} = \{\Delta\xi : \|\Delta\xi\|_p \leq 1\}$$

. So instead of partitioning set Ξ_p , we can always choose to partition set $\Xi_{\Delta,p}$ which is only dependent on the value of p , not the features of the original uncertainty region. Figure 2.5 shows shape of different normalized uncertainty regions bounded with different p -norms. It can be seen that the smallest box that contains any normalized uncertainty regions is the normalized uncertainty region bounded with the infinity-norm. This is formally stated as the following proposition and a proof for the proposition is given.

Proposition 1. *Let $\Xi_{\Delta,p} = \{\Delta\xi \in \mathbb{R}^n : \|\Delta\xi\|_p \leq 1\}$. $\forall p, q \in \mathbb{Z}_+ \cup \{\infty\}$, If $p < q$ then $\Xi_{\Delta,p} \subset \Xi_{\Delta,q}$. Here \mathbb{Z}_+ denotes the set of all positive integers.*

Proof. $\forall p \in \mathbb{Z}_+, \forall \Delta\xi \in \Xi_{\Delta,p}$, we can first see that

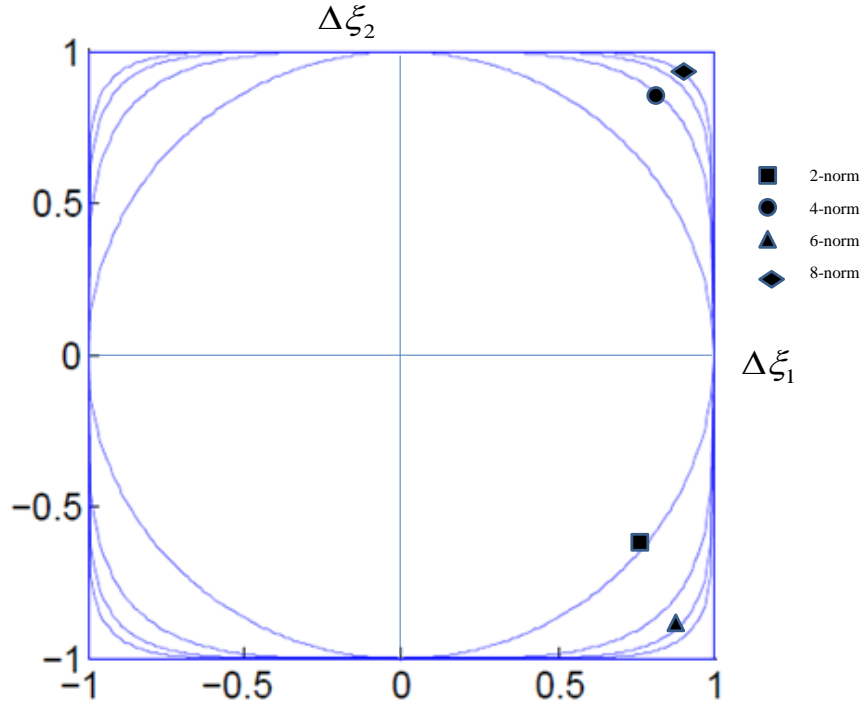


Figure 2.5: Normalized uncertainty regions bounded with different p -norms

$$\begin{aligned}
 1 &\geq \|\Delta\xi\|_p \\
 &= \left(\sum_{i=1}^n \{|\Delta\xi_i|^p\} \right)^{1/p}, \\
 &\geq \left(\max_{i=1,\dots,n} \{|\Delta\xi_i|^p\} \right)^{1/p}, \\
 &= \max_{i=1,\dots,n} \{|\Delta\xi_i|\}, \\
 &= \|\Delta\xi\|_\infty,
 \end{aligned} \tag{2.11}$$

which means that, $\Delta\xi \in \Xi_{\Delta,\infty}$ as well. So, $\Xi_{\Delta,p} \subset \Xi_{\Delta,\infty}$.

On the other hand,

$$\begin{aligned}
 & (\|\Delta\xi\|_{p+1})^{p+1} \\
 &= \sum_{i=1}^n |\Delta\xi_i|^p |\Delta\xi_i|, \\
 &\leq \sum_{i=1}^n |\Delta\xi_i|^p \|\Delta\xi\|_\infty, \\
 &= \left(\sum_{i=1}^n |\Delta\xi_i|^p\right) \cdot \|\Delta\xi\|_\infty, \\
 &= (\|\Delta\xi\|_p)^p \cdot \|\Delta\xi\|_\infty.
 \end{aligned} \tag{2.12}$$

Using Equation (2.11),

$$(\|\Delta\xi\|_p)^p \cdot \|\Delta\xi\|_\infty \leq (\|\Delta\xi\|_{p+1})^{p+1}. \tag{2.13}$$

Equation (2.12) and Equation (2.13) lead to $\|\Delta\xi\|_{p+1} \leq \|\Delta\xi\|_p$. So $\forall \Delta\xi \in \Xi_{\Delta,p}$, $\Delta\xi \in \Xi_{\Delta,p+1}$ as well. Therefore, $\Xi_{\Delta,p} \subset \Xi_{\Delta,p+1}$.

In summary of the above discussion, $\Xi_1 \subset \Xi_2 \subset \Xi_3 \dots \subset \Xi_\infty$ and the proposition is proved. □

Proposition 1 shows that set $\Xi_{\Delta,\infty}$ is the smallest box that contains all the normalized uncertainty regions bounded with the p -norm. In the remaining part of the thesis, we call this set the reference box.

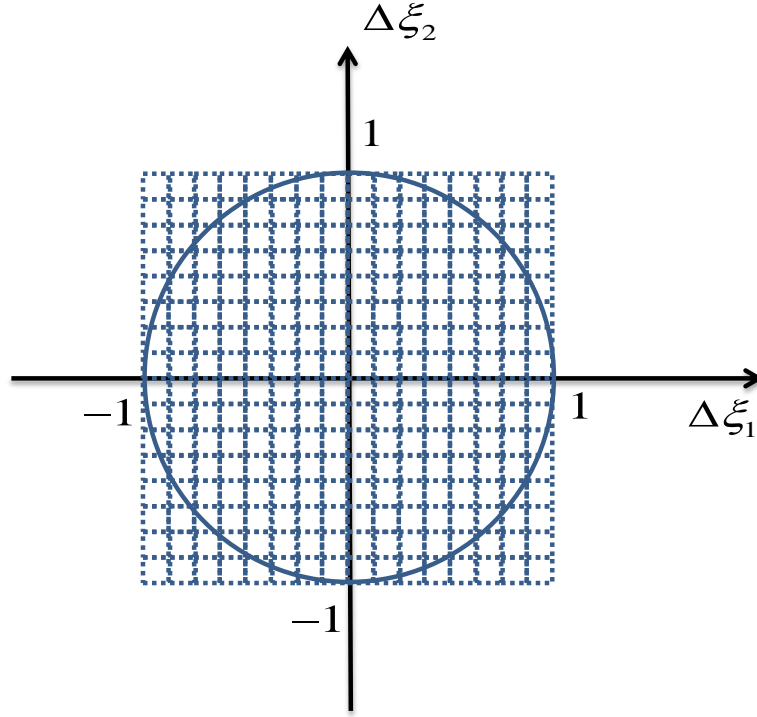


Figure 2.6: Division of the reference box into box-shaped sub-regions

2.2.3 Subregions Generated by Partitioning of the Reference Box

According to the discussion in Section 2.2.1, the reference box $\Xi_{\Delta, \infty}$ of any normalized uncertainty region $\Xi_{\Delta, p}$, can be readily partitioned into a number of box-shaped subregions, which can be represented as $\Xi_{\omega} = \{\Delta\xi_{\omega} : \|\Delta\xi_{\omega} - \Delta\bar{\xi}_{\omega}\|_{\infty} \leq \delta_{\omega}\}$. Here $\omega = 1, \dots, s$ and s is the total number of scenarios. Obviously, $\bigcup_{\omega=1}^s \Xi_{\omega} = \Xi_{\Delta, \infty} \supset \Xi_{\Delta, p}$. This is illustrated through Figure 2.6.

From Figure 2.6, it can be seen that, some of the box-shaped uncertainty subregions lie completely inside of the normalized uncertainty region and some of the box-shaped uncertainty sub-regions lie completely outside of the normalized uncertainty region. The box-shaped uncertainty sub-regions that lie completely outside

of the normalized uncertainty region can be screened out as those uncertainty sub-regions are not part of the normalized uncertainty region. The box-shaped uncertainty sub-regions that lie completely inside of the normalized uncertainty region will always be considered.

The box-shaped uncertainty sub-regions that lie on the boundary of normalized uncertainty region can either be screened out or considered. When they are considered, the optimization problem over-estimates the normalized uncertainty region; otherwise, the problem under-estimates the normalized uncertainty region. Figure 2.7 and Figure 2.8 illustrate the over-estimation and the under-estimation of the normalized uncertainty region, respectively. When the number of box-shaped uncertainty sub-regions is significantly large, the area of the uncertainty subregions on the boundary is sufficiently small, and the over-estimated and the under-estimated normalized uncertainty regions are sufficiently close, as illustrated in Figure 2.9. In this case, the two optimization problems will have almost the same optimal objective values. Once the normalization process is completed, then $\bar{\xi}_\omega$ in Formulation (RS-norm) will be replaced by $\bar{\xi} + M^{-1}\Delta\xi_\omega$.

2.2.4 Illustrative Example: Normalization and Partitioning

To better explain the normalization of original uncertainty region, subsequent partitioning of reference uncertainty region and the construction of over-estimated and under-estimated normalized uncertainty regions, an example will be discussed in this section. In this example, the original uncertainty region, defined by a quadratic constraint, is, $\Xi = \{\xi \in \mathbb{R}^2 : (\xi_1 - 2)^2 + (\xi_2 - 3)^2 \leq 4\}$. From the equation, it is found

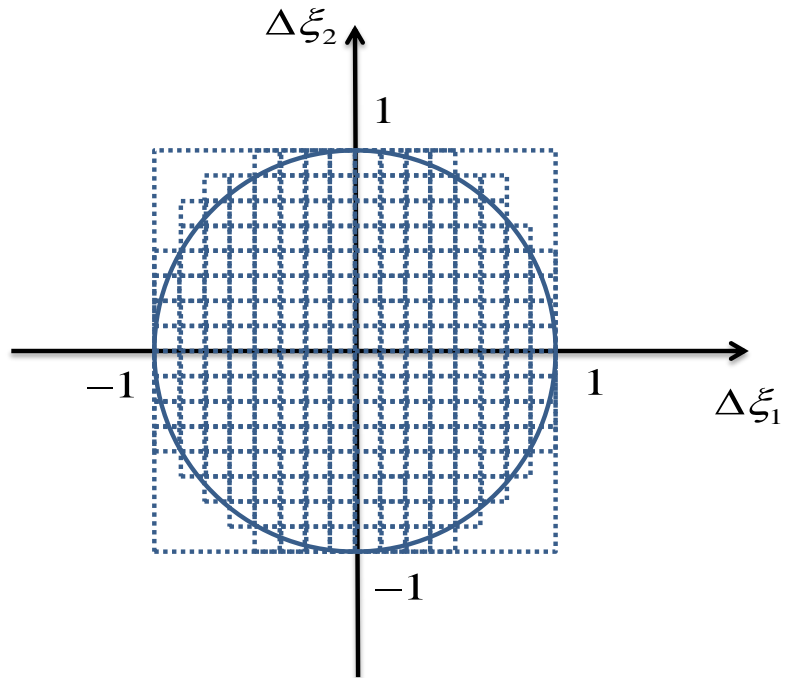


Figure 2.7: Over-estimation of the normalized uncertainty region

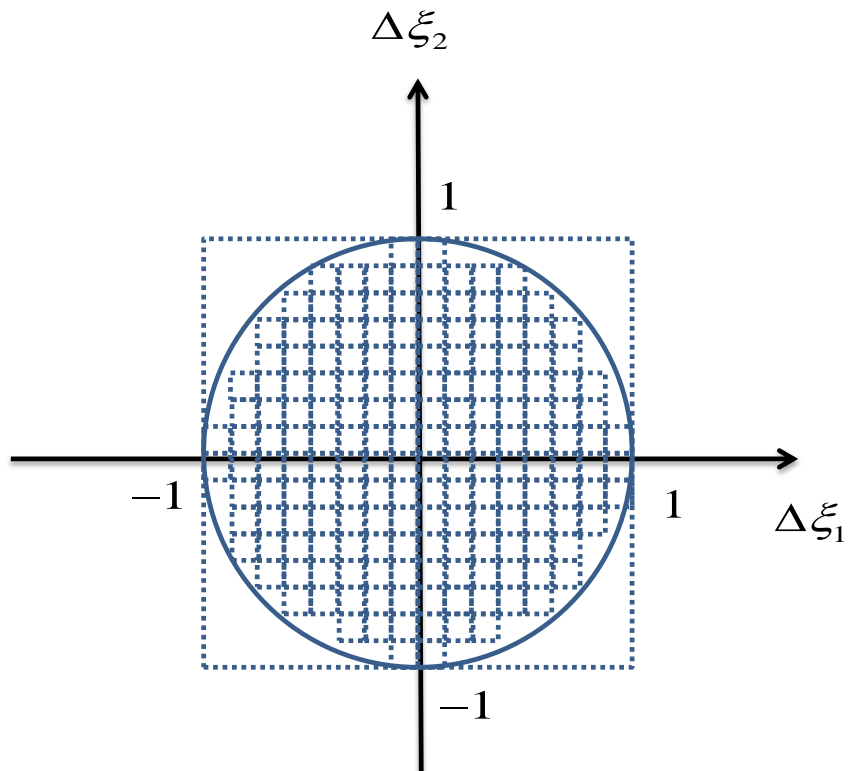


Figure 2.8: Under-estimation of the normalized uncertainty region

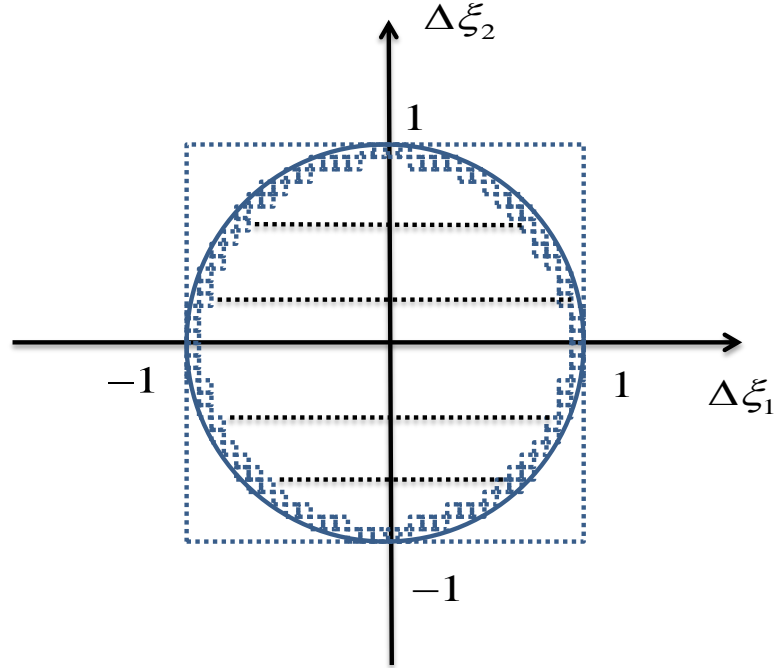


Figure 2.9: Approximation of the normalized uncertainty region with many scenarios that, the original uncertainty region is a circle having center (2,3) and radius 2. Figure 2.10 illustrates the original uncertainty region.

The normalization procedure is illustrated in Figure 2.11. First, the original uncertainty region can be expressed with the 2-norm, as $\Xi = \{\xi \in \mathbb{R}^2 : \|M(\xi - \bar{\xi})\|_2 \leq 1\}$, where

$$M = \begin{bmatrix} \frac{1}{2} & 0 \\ 0 & \frac{1}{2} \end{bmatrix}, \quad \bar{\xi} = \begin{bmatrix} 2 \\ 3 \end{bmatrix},$$

and $\bar{\xi}$ denotes the center of the region. By defining the new uncertain parameters $\hat{\xi} = \xi - \bar{\xi}$, the uncertainty region is shifted to the origin. The shifted uncertainty region can be expressed as $\hat{\Xi} = \{\hat{\xi} \in \mathbb{R}^2 : \|M\hat{\xi}\|_2 \leq 1\}$. Finally, resize the shifted

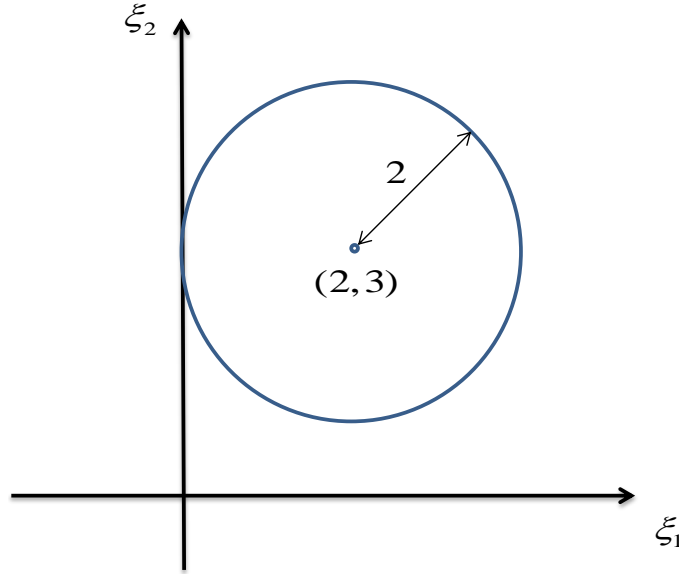


Figure 2.10: Original uncertainty region bounded with $(\xi_1 - 2)^2 + (\xi_2 - 3)^2 \leq 4$

uncertainty region into a unit circle, by defining $\Delta\xi = M\hat{\xi}$. The normalized uncertainty region can be expressed as $\Xi_{\Delta} = \{\Delta\xi \in \mathbb{R}^2 : \|\Delta\xi\|_2 \leq 1\}$.

Once the normalization process is completed, the normalized uncertainty region, Ξ_{Δ} , can now be covered with a box-shaped reference uncertainty region, $\Xi_{\Delta, \infty}$. This box-shaped reference uncertainty region can now be partitioned as described in the previous section. If there are 25 partitions of reference uncertainty region, then the over-estimation and under-estimation of normalized uncertainty region is shown in Figure 2.12. When uncertainty subregions that have at least one extreme point inside the normalized uncertainty region are considered, the normalized uncertainty regions is over-estimated, as shown in Figure 2.12(b). All 25 subregions are considered in this case. When uncertainty subregions that have all extreme points inside the normalized uncertainty region are considered, the normalized uncertainty region

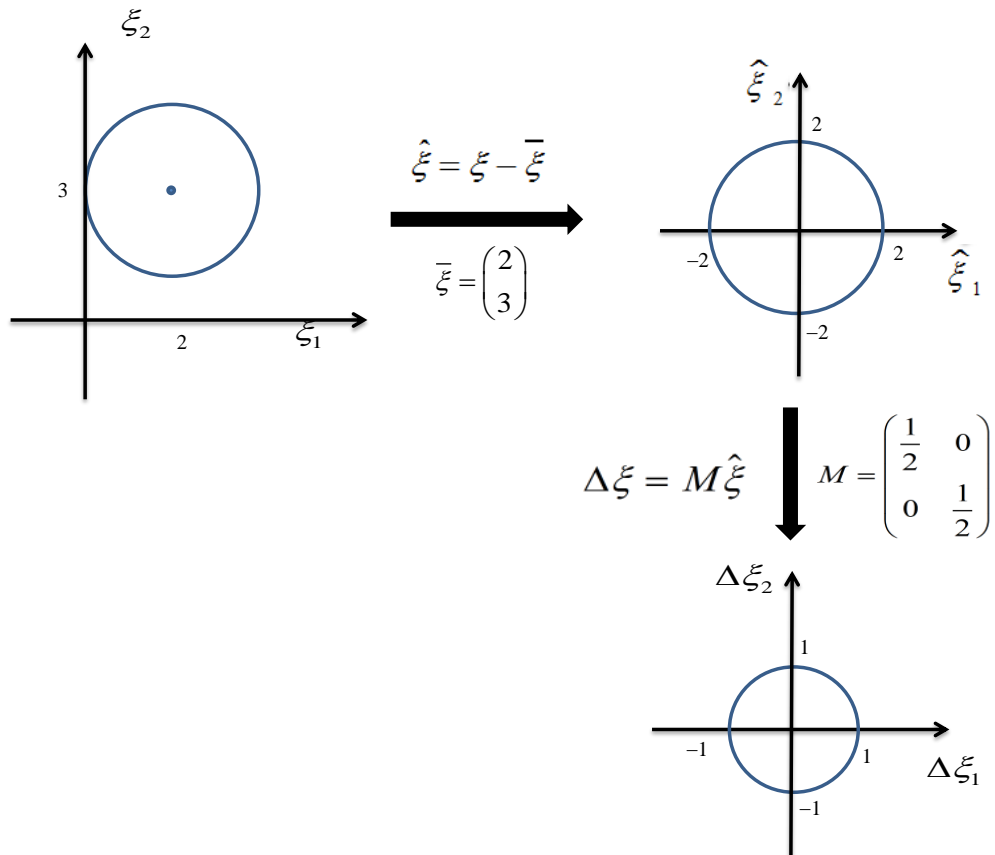


Figure 2.11: Normalization process of original uncertainty region bounded with $(\xi_1 - 2)^2 + (\xi_2 - 3)^2 \leq 4$

is under-estimated, as shown in Figure 2.12(c). In this case, only 9 uncertainty sub-regions are considered.

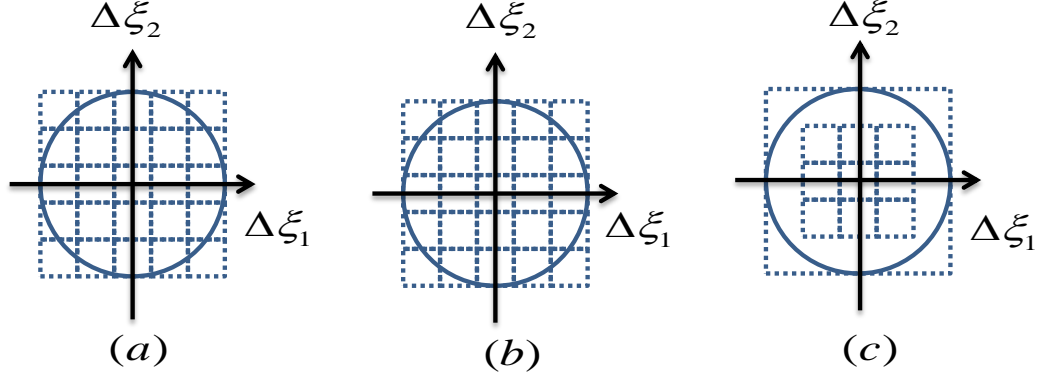


Figure 2.12: (a) Reference uncertainty region with 25 partition (b) Overestimation of normalized uncertainty region (c) Underestimation of normalized uncertainty region

2.3 Linear Programming Reformulations for the 1-Norm Constraints

With the proposed uncertainty region partitioning approach, uncertainty sub-regions, Ξ_ω , are always box-shaped and can be bounded with the infinity-norm, so Equation (2.7) of Formulation (RS-norm) can always be written as:

$$\beta_{t,i}^T x + w_i^T v_\omega + (x^T \alpha_{t,i} + w_i^T U_\omega) \bar{\xi}_\omega + \delta_\omega \|(x^T \alpha_{t,i} + w_i^T U_\omega) M^{-1}\|_1 \leq 0. \quad (2.14)$$

Equation (2.14) contains a term that is involved with the 1-norm. Let $y_\omega = (x^T \alpha_{t,i} + w_i^T U_\omega) M^{-1}$, then Equation (2.14) can be re-written as:

$$\beta_{t,i}^T x + w_i^T v_\omega + (x^T \alpha_{t,i} + w_i^T U_\omega) \bar{\xi}_\omega + \delta_\omega \sum_{j=1}^n |y_{\omega,j}| \leq 0. \quad (2.15)$$

Here, we explain how to reformulate the constraint involving absolute value operations into linear constraints. We use the following simplified optimization problem for convenience of discussion.

Formulation (1)

$$\min_{x \in X} c^T x \tag{2.16}$$

$$s.t. \quad Ax \leq b, \tag{2.17}$$

$$\bar{\xi}^T x + \sum_{i=1}^n |y_i| \leq 0, \tag{2.18}$$

$$y_i = x_i^T M^{-1}, \quad i = 1, \dots, n, \tag{2.19}$$

where n is the total number of components in y , which is also the number of uncertain parameters in the robust scenario formulation.

Equation (2.18) of this optimization problem can be re-written. One way of re-writing Equation (2.18) was discussed by McLean and Li [36]. It results in the following LP problem:

Formulation (2)

$$\min_{x \in X} c^T x \tag{2.20}$$

$$s.t. \quad Ax \leq b, \tag{2.21}$$

$$\bar{\xi}^T x + y_1 + y_2 + \dots + y_n \leq 0, \tag{2.22}$$

$$\bar{\xi}^T x - y_1 + y_2 + \dots + y_n \leq 0, \tag{2.23}$$

$$\bar{\xi}^T x + y_1 - y_2 + \dots + y_n \leq 0, \tag{2.24}$$

$$\bar{\xi}^T x - y_1 - y_2 + \dots + y_n \leq 0, \tag{2.25}$$

·
·
·

$$y_i = x_i^T M^{-1} \quad i = 1, \dots, n, \tag{2.26}$$

Comparing to the Formulation (1), this optimization problem has $2^n - 1$ extra constraints. So, with the increasing numbers of uncertain parameters, the number of constraints increases exponentially. If Formulation (1) involves a large number of uncertain parameters, then this approach can make the problem hard to solve. To avoid that, a new LP reformulation is proposed here.

Formulation (3)

$$\min_{x \in X} c^T x \tag{2.27}$$

$$s.t. \quad Ax \leq b, \tag{2.28}$$

$$\bar{\xi}^T x + \sum_{i=1}^n t_i \leq 0, \tag{2.29}$$

$$y_i = x_i^T M^{-1}, \quad i = 1, \dots, n, \tag{2.30}$$

$$-t_i \leq y_i \leq t_i, \quad i = 1, \dots, n, \tag{2.31}$$

$$t_i \geq 0, \quad i = 1, \dots, n. \tag{2.32}$$

Here, Formulation (1) and Formulation (3) are equivalent, because, (a) both of the optimization problems have the same objective function and (b) any x and y , that satisfy the constraints of formulation (1), also satisfy the constraints of formulation (3) and any x , y and t , that satisfy the constraints of formulation (3), also satisfy the constraints of formulation (1). As a result, the feasible sets of x in formulation (1) and formulation (3) are the same. Comparing to Formulation (1), Formulation (3) has n extra variables and $3n - 1$ extra constraints. So, the number of variables and constraints increase linearly with n in Formulation (3), which is better than Formulation (2). If the original optimization problem involves a large number of uncertain parameters, then Formulation (3) is expected to perform better in terms of computational time.

2.4 Case Study

2.4.1 An Industrial Chemical Supply Chain from DuPont

In this section, an industrial chemical supply chain case study will be discussed to show the effective implementation of the ideas described in the previous sections. The industrial chemical supply chain case study problem was formulated from the operational data, provided by DuPont [50]. The deterministic model contains 2335 variables and 1020 constraints. This supply chain network has 55 grades of Primary Raw Materials (PRM). There is only one PRM warehouse in which PRM can be stored. PRM can also be stored in one of the 5 on-site PRM warehouses. From the on-site warehouses, the raw materials are sent to one of the 5 production plants for processing into final products (FP). FP then sent to the on-site final product warehouses. The FP has 23 different grades and can either be transported to regional warehouses for additional storage or to the 5 regional markets to be sold to the customers. The complete network of the supply chain problem is illustrated through Figure 2.13.

The goal of this industrial chemical supply chain optimization problem is to determine the optimal capacity for each of the plants in a way such that, the total profit of supply chain network is maximized and the minimum customer demand at 5 different regional markets are satisfied. The uncertain parameters for this case study are minimum demand of the different final products at each of the regional markets. Capacities of different processing plants are the first-stage decision variables. The second-stage decision variables are the raw material flows and product flows associated with the operation of the supply chain network. Both first stage and second

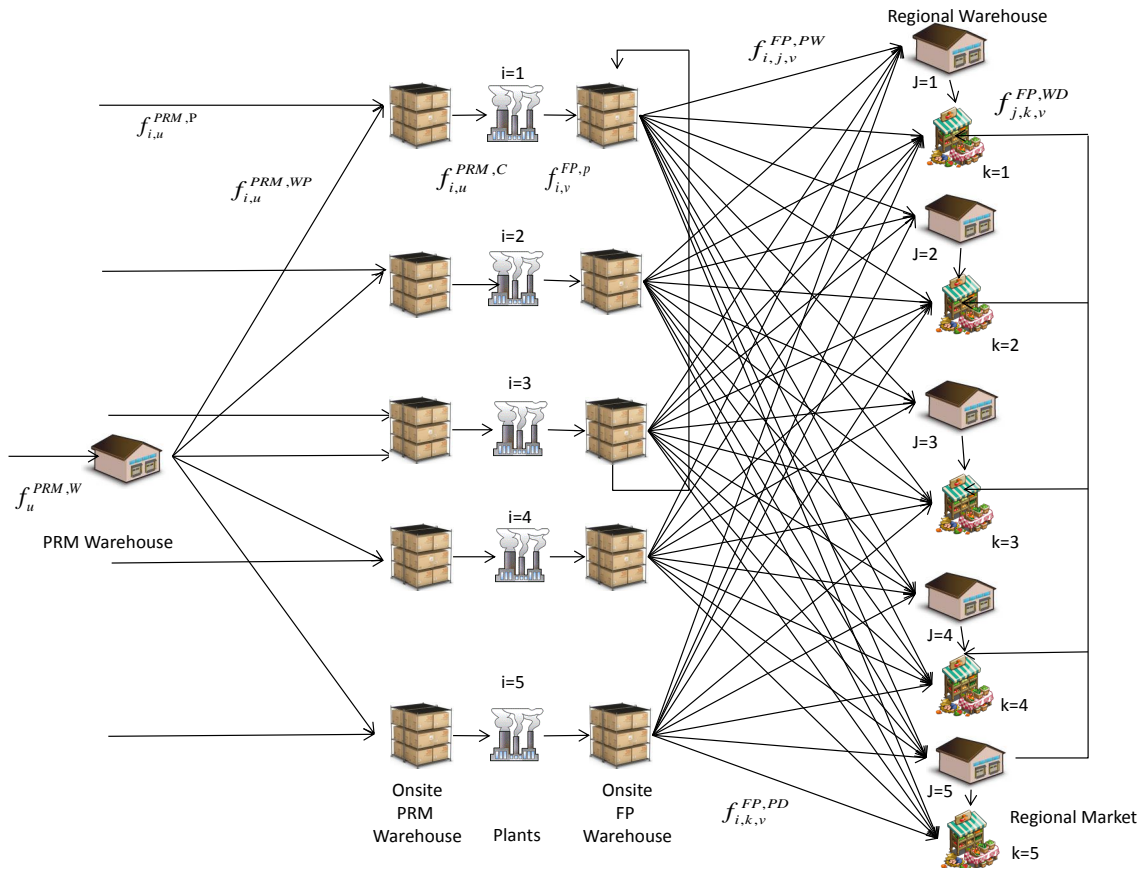


Figure 2.13: DuPont industrial chemical supply chain network

stage decision variables are represented by continuous variables in the optimization problem. The Robust Scenario Formulation for DuPont Industrial Chemical Supply Chain problem with its deterministic formulation, related nomenclature and list of symbols are given in Appendix A. Note that, here instead of arbitrary demand, minimum demand at different markets are to be met in order to satisfy the prior contract commitments between different markets and the producers.

2.4.2 Demand Uncertainty

We assume that the minimum demands ($D_{v,k}^{min}$) for different grades of final products (v) in regional markets (k) are uncertain. Specifically,

$$D_{v,k}^{min} = \bar{D}_{v,k}^{min} \cdot \xi_1, \quad k = 1, 2, 3$$

$$D_{v,k}^{min} = \bar{D}_{v,k}^{min} \cdot \xi_2, \quad k = 4, 5$$

Here, $\bar{D}_{v,k}^{min}$ denotes the nominal demand, which is a known constant, of different grades of final products at different regional markets. Due to different geographical locations, there are two different groups of market. First group consists of $k = 1, 2, 3$ and second group consists of $k = 4, 5$. The uncertain parameter ξ_1 determines the minimum demands at market 1, 2, and 3, and the uncertain parameter ξ_2 determines the minimum demands at market 4 and 5. ξ_1 follows a normal distribution with mean 1 and standard deviation 0.1634, and ξ_2 follows normal distribution with mean 1 and standard deviation 0.1226. The two uncertain parameters are independent of each other. Therefore, the 95% confidence region of the two uncertain parameters is [51]:

$$\Xi = \{ \xi \in \mathbb{R}^2 : (\xi - \bar{\xi})^T \Sigma^{-1} (\xi - \bar{\xi}) \leq \chi_{0.05,2}^2 \}.$$

Here, the covariance matrix and the center of the confidence region are

$$\Sigma = \begin{bmatrix} 0.0267 & 0 \\ 0 & 0.0150 \end{bmatrix}, \quad \bar{\xi} = \begin{bmatrix} 1 \\ 1 \end{bmatrix},$$

and $\chi_{0.05,2}^2 = 5.9915$ denotes the percentage point for 5% tail for chi-squared distribution (degrees of freedom = 2). Ξ can also be expressed with the 2-norm, as

$$\Xi = \{\xi \in \mathbb{R}^2 : \|M(\xi - \bar{\xi})\|_2 \leq 1\},$$

where

$$M = \begin{bmatrix} 0.4^{-1} & 0 \\ 0 & 0.3^{-1} \end{bmatrix}.$$

In order to normalize the uncertainty region, define $\Delta\xi = M(\xi - \bar{\xi})$, then the normalized uncertainty region is $\Xi_{\Delta} = \{\Delta\xi \in \mathbb{R}^2 : \|\Delta\xi\|_2 \leq 1\}$. The robust scenario formulation using the normalized uncertainty region for the DuPont industrial chemical supply chain optimization problem is also given in Appendix A.

Next, we discuss how to calculate the probability for each scenario/uncertainty subregion in the robust scenario formulation. Let's assume that we are to partition the reference box for the normalized uncertainty region into 16 identical box subregions, as illustrated in Figure 2.14. According to its definition, either $\Delta\xi_1$ or $\Delta\xi_2$ follows a normal distribution with a mean of 0 and a standard deviation of 0.4086. In other words, either $\Delta\xi_1/0.4086$ or $\Delta\xi_2/0.4086$ follows the standard normal distribution. Therefore, the probability of the 14th uncertainty subregion in Figure 2.14 can be calculated as:

$$P_{14} = \left[\Phi^{-1} \left(\frac{-1 + \frac{2}{4} \cdot 2}{0.4086} \right) - \Phi^{-1} \left(\frac{-1 + \frac{2}{4} \cdot 1}{0.4086} \right) \right] \times \left[\Phi^{-1} \left(\frac{-1 + \frac{2}{4} \cdot 1}{0.4086} \right) - \Phi^{-1} \left(\frac{-1 + \frac{2}{4} \cdot 0}{0.4086} \right) \right]. \quad (2.33)$$

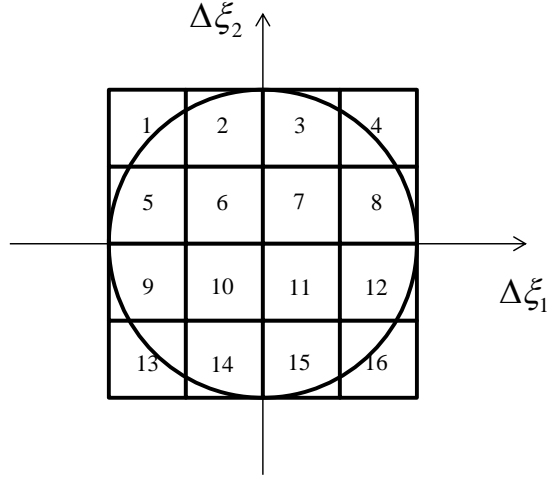


Figure 2.14: Normalized uncertainty region with 16 sub-regions

Here Φ^{-1} is the inverse cumulative distribution function for standard normal distribution. Note that, here standard deviation of $\Delta\xi_1$ and $\Delta\xi_2$ are found from the covariance matrix, Σ_n . If, 95% joint confidence region of normalized uncertain parameters, $\Xi_\Delta = \{\Delta\xi \in \mathbb{R}^2 : \Delta\xi^T \Sigma_n^{-1} \Delta\xi \leq \chi_{0.05,2}^2\}$, and the equation of normalized uncertainty region, $\Xi_\Delta = \{\Delta\xi \in \mathbb{R}^2 : \|\Delta\xi\|_2 \leq 1\}$ are compared, then the covariance matrix, Σ_n , can be written as $\Sigma_n = \frac{1}{\chi_{0.05,2}^2} I$, where I is the identity matrix and $\chi_{0.05,2}^2 = 5.9915$. From the above equation, covariance matrix is,

$$\Sigma_n = \begin{bmatrix} 0.1669 & 0 \\ 0 & 0.1669 \end{bmatrix}$$

. From this covariance matrix, standard deviations of both $\Delta\xi_1$ and $\Delta\xi_2$ can be calculated and the standard deviations of $\Delta\xi_1$ and $\Delta\xi_2$ are, $\sqrt{0.1669} = 0.4085$ and $\sqrt{0.1669} = 0.4085$ respectively.

In general, if the range of each uncertain parameter is divided into b subranges,

then the probability associated with h^{th} subrange ($h = 1, \dots, b$) is

$$P_h = \Phi^{-1} \left(\frac{-1 + \frac{2h}{b}}{0.4086} \right) - \Phi^{-1} \left(\frac{-1 + \frac{2}{b}(h-1)}{0.4086} \right).$$

In addition, the total number of scenarios is $s = b^2$, and the probability for each scenario ω ($\omega = 1, \dots, s$), P_ω , is the product of the probabilities associated with the two uncertain parameters. Note that the sum of P_ω over all selected uncertainty subregions, P_{total} , is not equal to 1 in general. In order to calculate the expected cost for the uncertainty realizations considered in the formulation, we use the following scaled probability, $P_{scaled,\omega}$, for each considered scenario:

$$P_{scaled,\omega} = \frac{P_\omega}{P_{total}}. \quad (2.34)$$

$P_{scaled,\omega}$ can be viewed as the conditional probability, under the condition that only the points in the considered uncertainty subregions can be realized.

2.4.3 Case Study Results

In this case study, we first solve the DuPont industrial chemical supply chain optimization problem using the new robust scenario approach, and then assess the optimality and the feasibility of the solution using Monte Carlo simulation. The case study problem was modeled using GAMS 24.3.1 [52], and solved in a machine with 3.40GHz CPU and Linux operating system using CPLEX 12.4 solver [45]. A relative termination criterion of 1% was used for all the problems. For linear programming reformulation of constraints involving the 1-norm, Formulation 3 proposed in Section 2.3, was used.

(a) *Convergence to Optimal Solution*

We call the robust scenario formulation using the over-estimated uncertainty region RSF-OE, and the one using the under-estimated uncertainty region RSE-UE. Figure 2.15 shows how the optimal objective values of the two formulations converge with the increase of the number of scenarios. It can be seen that with increasing number of scenarios, the optimal objective value of RSF-OE converges to the optimal objective value of RSE-UE, within a relative tolerance of 1%. Initially, when the number of scenarios is 9 or 16, there is a significant difference (relative tolerance is more than 1%) between the optimal objective values of RSF-OE and RSE-UE. The reason behind it is, lack of sufficient number of scenarios for RSF-UE and RSF-OE to completely represent the normalized uncertainty region. When the number of scenarios increased to 25, both optimal objective values converge within the relative tolerance, which indicates that 25 scenarios are good enough to represent the normalized uncertainty region bounded with the 2-norm. The converged optimal objective value is \$22092, and this value can be viewed as the expected profit predicted by the robust scenario formulations at the convergence. Here, the first stage decisions, which are the capacity of five processing plants are, 7383.81t, 1626.32t, 577.04t, 1334.23t, and 1793.55t respectively. Note that, these first stage decisions might be inconvenient to implement due to practical purposes. For example, while building the processing plants, if the choice of the capacity for first processing plant is 7000t or 7500t, then the capacity of first processing plant can be expressed as $7000\delta_1 + 7500\delta_2$ in the optimization problem, where δ_1 and δ_2 are binary variables and follow the equation, $\delta_1 + \delta_2 = 1$.

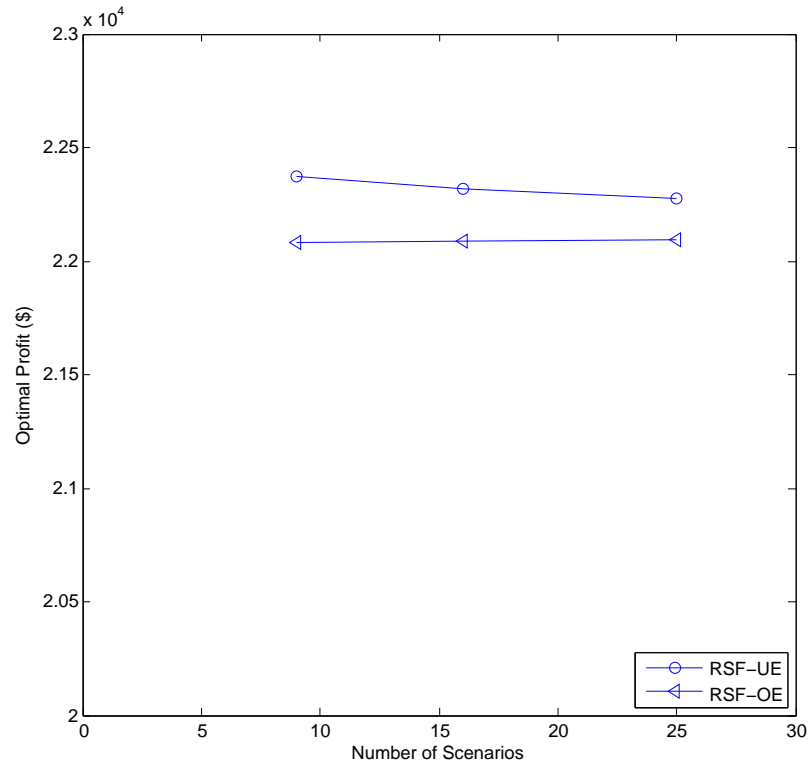


Figure 2.15: Convergence of RSF-OE and RSF-UE

(b) Evaluation of Optimality and Feasibility of Solution

The robust scenario formulation is different from the rigorous two-stage stochastic programming formulation in the sense that the second-stage decisions are approximated as affine functions of uncertainty realizations. So we need to assess whether the first-stage decisions obtained by solving the robust scenario formulation are as optimal as predicted and feasible with the predefined confidence.

We use Monte Carlo simulation for this purpose. We fix the first-stage decision variables, i.e., capacities of the processing plants, to their values at the optimal solution. And then solve a full recourse problem for each sampled uncertainty realization.

In order to know how many sampled realizations are needed to reflect the true expected profit and the true percentage of feasibility, we keep increase the number of sampled scenarios until the simulated expected profit and percentage of feasibility do not change.

Figure 2.16 and Figure 2.17 give the simulation results.

Figure 2.16 illustrates the optimality test for DuPont industrial Chemical Supply Chain problem. From Figure 2.16 it can be seen that, with sufficiently large number of samples for normalized uncertain parameters, the predicted expected profit can be very close to the achieved expected profit.

From Figure 2.16, at the beginning, when number of samples were small (less than 100), the difference between achieved expected profit and the predicted expected profit was very high. With the increasing number of samples, the achieved expected profit decreased quickly till 1000 samples. After 1000 samples, the achieved expected profit again incresed and at 2000 samples and onwards the change in two consecutive profits are within the relative tolerance of 1%. The profit at 2000 samples is \$22096 which is better than the predicted expected profit of \$22092.

While calculating the achieved expected profit, Monte-Carlo simulation was conducted with a large number of normally distributed random samples. In that case, feasibility of the problem can be an issue. Here, the minimum desired rate of feasibility is 95% which means that for all the normally distributed random samples, atleast 95% of the problems has to be feasible. This procedure is named as feasibility test. Figure 2.17 illustrates the feasibility test of DuPont industrial Chemical Supply Chain problem.

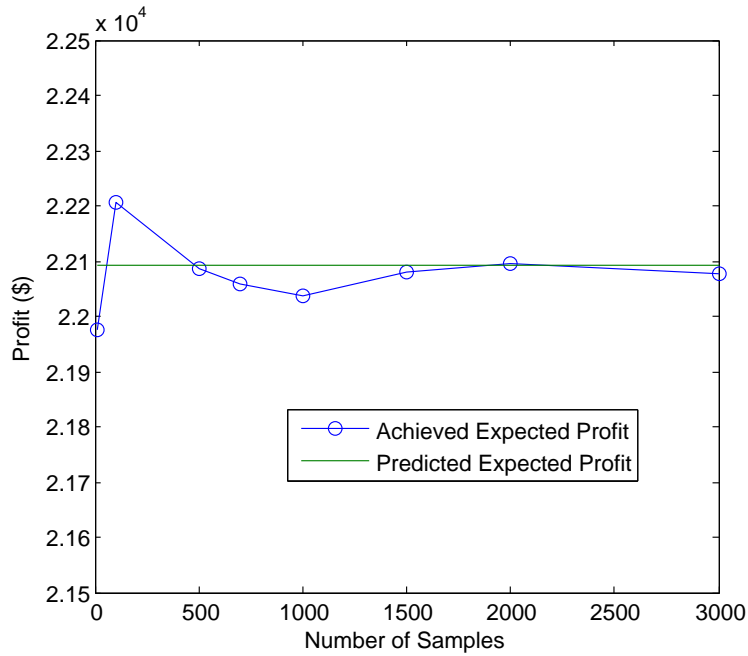


Figure 2.16: Optimality test for DuPont Industrial Chemical Supply Chain Problem

In that case, 10, 100, 500, 700, 1000, 1500, 2000, 3000 and 4000 normally distributed random uncertainty realizations for normalized uncertain parameters, $\Delta\xi$, were used. From Figure 2.17 it is clear that initially when the number of samples are low, the rate of feasible problems decreases very quickly. With the increasing number of samples, the percentage of feasibility slowly becomes constant. At 2000 samples, the percentage of feasible problems become 99.55% which almost remained constant (99.61%) even at 4000 samples. The feasibility rate, which is 99.55% for 2000 samples is far better than the initial expectation of 95% feasibility.

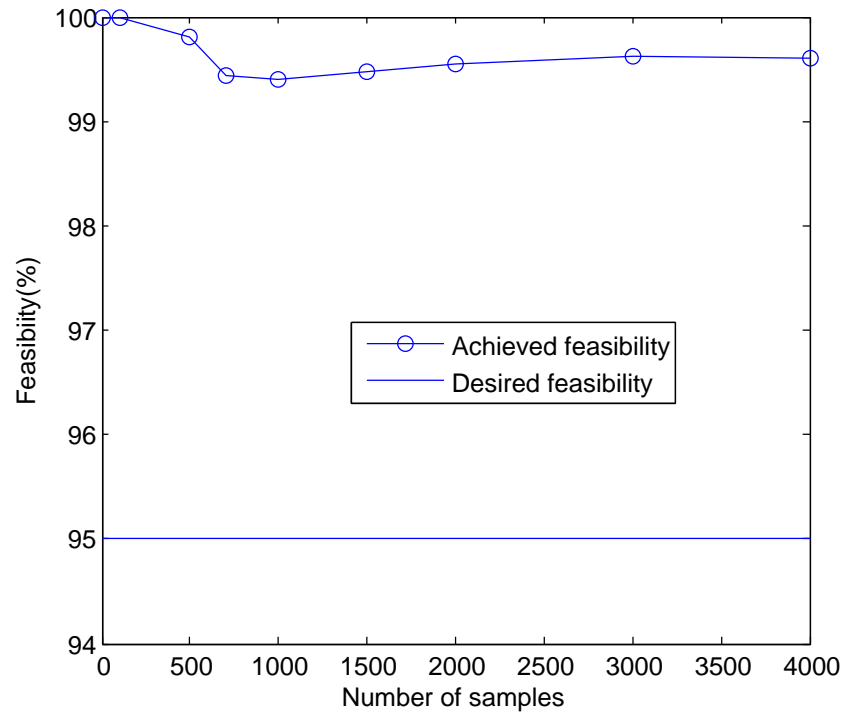


Figure 2.17: Feasibility test for DuPont Industrial Chemical Supply Chain Problem

Chapter 3

Robust Scenario Approaches for Robust Optimization and Data Driven Stochastic Programming

In Chapter 2, a general approach has been developed to effectively address uncertainty regions bounded with the p-norm, in two-stage stochastic programming. Uncertainty regions bounded with the p-norm can be used to represent or approximate many symmetric and convex uncertainty regions. However, in the real life, there are cases where uncertainty regions are asymmetric and nonconvex [53]. In this chapter, the approach proposed in Chapter 2 will be extended to all bounded uncertainty regions. The potential benefits of rotation of the original uncertainty region will also be discussed.

In real life industrial cases, uncertain parameters are often characterized through historic data [54]. A data driven robust scenario formulation will be discussed for these cases, in the second part of this chapter.

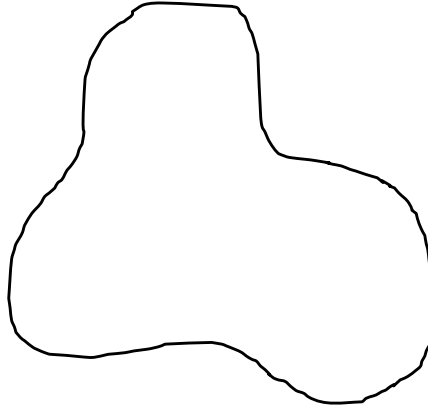


Figure 3.1: An asymmetric and nonconvex bounded uncertainty region

3.1 A Robust Scenario Approach for Robust Optimization

While a robust scenario approach is developed in Chapter 2 for uncertainty regions bounded with the p-norm, a real life problem may have an asymmetric and nonconvex bounded uncertainty region, such as the one shown in Figure 3.1.

Asymmetric or nonconvex uncertainty regions often arise from problems where uncertainty regions are defined explicitly by a set of constraints, such as those from many robust optimization problems. These robust optimization problems are often treated as semi-infinite programming problems and solved using iterative approaches [55] [56]. Here we discuss robust optimization problems in the following form:

$$\min_{x \in X} f(x) \tag{3.1}$$

$$s.t. \quad g(x, \xi) \leq 0, \quad \forall \xi \in \Xi, \tag{3.2}$$

where Ξ denotes the original bounded uncertainty region that can be defined by a set of equations and can have an arbitrary shape and $f(x)$ is a nominal objective function.

Like uncertainty regions bounded with the p-norm, a general bounded uncertainty region can be normalized such that the ranges of all uncertain parameters are $[-1, 1]$. Take the uncertainty region in Figure 3.1 as an example, the first step towards the normalization of the region is to determine the range of the uncertain parameters, by solving the following optimization problems:

$$\min \quad \xi_1 \tag{3.3}$$

$$s.t. \quad (\xi_1, \xi_2) \in \Xi, \tag{3.4}$$

$$\max \quad \xi_1 \tag{3.5}$$

$$s.t. \quad (\xi_1, \xi_2) \in \Xi, \tag{3.6}$$

$$\min \quad \xi_2 \tag{3.7}$$

$$s.t. \quad (\xi_1, \xi_2) \in \Xi, \tag{3.8}$$

$$\max \quad \xi_2 \tag{3.9}$$

$$s.t. \quad (\xi_1, \xi_2) \in \Xi. \tag{3.10}$$

Let the optimal values of the problems are $\xi_{1,min}$, $\xi_{1,max}$, $\xi_{2,min}$, $\xi_{2,max}$, then the ranges of the two uncertain parameters are $[\xi_{1,min}, \xi_{1,max}]$, $[\xi_{2,min}, \xi_{2,max}]$, and the center point of the uncertainty region is defined as $[\bar{\xi}_1, \bar{\xi}_2] = [\frac{\xi_{1,max} + \xi_{1,min}}{2}, \frac{\xi_{2,max} + \xi_{2,min}}{2}]$. Define the new uncertain parameter vector $\hat{\xi} = \xi - \bar{\xi}$, then the new uncertainty region is centered at the origin. In addition, define the deviated uncertainty parameter

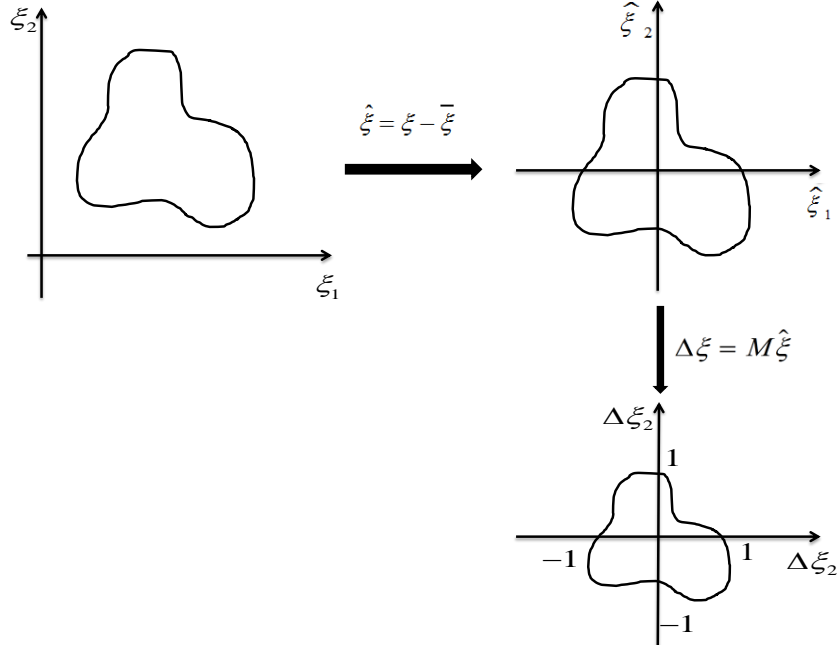


Figure 3.2: Normalization process for a bounded uncertainty region

vector $\Delta\xi = M\hat{\xi}$, where

$$M = \begin{bmatrix} \frac{\xi_{1,max} - \xi_{1,min}}{2} & 0 \\ 0 & \frac{\xi_{2,max} - \xi_{2,min}}{2} \end{bmatrix}^{-1},$$

then the ranges of $\Delta\xi_1$ and $\Delta\xi_2$ will become $[-1 \ 1]$. Figure 3.2 illustrates the normalization process of original uncertainty region.

Once the normalization process is completed, then the normalized uncertainty region can be covered with the reference box $\Xi_{\Delta,\infty} = \{\Delta\xi \in \mathbb{R}^2 : \|\Delta\xi\|_\infty \leq 1\}$, and the reference box can be partitioned into s box-shaped uncertainty sub-regions defined as $\Xi_\omega = \{\Delta\xi \in \mathbb{R}^2 : \|\Delta\xi_\omega - \Delta\bar{\xi}_\omega\|_\infty \leq \delta_\omega\}$ ($\omega = 1, \dots, s$), according to the approach discussed in Chapter 2.

The optimization problem, RSF-OE, that over-estimates the normalized uncertainty region can be written as:

$$\min_{x \in X} f(x) \tag{3.11}$$

$$s.t. \quad g(x, \xi_\omega) \leq 0, \quad \forall \xi_\omega \in \Xi_\omega^{OE}, \omega = 1, \dots, s. \tag{3.12}$$

The optimization problem, RSF-UE, that under-estimates the normalized uncertainty region can be written as following

$$\min_{x \in X} f(x) \tag{3.13}$$

$$s.t. \quad g(x, \xi_\omega) \leq 0, \quad \forall \xi_\omega \in \Xi_\omega^{UE}, \omega = 1, \dots, s. \tag{3.14}$$

Here, Ξ_ω^{OE} indicates the box-shaped uncertainty sub-regions when the normalized uncertainty region is over-estimated and Ξ_ω^{UE} indicates the box-shaped uncertainty sub-regions when the normalized uncertainty region is under-estimated.

3.1.1 An Illustrative Example

To demonstrate the idea of solving an optimization problem with any bounded uncertainty region, the following simple example will be considered, where there are two uncertain parameters (ξ_1 and ξ_2) and two decision variables (x_1 and x_2)

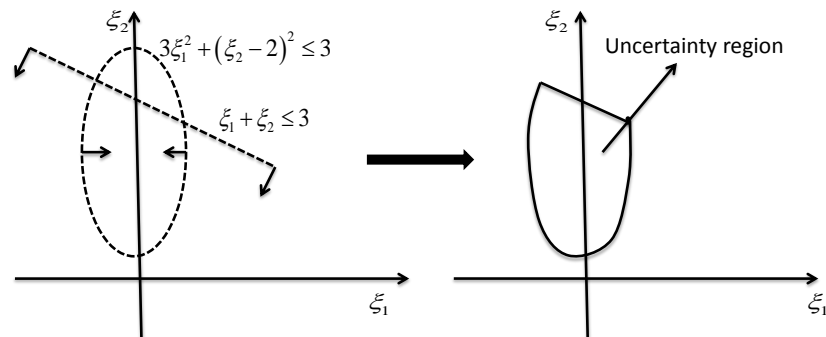


Figure 3.3: Uncertainty region, Ξ of Problem (1)

Problem 1

$$\min \quad x_2^2 - \frac{1}{2}x_1 \tag{3.15}$$

$$s.t. \quad \xi_1 x_1 + \xi_2 x_2 - 1 \leq 0, \quad \forall (\xi_1, \xi_2) \in \Xi. \tag{3.16}$$

Here the uncertainty region is defined as:

$$\Xi = \{ \xi \in \mathbb{R}^2 : 3\xi_1^2 + (\xi_2 - 2)^2 \leq 3, \xi_1 + \xi_2 \leq 3 \}.$$

This uncertainty region is shown in Figure 3.3.

To determine the ranges of ξ_1 and ξ_2 , following optimization problems are solved:

$$\min \xi_1 \tag{3.17}$$

$$s.t. \quad 3\xi_1^2 + (\xi_2 - 2)^2 \leq 3, \quad \xi_1 + \xi_2 \leq 3, \tag{3.18}$$

$$\max \xi_1 \tag{3.19}$$

$$s.t. \quad 3\xi_1^2 + (\xi_2 - 2)^2 \leq 3, \quad \xi_1 + \xi_2 \leq 3, \tag{3.20}$$

$$\min \xi_2 \tag{3.21}$$

$$s.t. \quad 3\xi_1^2 + (\xi_2 - 2)^2 \leq 3, \quad \xi_1 + \xi_2 \leq 3, \tag{3.22}$$

$$\max \xi_2 \tag{3.23}$$

$$s.t. \quad 3\xi_1^2 + (\xi_2 - 2)^2 \leq 3, \quad \xi_1 + \xi_2 \leq 3. \tag{3.24}$$

From the solutions of the optimization problems, the ranges of ξ_1 and ξ_2 are $[-1, 1]$ and $[0.268, 3.50]$. Define $\hat{\xi} = \xi - \bar{\xi}$, where

$$\bar{\xi} = \begin{bmatrix} \frac{-1+1}{2} \\ \frac{0.268+3.50}{2} \end{bmatrix} = \begin{bmatrix} 0 \\ 1.884 \end{bmatrix},$$

which shifts the center of the uncertainty region to the origin. Then define $\Delta\xi = M\hat{\xi}$, and

$$M = \begin{bmatrix} 1 & 0 \\ 0 & 1.616 \end{bmatrix}^{-1}.$$

Now the normalized uncertainty region is the following region for $\Delta\xi$:

$$\Xi_{\Delta} = \{\Delta\xi \in \mathbb{R}^2 : \Delta\xi = M(\xi - \bar{\xi}), 3\xi_1^2 + (\xi_2 - 2)^2 \leq 3, \xi_1 + \xi_2 \leq 3\}$$

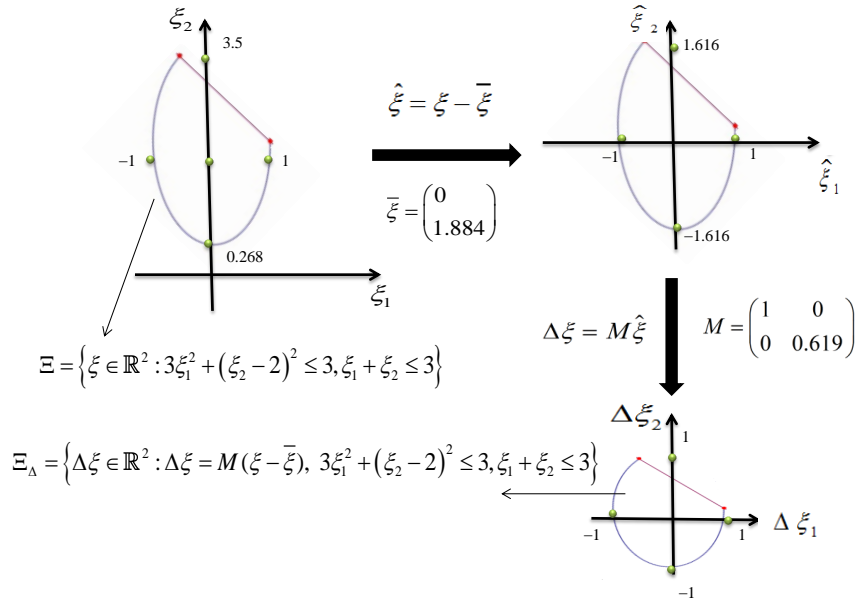


Figure 3.4: Normalization process for Ξ

The normalization process is shown in Figure 3.4.

Now, the smallest box region that covers the normalized uncertainty region is $\Xi_{\Delta, \infty} = \{\Delta\xi \in \mathbb{R}^2 : \|\Delta\xi\|_{\infty} \leq 1\}$, which can be partitioned to generate a set of box-shaped subregions that over-estimates Ξ_{Δ} and a set of box-shaped subregions that under-estimates Ξ_{Δ} . Figure 3.5 shows the case in which $\Xi_{\Delta, \infty}$ is partitioned into 25 scenarios, resulting in an over-estimation of Ξ_{Δ} with 23 subregions and an under-estimation of Ξ_{Δ} with 8 subregions.

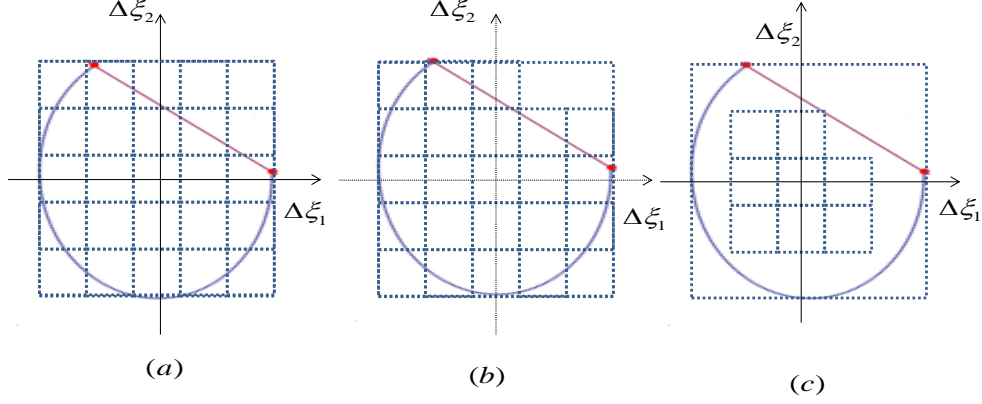


Figure 3.5: (a) Reference uncertainty region with 25 scenarios (b) Overestimation of normalized uncertainty region (c) Underestimation of normalized uncertainty region

The LP reformulation for either RSF-OE or RSF-UE, is given below

$$\min \quad x_2^2 - \frac{1}{2}x_1 \tag{3.25}$$

$$s.t. \quad \bar{\xi}^T x + \Delta \bar{\xi}_\omega^T ((M^{-1})^T x) + \delta_\omega \sum_{i=1}^{n_\xi} t_i \leq 1, \quad \omega = 1, \dots, s,$$

$$-t \leq (M^{-1})^T x \leq t, \tag{3.26}$$

$$t \geq 0. \tag{3.27}$$

Here, $t = (t_1, t_2)$, $x = (x_1, x_2)$. M determines the shape of the original uncertainty region, $\bar{\xi}$ is center of the original uncertainty region, $\Delta \bar{\xi}_\omega$ is the center of each uncertainty subregions generated from partitioning the normalized uncertainty region, and δ_ω determines the size of each uncertainty subregion. The derivation of robust scenario formulation of Problem (1) is given in Appendix B.

3.1.2 A Different Way to Partition the Original Uncertainty Region

In this section, we will first rotate the original uncertainty region and then apply the partitioning procedure. This is motivated by the fact that, one edge of the original uncertainty region is a straight line. If the region is rotated such that this edge is aligned with one of the coordinate axes, then the partitioning may be more efficient and effective.

Figure 3.6 illustrates the normalization process of original uncertainty region, when the original uncertainty region of Problem (1) is rotated around the origin by 45° counter clockwise using the following rotation matrix:

$$M^\theta = \begin{bmatrix} \cos 45^\circ & -\sin 45^\circ \\ \sin 45^\circ & \cos 45^\circ \end{bmatrix} = \begin{bmatrix} \frac{1}{\sqrt{2}} & \frac{-1}{\sqrt{2}} \\ \frac{1}{\sqrt{2}} & \frac{1}{\sqrt{2}} \end{bmatrix}.$$

The relationship between the original uncertain parameters ξ , and the normalized uncertain parameters $\Delta\xi^r$, is $\xi = (M^\theta)^{-1}(\bar{\xi}^r + M^{-1}\Delta\xi^r)$. Partitioning of the reference box and the resulting overestimation of the normalized uncertainty region and underestimation of the normalized uncertainty region are illustrated in Figure 3.7.

The LP reformulation for RSF-OE or RSF-UE is given below:

$$\min \quad x_2^2 - \frac{1}{2}x_1 \tag{3.28}$$

$$s.t. \quad \tilde{\xi}^r T x + (\Delta\tilde{\xi}_\omega^r)^T (\hat{M}^T x) + \delta_\omega \sum_{i=1}^{n_\omega} t_i \leq 1, \quad \omega = 1, \dots, s,$$

$$-t \leq \hat{M}^T x \leq t, \tag{3.29}$$

$$t \geq 0, \tag{3.30}$$

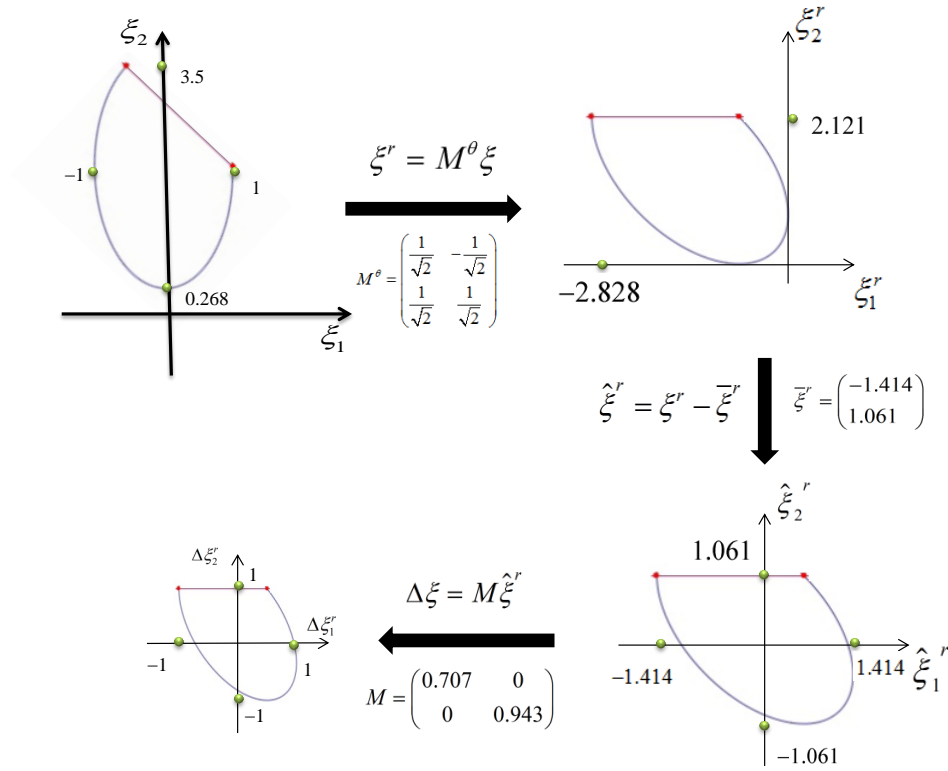


Figure 3.6: Uncertainty region rotation and normalization

Here, $\tilde{\xi}_\omega^r = (M^\theta)^{-1} \bar{\xi}_\omega^r$ and $\hat{M} = (M^\theta)^{-1} M^{-1} = \begin{bmatrix} 0.707 & -0.707 \\ 1.143 & 1.143 \end{bmatrix}$.

3.1.3 Benefit of Rotation of the Uncertainty Region

Figure 3.8 shows the optimal objective values of RSF-OE and RSF-UE for both rotated and un-rotated original uncertainty region cases, for up to 900 scenarios. It can be seen that, initially there are large differences between the optimal objective values of RSF-OE and RSF-UE (for both un-rotated and rotated original uncertainty regions), which indicates that, the numbers of scenarios are not sufficient to

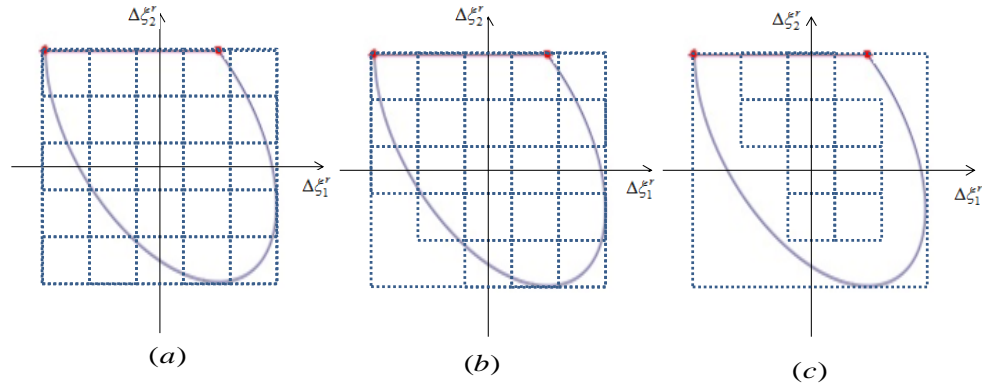


Figure 3.7: (a) Reference uncertainty region with 25 scenarios (b) Overestimation of uncertainty region (c) Underestimation of uncertainty region

completely represent the normalized uncertainty region. Figure 3.9 illustrates the optimal objective values of RSF-OE and RSF-UE for both rotated and un-rotated original uncertainty region cases from 2500 to 22500 scenarios. It can be seen that, with the increasing number of scenarios, the difference between the optimal objective values of RSF-OE and RSF-UE decreases (for both un-rotated and rotated original uncertainty regions), which indicates, when the number of scenarios are large, the normalized uncertainty region is better represented comparing to the situation where number of scenarios were low.

From Figure 3.9, the optimal objective values of RSF-OE and RSF-UE optimization problems converge at 22500 scenarios (within the relative tolerance of 1%), for un-rotated original uncertainty region case and the optimal objective value is 0.658.

The number of scenarios required for the convergence of RSF-OE and RSF-UE for the rotated original uncertainty region case are 16900 and the optimal objective value

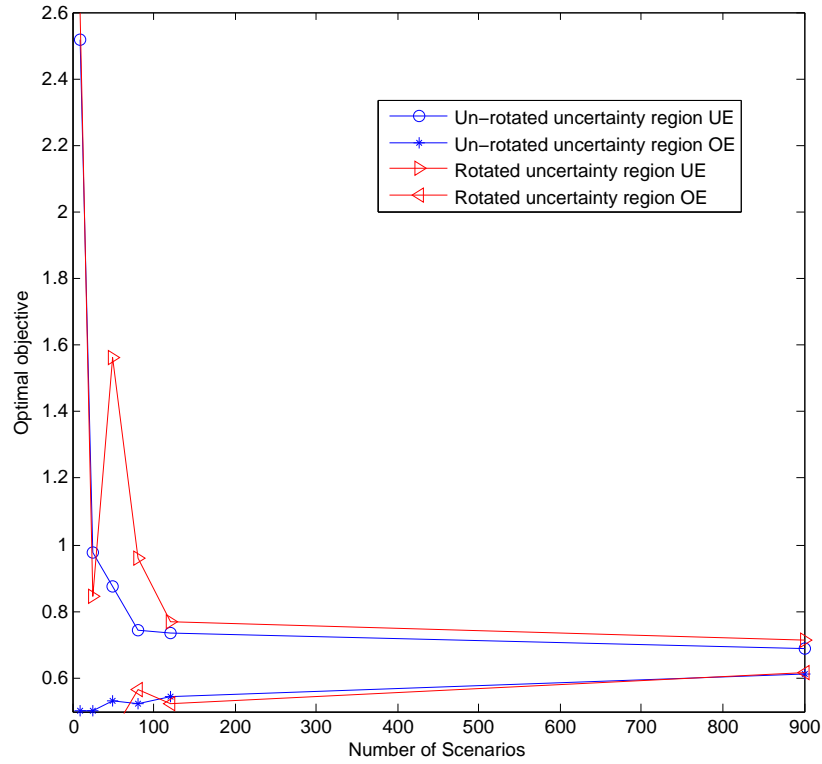


Figure 3.8: Convergence of RSF-OE and RSF-UE, Scenario 9-900

is 0.654. When original uncertainty region was rotated 45° counter clockwise, it took a less number of scenarios for the convergence of RSF-OE and RSF-UE comparing to the case of un-rotated original uncertainty region.

3.2 A Robust Scenario Approach for Data Driven Stochastic Programming

In the industry, the values of uncertain parameters over the previous time periods are often recorded, so the uncertainty region for the parameters can be reflected by the historic data. For example, if there are two uncertain parameters, the uncertainty

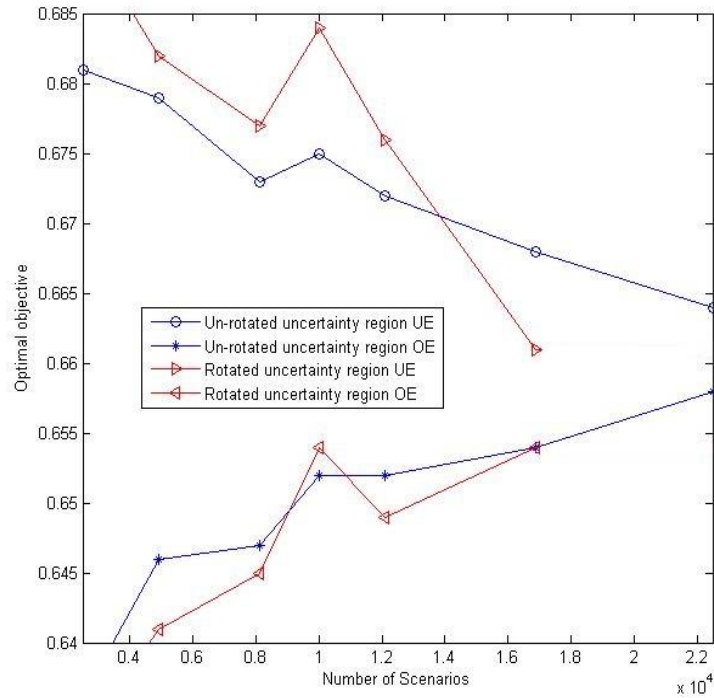


Figure 3.9: Convergence of RSF-OE and RSF-UE, Scenario 2500-22500

region can be reflected by a scatter plot with historical data, as shown in Figure 3.10. In this section we give some preliminary discussion regarding the solution of data driven stochastic programming problems via a robust scenario approach.

3.2.1 Normalization and Partitioning Process for Data Driven Stochastic Programming

We use the example in Figure 3.10 to demonstrate how the data set can be normalized, a bounded box can be constructed and partitioned to formulate a robust scenario formulation. First, find out the ranges of each uncertain parameter, and the mid points of the uncertain parameter ranges give the center of the data set, $\bar{\xi}$. Then

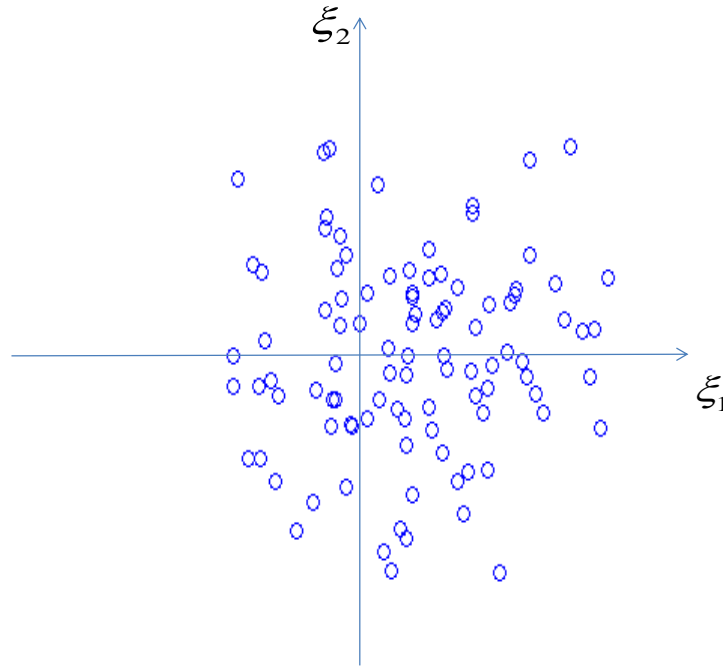


Figure 3.10: Representation of uncertain parameters using a data set

shift the center to the original by defining $\hat{\xi} = \xi - \bar{\xi}$.

Next, construct the smallest box that covers a given percentage, say 95%, of the data points. Enforce the ratio of the two edges of the box to be $\frac{\sigma_1}{\sigma_2}$, where σ_1 is the standard deviation of data set of ξ_1 and σ_2 is the standard deviation of data set of ξ_2 . The size of the box can be determined by a trial and error procedure. For example, one can start the procedure with a box that covers all the data points, and keep reducing the size of the box until only 95% of data points are covered. We call the box obtained at the end of this procedure be the reference box, and let the edges of the box be a and b .

After the reference box is constructed, define the normalized uncertain parameters

$\Delta\xi = M\hat{\xi}$, where

$$M = \begin{bmatrix} a & 0 \\ 0 & b \end{bmatrix}^{-1}.$$

Finally, the reference box can be readily partitioned into a number of box-shaped uncertainty subregions. Figure 3.11 illustrates the overall process, in which 9 box uncertainty subregions are generated at the end.

The probability of each uncertainty sub-region can be calculated according to the percentage of data points inside the sub-region.

$$P_\omega = \frac{n_\omega}{n}, \quad \omega = 1, \dots, s \tag{3.31}$$

Where,

P_ω = Probability of uncertainty subregion ω ,

n_ω = Number of data point inside uncertainty subregion ω ,

n = Total number of data point inside the reference box.

3.2.2 Case Study Results

The DuPont industrial chemical supply chain problem studied in Chapter 2 is again used for a case study. Here we assume that we do not know the distributions of the two uncertain parameters, but know some data points for the parameters that were previously recorded. We need to guarantee the feasibility of the solution with a confidence level of 95%. We consider three cases here, where 100, 500, and 1000 data points are available for stochastic programming. We sample the data points randomly

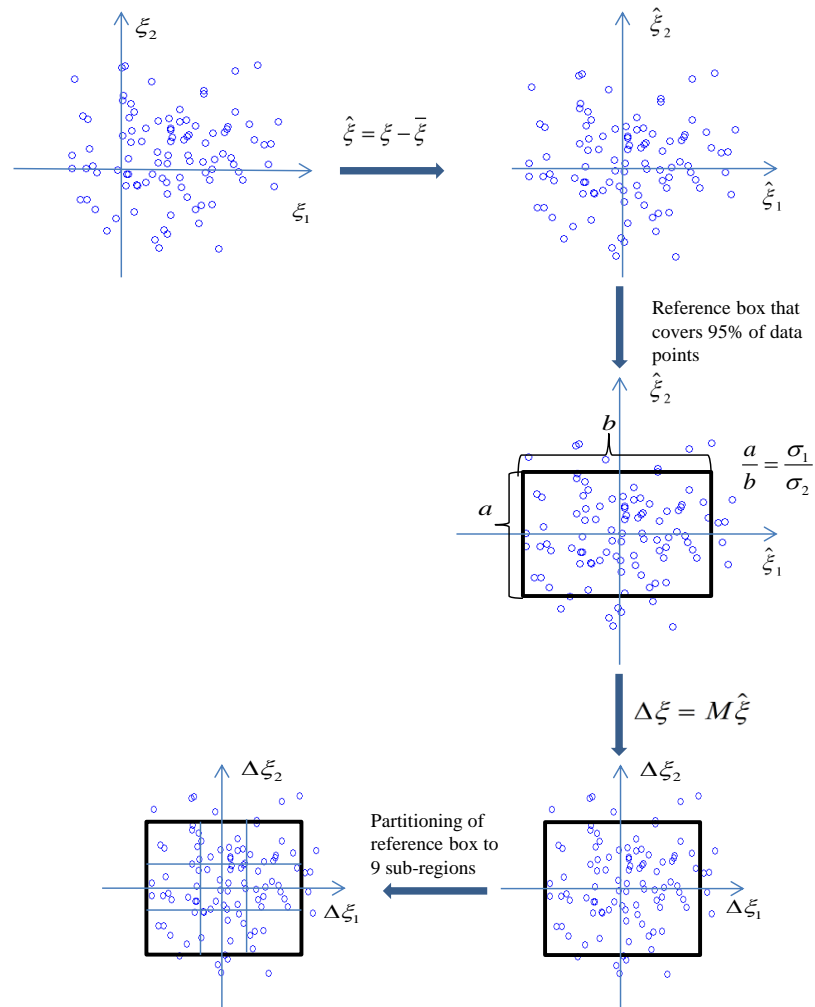


Figure 3.11: Normalization of original uncertainty region described as data set and partitioning of reference box

using the normal distributions considered in Chapter 2. The relative tolerance for solving all optimization problems was 1%.

Table 3.1 summarize the solution results for the three cases. The predicted expected profit refers to the optimal objective value of the robust scenario formulation, i.e., the profit predicted by the formulation. The achieved expected profit refers to

the expected profit that can be really achieved by the obtained solution, and the percentage of feasibility refers to the probability of the solution for satisfying all constraints. The achieved expected profit and the percentage of feasibility are estimated by first fixing the first-stage decision variables to the solution, and then calculate the average profit and the percentage of feasibility for 8000 randomly sampled uncertainty realizations. 8000 samples are enough for a good estimation, as the estimation results do not change when more samples are generated.

It can be seen from Table 3.1 that, when 100 and 500 samples were considered, the percentage of feasibility were below the desired confidence level of 95%. This is due to the fact that, the numbers of data points available for charactering the desired uncertainty region were not enough. When the number of available data points was 1000, the obtained solution achieved a satisfactory percentage of constraint satisfaction. On the other hand, the difference between the predicted and achieved expected profits deceases slightly with the increase of available samples, but the differences are all within the optimization tolerance.

Here we also give more details about the uncertainty region construction and

Table 3.1: Computational Results for the data driven robust scenario formulation with different numbers of available samples

Number of Samples	Predicted Expected Profit (\$)	Achieved Expected Profit (\$)	Percentage of Feasibility (%)
100	22654	22870	94.05
500	22704	22913	93.15
1000	22579	22786	98.76

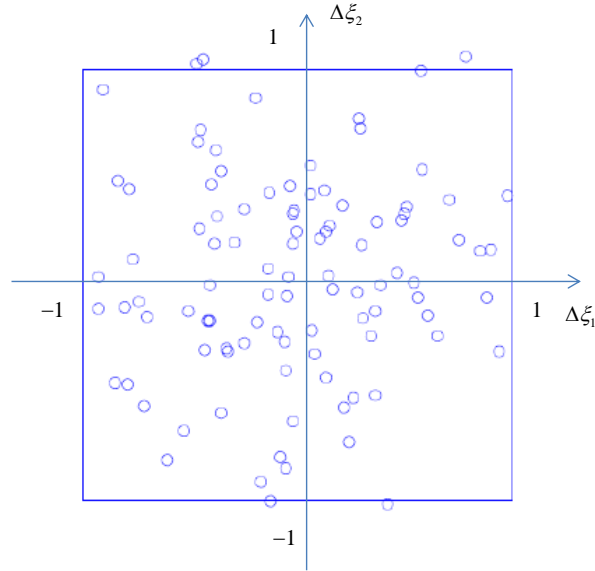


Figure 3.12: 100 samples and the corresponding reference uncertainty box

normalization. When there was 100 available samples,

$$\bar{\xi} = \begin{bmatrix} 0.8924 \\ 1.0119 \end{bmatrix}, \quad \frac{\sigma_1}{\sigma_2} = 0.967, \quad M^{-1} = \begin{bmatrix} 0.4 & 0 \\ 0 & 0.3 \end{bmatrix},$$

and the normalized data points and reference box are shown in Figure 3.12.

When there were 500 available samples,

$$\bar{\xi} = \begin{bmatrix} 1.0018 \\ 1.0047 \end{bmatrix}, \quad \frac{\sigma_1}{\sigma_2} = 1.054, \quad M^{-1} = \begin{bmatrix} 0.4 & 0 \\ 0 & 0.3 \end{bmatrix},$$

and the normalized data points and reference box are shown in Figure 3.13.

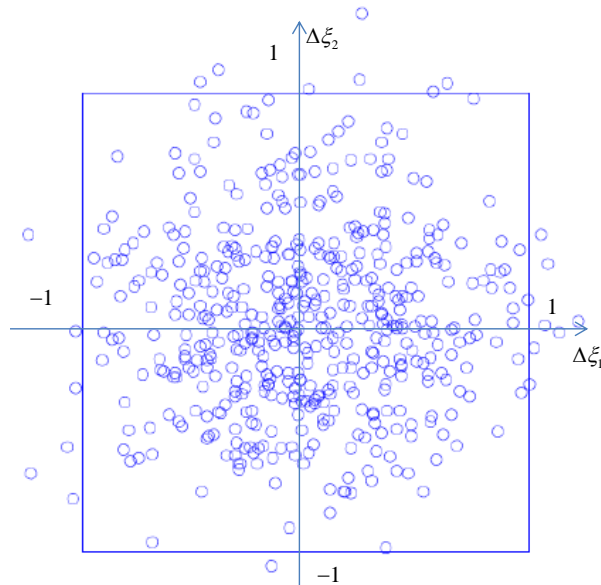


Figure 3.13: 500 samples and the corresponding reference uncertainty box

When there were 1000 available samples,

$$\bar{\xi} = \begin{bmatrix} 0.9986 \\ 1.0038 \end{bmatrix}, \quad \frac{\sigma_1}{\sigma_2} = 1.030, \quad M^{-1} = \begin{bmatrix} 0.4 & 0 \\ 0 & 0.3 \end{bmatrix},$$

and the normalized data points and reference box are shown in Figure 3.14.

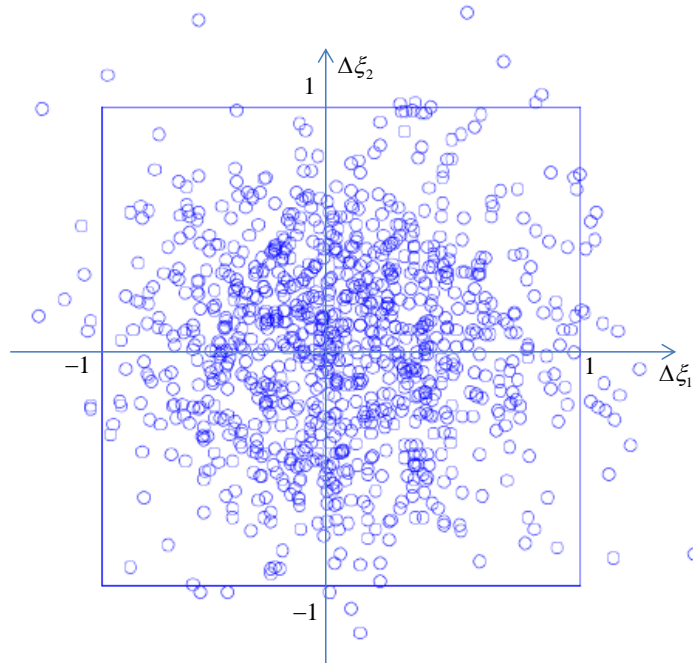


Figure 3.14: 1000 samples and the corresponding reference uncertainty box

Chapter 4

Nonlinear Robust Constraints and Decomposition Based Optimization

In Chapters 2 and 3, the normalized bounded uncertainty region is partitioned into box-shaped uncertainty subregions that are bounded with the infinity-norm. The resulting robust constraints can be reformulated into linear constraints and then the robust scenario formulation becomes a LP problem that can be solved efficiently with start-of-the-art LP solvers such as CPLEX. However, when the uncertainty subregions are bounded with nonlinear constraints, the resulting robust scenario formulation is a nonlinear programming (NLP) problem. When the size of the NLP problem is large, the solution time may be prohibitively large, even if the problem is convex. In this chapter, we discuss applying a decomposition-based optimization method for solving nonlinear robust scenario formulations and demonstrate the benefit of it through a case study.

4.1 Non-linear Robust Constraints

In Chapter 2, a new robust scenario approach was discussed where after normalization, the normalized uncertainty region was partitioned into box shaped uncertainty subregions, and over-estimation and under-estimation of the normalized uncertainty region are achieved with parts of the uncertainty subregions. When the normalized uncertainty region is partitioned into more uncertainty subregions with smaller sizes, the over- and under-estimated uncertainty region will converge. In principle, the normalized uncertainty region can be partitioned into uncertainty subregions with other shapes that are defined by nonlinear constraints (such as ellipsoids). Using uncertainty subregions defined by nonlinear constraints may be beneficial if (a) the normalized uncertainty region is shaped or structured in a way that, when nonlinearly constrained subregions are used, fewer number of uncertainty subregions are needed for the convergence; or (b) from the uncertainty distribution, nonlinearly constrained subregions can lead to more precise estimate of expected costs. Figure 4.1 compares the cases where the normalized uncertainty is approximated by box subregions and ellipsoidal subregions.

With nonlinearly constrained uncertainty subregions, the robust scenario formulation is nonlinear. For example, if circular uncertainty subregions are used, i.e., the subregions can be expressed as

$$\Xi_{\omega} = \{\Delta\xi_{\omega} \in \mathbb{R}^2 : \|\Delta\xi_{\omega} - \Delta\bar{\xi}_{\omega}\|_2 \leq \delta_{\omega}\}, \quad \omega = 1, \dots, s.$$

Here, $(\Delta\bar{\xi}_{\omega})$ indicates the center of each circular uncertainty sub-regions. In this case, the robust scenario formulation can be written as:

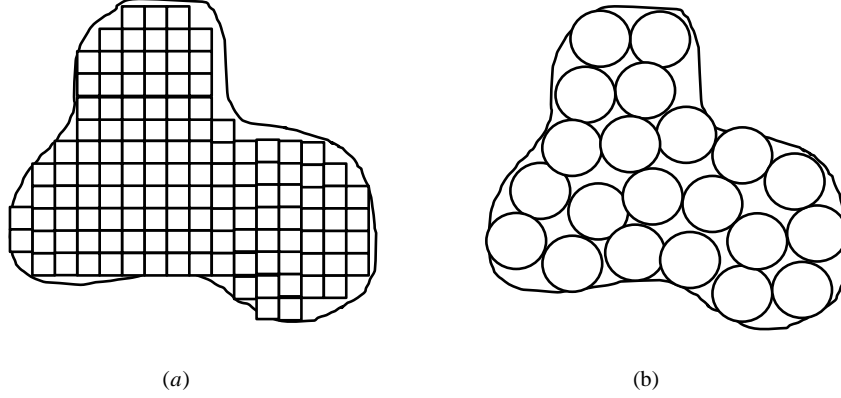


Figure 4.1: (a) Uncertainty sub-regions are bounded with the infinity-norm (b) Uncertainty sub-regions are bounded with the 2-norm

Formulation (RS-norm-2)

$$\min_{\substack{x \in X \\ U_1, \dots, U_s \\ v_1, \dots, v_s}} c^T x + \sum_{\omega=1}^s P_{\omega}(\alpha_q \bar{\xi}_{\omega} + \beta_q)^T (U_{\omega} \bar{\xi}_{\omega} + v_{\omega}) \quad (4.1)$$

$$s.t. \quad Ax \leq b, \quad (4.2)$$

$$\beta_{t,i}^T x + w_i^T v_{\omega} + (x^T \alpha_{t,i} + w_i^T U_{\omega}) \bar{\xi}_{\omega} + \delta_{\omega} \|(x^T \alpha_{t,i} + w_i^T U_{\omega}) M^{-1}\|_2 \leq 0, \quad (4.3)$$

$$i = 1, \dots, m, \quad \omega = 1, \dots, s.$$

The above problem has a L-shaped structure as shown in Figure 1.2 in Chapter 1, and it is a second-order cone programming (SOCP) problem which is convex [57]. Therefore, this problem can be solved via generalized Benders decomposition that is introduced in Chapter 1, which can be much more efficient than any classical convex optimization method, especially when the problem size is large.

4.2 Generalized Benders Decomposition Algorithm

This section describes the generalized Benders decomposition algorithm for solving the robust scenario problem. Consider the following form of problem, which the robust scenario problem can be written into:

Problem (P)

$$\min_{x, y_1, \dots, y_s} \sum_{\omega=1}^s (c_{x,\omega}^T x + c_{y,\omega}^T y_\omega) \quad (4.4)$$

$$s.t. \quad A_\omega x + g_\omega(y_\omega) \leq 0 \quad (4.5)$$

$$x \in X \quad (4.6)$$

$$y_\omega \in Y_\omega, \quad \omega = 1, \dots, s \quad (4.7)$$

Here X is a nonempty compact set, $g_\omega(y_\omega)$ is a convex function of y_ω , and Y_ω is a convex set, for all the scenarios ($\omega = 1, \dots, s$) used in the optimization problem. In generalized Benders decomposition, Problem (P) is solved by solving a number of subproblems iteratively, namely, primal problem, feasibility problem, relaxed master problem, and feasibility relaxed master problem.

The primal problem is constructed by fixing $x = x_k$ at the k^{th} iteration of generalized Benders decomposition algorithm, and it can be decomposed into s subproblems, each in the following form:

Problem (PP_ω^k)

$$obj_{PP_\omega^k} = \min_{x, y_1, \dots, y_s} \sum_{\omega=1}^s (c_{x,\omega}^T x + c_{y,\omega}^T y_\omega) \quad (4.8)$$

$$s.t. \quad A_\omega x^k + g_\omega(y_\omega) \leq 0 \quad (4.9)$$

$$y_\omega \in Y_\omega \quad (4.10)$$

From the formulation it can be seen that, Problem (PP_ω^k) is easy to solve comparing to the problem (P) . The reason for that is, it only involves second stage decision variables as x^k is fixed to a constant value in this problem and also the size of the problem (PP_ω^k) is not dependent on the number of scenarios involved in the original problem (P) .

There is a possibility that problem (PP_ω^k) might be infeasible. In that case a feasibility problem will be solved and that too can be decomposed into s sub-problems in the following form.

Problem (FP_ω^k)

$$obj_{FP_\omega^k} = \min_{y_\omega, G_\omega} \|G_\omega\|_1 \quad (4.11)$$

$$s.t. \quad A_\omega x^k + g_\omega(y_\omega) \leq 0 \quad (4.12)$$

$$y_\omega \in Y_\omega \quad (4.13)$$

$$z_\omega \geq 0 \quad (4.14)$$

Here, $\|\cdot\|_1$ denotes the 1-norm and G_ω is slack variable. In the first iteration, x is

chosen as any arbitrary value. In the subsequent iterations, the value of x is generated by solving another optimization problem, named, relaxed master problem.

Problem (RMP^k)

$$\min_{x,\eta} \eta \tag{4.15}$$

$$s.t. \quad \eta \geq \sum_{\omega=1}^s obj_{PP_\omega^j} + \left[\sum_{\omega=1}^s (c_{x,\omega}^T + (\lambda_\omega^j) A_\omega) \right] (x - x^j), \quad \forall j \in T^k \tag{4.16}$$

$$0 \geq \sum_{\omega=1}^s obj_{FP_\omega^j} + \left[\sum_{\omega=1}^s (\mu_\omega^i)^T A_\omega \right] (x - x^j), \quad \forall i \in R^k \tag{4.17}$$

$$x \in X \tag{4.18}$$

Here the index set can be defined as following.

$$T^k = \{j \in \{1, \dots, k\} : \text{Problem (P) is feasible for } x = x^j\}$$

$$R^k = \{i \in \{1, \dots, k\} : \text{Problem (P) is infeasible for } x = x^i\}$$

Here λ_ω^j indicates the Lagrangian multipliers for Equations (4.9) of Problem (PP_ω^k) and μ_ω^j indicates the Lagrangian multipliers for Equations (4.12) of Problem (FP_ω^k). Equations (4.16), which are obtained from the solution of primal sub-problems, are known as optimality cut. Equations (4.17), which are obtained from the solution of the feasibility sub-problems, are known as feasibility cut. As Problem (RMP^k) contains only first stage decision variable x and it's size is independent of the number of scenarios, hence Problem (RMP^k) is much easier to solve comparing to the original Problem (P). At the initial iterations, the set T^k might be empty because of

the possible infeasibility of Problem (P) for all the chosen value of x . Because of this, Problem (RMP^k) may be unbounded at initial few iterations. For these iterations, feasibility relaxed master problem is solved.

Problem ($FRMP^k$)

$$\min_x \|x\|_1 \tag{4.19}$$

$$s.t. \quad 0 \geq \sum_{\omega=1}^s obj_{FP_{\omega}^j} + \left[\sum_{\omega=1}^s (\mu_{\omega}^i)^T A_{\omega} \right] (x - x^j), \quad \forall i \in R^k \tag{4.20}$$

$$x \in X \tag{4.21}$$

Generalized Benders decomposition solves the primal problem (PP_{ω}^k) or Feasibility problem (FP_{ω}^k) and Relaxed Master Problem (RMP^k) or Feasibility Relaxed Master Problem ($FRMP^k$) in an iterative manner. The solutions of Problem (PP_{ω}^k) provides a sequence of upper bounds for the Problem (P) and the solutions of Problem (RMP^k) provides a sequence of lower bounds for the Problem (P). When the upper bound and lower bound converges then an optimal solution is obtained. The generalized benders decomposition algorithm is given below.

1. **Initiation:** Set a sufficiently large upper bound, $UBD = M$ and a large lower bound, $LBD = -M$. Here, $M > 0$, tolerance limit, $\epsilon > 0$, iteration counter, $k = 1$ and $T^0 = R^0 = \emptyset$. The initial value of x is selected as x_0^1 .

2. **Primal Problem:** Primal Problem (PP_{ω}^k) is solved for all the scenarios, $\omega = 1, \dots, s$.

3. **Feasible Primal:** If Problem (PP_ω^k) is feasible for all the scenarios, $\omega = 1, \dots, s$, then an optimal solution y_ω^k , the associated Lagrange multipliers λ_ω^k and the optimal objective value $obj_{PP_\omega^k}$ can be obtained. Set $T^k = T^{k-1} \cup \{k\}$, $R^k = R^{k-1}$, and add an optimality cut to the relaxed master problem. If $\sum_{\omega=1}^s obj_{PP_\omega^k} < UBD$, then set $UBD = \sum_{\omega=1}^s$ and $(x^*, y_1^*, \dots, y_s^*) = (x^k, y_1^k, \dots, y_s^k)$.

4. **Infeasible Primal:** If Problem (PP_ω^k) is infeasible for some ω , then solve (FP_ω^k) and obtain Lagrange multipliers μ_ω^k and the optimal objective value $obj_{FP_\omega^k}$. Set $R^k = R^{k-1} \cup \{k\}$, $T = T^{k-1}$, and add a feasibility cut to the relaxed master problem.

5. **Relaxed Master problem:**

- (a) If $T^k = \emptyset$, solve Problem $(FRMP^k)$. If the problem is feasible and an optimal solution \hat{x} is obtained, set $x^{k+1} = \hat{x}$.
- (b) If $T^k \neq \emptyset$, solve RMP^k . If the problem is feasible and an optimal solution $(\hat{x}, \hat{\eta})$ is obtained, set $x^{k+1} = \hat{x}$ and $LBD = \hat{\eta}$.

6. **Termination Check:** If Problem $(FRMP^k)$ or (RMP^k) is infeasible, terminate and Problem (P) is infeasible. If $UBD \leq LBD + \epsilon$, terminate and $(x^*, y_1^*, \dots, y_s^*)$ is an optimal solution of Problem (P); otherwise, set $k = k + 1$ and go to step 2.

4.3 Computational Study

The goal of the case study is to apply the generalized Benders Decomposition algorithm to solve a nonlinear robust scenario formulation for the DuPont industrial supply chain problem. This formulation is modified from the one studied in Chapter 2. In this formulation, first-stage decisions (i.e., the capacities of the processing plants) are integer rather than continuous variables, and the impurity constraints are removed to avoid some numerical problems. The full formulation and the subproblems that are to be solved in generalized Benders decomposition are given in Appendix C. The dual norm functions involved in the subproblems are assumed to be the 2-norm (i.e., the uncertainty subregions are assumed to be ellipsoidal). This assumption is merely to yield nonlinear robust constraints for the computational study, and it does not mean that the ellipsoidal uncertainty subregions are better than box uncertainty subregions in terms of approximating the original uncertainty region.

All the case study problems and subproblems solved in generalized Benders decomposition algorithm were modeled in GAMS 24.3.1 and the main algorithm of Benders decomposition was implemented in MATLAB 2014a. GDX facility, provided by MTLAB, was used to exchange operational data of the case study between GAMS and MATLAB. Primal problem (PP_{ω}^k) and feasibility problem (FP_{ω}^k) was solved using MOSEK 7.1. Relaxed master problem (RMP^k) and Feasibility relaxed master problem ($FRMP^k$) was solved in CPLEX 12.4. A machine having 3.40 GHz CPU, 8 GB RAM and Linux operating system was used to solve all the sub-problems. A relative termination criterion of 1% was used for solving the supply chain optimization problem.

Table 4.1: Comparison of computational times for different numbers of scenarios

Scenarios	MOSEK time (s)	GBD total time (s)	GBD solving time (s)
1	1.80	11.03	3.08
9	19.57	14.85	5.48
25	256.46	194.58	67.54
49	424.23	364.87	147.31
81	564.47	487.79	189.54
121	387.92	346.12	126.48
169	641.29	488.31	154.73

The computational results for the robust scenario are given in Table 4.1. MOSEK time refers to the CPU time for MOSEK to solve the robust scenario problem directly. GBD solver time refers to the CPU for generalized Benders decomposition to solve all subproblems before the convergence. GBD total time refers to the wall time for generalized Benders decomposition to solve all subproblems before the convergence, including the GBD solving time and the computing overhead.

It can be seen from Table 4.1 that, MOSEK solution time is much faster than Benders decomposition for the case where only one scenario was involved. With the increasing number of scenarios, MOSEK solution time increased rapidly. As a result, when the number of scenarios was greater than 1, generalized Benders decomposition requires less time than MOSEK to solve the problem. It can also be seen that, solving time for generalized Benders decomposition is significantly shorter than the total time for executing the generalized Benders decomposition. This significant difference is due to the data exchange from GAMS to MATLAB through GDX facility. More

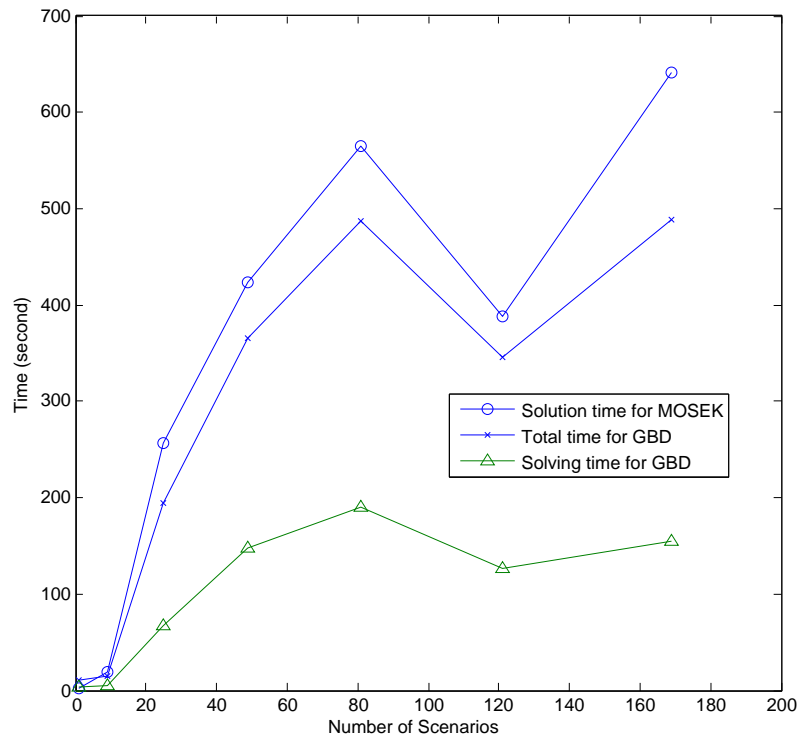


Figure 4.2: Comparison of computational times

efficient implementation of Benders decomposition, e.g. using a unified programming language/platform such as C++ and Python, can reduce the time required for data exchange and therefore reduce the total time required. The computational results in the table are also visualized in Figure 4.2. With the increasing number of scenarios, the problem size also increases, as a result, it should take more time to solve GBD algorithm when problem size is large. But, when the number of scenarios are 121, it took less time for GBD to solve the problem. The main reason behind it is less number of iterations to solve GBD when number of scenarios are 121.

Table 4.2 provides more details of the computational study results for different

Table 4.2: Other computational results

Scenarios	1	9	25	49	81	121	169
GBD Iterations	8	12	23	38	48	29	35
PP solving time	1.9	2.54	29.28	59.27	97.85	42.65	54.78
FP solving time	1	1.12	30.42	59.98	76.9	83.51	68.92
RMP solving time	0.176	0.006	0.232	0.085	0.033	0.058	0.048
FRMP solving time	0	0	0.025	0.058	0.029	0.263	0.182
Constraints	13850	126411	290750	512270	955311	1342970	18996770
Continuous variables	18531	166731	389031	685431	1278231	1796931	2537931
Integer Variables	5	5	5	5	5	5	5

numbers of scenarios, including the problem size, number of iterations, times for different subproblems.

Chapter 5

Summary and Conclusions

A general approach is proposed in this thesis to solve two-stage stochastic programming with recourse that comes from strategic supply chain optimization problem where uncertainty region is bounded with the p -norm. The synergy of the classical scenario approach, which commonly provides good optimality and the robust approach, that can guarantee feasibility of a problem, named robust scenario formulation, was used in this thesis to solve the two-stage stochastic programming with recourse. In this general approach, after the normalization of uncertainty region bounded with the p -norm, the normalized uncertainty region can be covered with a reference uncertainty region which is bounded with the infinity-norm. That reference uncertainty region was divided into box shaped subregions. A optimization problem was solved where the original p -norm bounded uncertainty region was overestimated with boxes. The criterion of overestimation was, if any one extreme points of an uncertainty subregion was inside the original p -norm bounded uncertainty region, then that uncertainty sub-region was included in the optimization problem. Another optimization problem was solved where the original p -norm bounded uncertainty region was underestimated

with boxes. The criterion of underestimation was, if all extreme points of an uncertainty subregion was inside the original p-norm bounded uncertainty region, then that uncertainty sub-region was included in the optimization problem. When the optimum objective of both of the optimization problems were converged to a constant within a given tolerance then it was assumed that, enough partitioning was done to represent the uncertainty region bounded with the p-norm. Since the rectangular uncertainty sub-regions were described by the infinity-norm, the optimization problems to be solved had constraints involving the 1-norm, and these constraints were transformed into linear constraints. A new approach was introduced to reform the constraint involving 1-norm which prevent the exponential growth of constraints comparing to the procedure applied in the literature [36]. Here in the new approach, the growth rate of constraints was linear. A case study provided by DuPont successfully demonstrated all the concepts mentioned above where profit was maximized by satisfying minimum demand of final products in the market.

To verify the optimality of the optimal profit obtained via the robust scenario approach, Monte Carlo simulation was conducted. In Monte Carlo simulation, different number of samples of uncertain parameters were used to calculate the expected profit. With very large number of samples, the calculated expected profit was higher than the predicted profit from the model. To verify the feasibility of the solution obtained via the robust scenario approach, again Monte Carlo simulation was conducted. In Monte Carlo simulation, different number of samples of uncertain parameters were used to calculate the percentage of feasibility. For each case, the percentage of the samples for which the solution was feasible, calculated. With very large number of

samples, the calculated feasible percentage was greater than the initial target of 95%.

When the uncertainty region had any bounded arbitrary shape then the approach of normalization, underestimation of uncertainty region, overestimation of uncertainty region was applied. In that case, a nominal objective function was used. In this thesis, an example was showed in that regard where uncertainty region has arbitrary bounded shape. Rotation of uncertainty region might have influence reducing the number of scenarios required to represent the uncertainty region. Another example was showed where the same uncertainty region was rotated to 45^0 counter clockwise and then the similar approach of normalization, underestimation of uncertainty region, overestimation of uncertainty region was be applied. From the result it was evident that, rotation of uncertainty region reduced the number of scenarios required to converge to the optimal solution.

In industrial practice, it is more practical to represent uncertain parameter with scattered data point instead of a given uncertainty region. In that case a new approach was proposed named data driven robust scenario formulation. In that approach, after rejecting the outliers, a reference box, bounded with the infinity-norm, was chosen which covered 95% of the data points. Then, after normalization, the reference uncertainty box was partitioned into smaller uncertainty sub-regions of box shape. The exclusion criterion of an uncertainty sub-region form the optimization problem was, it must contain atleast one data point. The expected value of the uncertainty sub-region in that case was the average of all the data point inside the uncertainty sub-region. DuPont industrial chemical supply chain case study was also chosen to demonstrate

the effectiveness of the approach. In that case study, different number of samples for uncertain parameters (100, 500 and 1000) were used. When the number of samples were 100 and 500, the achieved expected profit was higher than the predicted expected profit but the percentage of feasible cases were less than the desired target of 95%. It indicates less number of samples were considered to represent uncertain parameters. When the number of samples for uncertain parameters were 1000, the achieved expected profit was also higher than the predicted expected profit. This time the percentage of feasibility was greater than the desired target of 95%. It indicates enough samples were considered to completely represent uncertainty region.

Previously, for the p -norm bounded uncertainty region, it was assumed that, the uncertainty subregions were bounded with the infinity-norm resulting in the linear robust constraint as dual norm of the infinity-norm is the 1-norm. But if it is assumed that, uncertainty subregions are bounded with the 2-norm then resulting robust constraint will be non-linear as dual norm of the 2-norm is the 2-norm itself. In this thesis, generalized Benders decomposition algorithm was studied for simplified DuPont industrial chemical supply chain problem where the uncertainty subregions were bounded with the 2-norm. It was found from the DuPont industrial chemical supply chain case study that, with the increasing number of scenarios, MOSEK solution time increased. As a result, when the number of scenarios were greater than 1, generalized Benders decomposition required lesser time than MOSEK to solve the problem.

Future work of this thesis may involve to find out a general framework to determine the best rotation angle of original uncertainty region so that minimum screening of uncertainty sub-regions from reference uncertainty region is required. Also, instead of using box shaped uncertainty sub-regions, p-norm bounded uncertainty subregion or a combination of box shaped uncertainty subregion and p-norm bounded uncertainty subregion can be considered. When uncertainty subregions are bounded with the p-norm, then that uncertainty subregions can be mapped into spherical coordinate system, resulting in a box-shaped uncertainty subregion. This procedure may lead to non-linear relationship between, q_ω and ξ_ω , $t_{i,\omega}$ and ξ_ω , y_ω and ξ_ω . In that case, tractable reformulation of robust constraint in Formulation (RS) is currently not known and determining the tractable reformulation of robust constraint in that particular case can be considered as future research direction. In future, there may be a requirement to transfer the single period optimization problem to multi-period optimization problem for better operational performance. In that case the single period optimization problem can be transformed into multi-period optimization problem.

Bibliography

- [1] MOSEK Modeling Manual. pages 1–98, 2014.
- [2] J. Geunes and P. M. Pardalos. *Supply Chain optimization*. Springer, New York, 2005.
- [3] Gabriela P. Ribas, S. Hamacher, and A. Street. Optimization under uncertainty of the integrated oil supply chain using stochastic and robust programming. *International Transaction in Operation Research*, 17(6):777–796, 2010.
- [4] H. M. S. Lababidi, M.A. Ahmed, and I. M. Alatiqi. Optimizing the supply chain of a petrochemical company under uncertain operating and economic conditions. *Industrial and Engineering Chemistry*, 43(9):63 – 73, 2004.
- [5] B. E. Wafa, H. M. S. Lababidi, and I. M. Alatiqi. Supply chain optimization of petroleum organization under uncertainty in market demands and prices. *European Journal of Operation Research*, 189(3):822 – 840, 2008.
- [6] A. Heungjo, W. E. Wilhelm, and S.W. Searcy. Biofuel and petroleum-based fuel supply chain research: A literature review. *Biomass and Energy*, 35(9):3763–3774, 2011.

-
- [7] X. Li, E. Armagan, A. Tomasgard, and P.I. Barton. Stochastic pooling problem for natural gas production network design and operation under uncertainty. *AIChE Journal*, 57(8):2120–2135, 2011.
- [8] M. Lalmazlounian, K. Y. Wong, K. Govindan, and D. Kannan. A robust optimization model for agile and build-to-order supply chain planning under uncertainties. *Annals of Operations Research*, 5(1):1–37, 2013.
- [9] S. Barker, E. Audsley, and D. Parsons. A two-stage stochastic programming with recourse model for determining robust planting plans in horticulture. *The Journal of Operation Research Society*, 51(1):83–89, 2014.
- [10] N. Shah. Pharmaceutical supply chains: key issues and strategies for optimisation. *Computers and Chemical Engineering*, 28(6-7):929–941, 2004.
- [11] L. Papageorgiou, G. Rotstein, and N. Shah. A two-stage stochastic programming with recourse model for determining robust planting plans in horticulture. *Industrial and Engineering Chemistry Research*, 40(1):275–286, 2001.
- [12] G. Gatica, L. Papageorgiou, and N. Shah. Capacity planning under uncertainty for the pharmaceutical industry. *Trans IChemE*, 81(July):665–678, 2003.
- [13] R. Sausa, S. Liu, and L. Papageorgiou. Global supply chain planning for pharmaceuticals. *Chemical Engineering Research and Design*, 89(11):2396–2409, 2011.
- [14] O. Akgul, N. Shah, and L. Papageorgiou. Design under uncertainty of hydrocarbon biorefinery supply chains: Multiobjective stochastic programming models, decomposition algorithm, and a comparison between cvar and downside risk. *AIChE Journal*, 58(7):101–114, 2012.

-
- [15] H. An, W. Wilhelm, and S. Searcy. Biofuel and petroleum-based fuel supply chain research: A literature review. *Biomass and Bioenergy*, 35(9):3763–3774, 2011.
- [16] C. Chen and Y. Fan. Bioethanol supply chain system planning under supply and demand uncertainties. *Transportation Research Part E: Logistics and Transportation Review*, 48(1):150–164, 2012.
- [17] B. Gebreslassie, Y. Yao, and F. You. Design under uncertainty of hydrocarbon biorefinery supply chains : Multiobjective stochastic programming models , decomposition algorithm , and a comparison between cvar and downside risk. *AIChE Journal*, 58(7):2155–2179, 2012.
- [18] M. Dal-mas, S. Giarola, S. Zamboni, A. Bezzo, and Fabrizio. Strategic design and investment capacity planning of the ethanol supply chain under price uncertainty. *Biomass and Bioenergy*, 35(5):2059–2071, 2011.
- [19] W. Chen, Y. Li, and G. Huang. A two-stage inexact-stochastic programming model for planning carbon dioxide emission trading under uncertainty. *Applied Energy*, 87(3):1033–1047, 2010.
- [20] S. Liu, J. Jian, and Y. Wang. A robust optimization approach to wind farm diversification. *International Journal of Electrical Power and Energy Systems*, 53(1):409–415, 2013.
- [21] M. Dal-mas, S. Giarola, S. Zamboni, A. Bezzo, and Fabrizio. Stochastic optimization of medical supply location and distribution in disaster management. *International Journal of Production Economics*, 126(1):76–84, 2010.

- [22] G. Zhu, J. Bird, and G. Yu. A two-stage stochastic programming approach for project planning with uncertain activity durations. *Journal of Scheduling*, 10(3):167–180, 2007.
- [23] F. Bobonneau, J. Vial, and R. Apparigliato. Uncertainty and environmental decision making. *Biomass and Bioenergy*, 35(5):2059–2071, 2011.
- [24] G. Guille and I. Grossmann. Optimal design and planning of sustainable chemical supply chains under uncertainty. *AIChE Journal*, 55(1):99–121, 2009.
- [25] A. Nikolopoulou and M.G. Ierapetritou. Optimal design of sustainable chemical process and supply chains: A review. *Computers and Chemical Engineering*, 44(1):94–109, 2012.
- [26] L. G. Papageorgiou. Supply chain optimisation for the process industries: Advances and opportunities. *Computers and Chemical Engineering*, 33(1):1931–1938, 2009.
- [27] L. E. Grossmann and G. Guillen-Gosalbez. Scope for the application of mathematical programming techniques in the synthesis and planning of sustainable processes. *Computers and Chemical Engineering*, 34(1):1365–1376, 2010.
- [28] A. Gupta and C. Manaras. Managing demand uncertainty in supply chain planning. *Computers and Chemical Engineering*, 27(8-9):1219–1227, 2003.
- [29] M. Dal-mas, S. Giarola, S. Zamboni, A. Bezzo, and Fabrizio. Strategic design and investment capacity planning of the ethanol supply chain under price uncertainty. *Biomass and Bioenergy*, 35(5):2059–2071, 2011.

-
- [30] N. B. Sahinidis. Optimization under uncertainty: State-of-the-art opportunities. *Computers and Chemical Engineering*, 28(1):971–983, 2004.
- [31] L. E. Grossmann and G. Guillen-Gosalbez. Multi-stage stochastic optimization applied to energy planning. *Mathematical Programming*, 52(1):359–375, 1991.
- [32] K. Huang. *Multi-stage stochastic programming models for production planning*. PhD thesis, Georgia Institute of Technology, 2005.
- [33] J. R. Birge and F. Louveaux. *Introduction to Stochastic Programming*. Springer, New York, 1997.
- [34] A. Bental, A. Goryashko, E. Guslitzer, and A. Nemirovski. Adjustable robust solutions of uncertain linear programs. *Mathematical Programming*, 99:351–376, 2004.
- [35] A. Bental and A. Nemirovski. Robust convex optimization. *Mathematics of Operations Research*, 23(4):769–805, 1998.
- [36] K. Mclean and X. Li. Robust scenario formulations for strategic supply chain optimization under uncertainty. *Industrial and Engineering Chemistry Research*, 52(16):5721–5734, 2013.
- [37] A. Bental and A. Nemirovski. Robust solutions of linear programming problems contaminated with uncertain data. *Mathematical Programming*, 88:411–424, 2000.
- [38] A. Bental and A. Nemirovski. A. robust solutions of uncertain linear programs. *Operation Research letter*, 25(1):1–13, 1999.

- [39] L. El-Ghauri and H. Lebert. Robust solutions to least-squares problems with uncertain data. *SIAM Journal of Matrix Analysis Application*, 18(4):1035–1064, 1997.
- [40] L. El-Ghauri, F. Oustry, and H. Lebert. Robust solutions to uncertain semi-definite programs. *Journal of Optimization Theory and Applications*, 9:32–52, 1998.
- [41] Z. Li, R. Ding, and C. A. Floudas. A comparative theoretical and computational study on robust counterpart optimization: i. robust linear optimization and robust mixed integer linear optimization. *Industrial and Engineering Chemistry Research*, 50(1):10567–10603, 2011.
- [42] Z. Li and C. A. Floudas. A comparative theoretical and computational study on robust counterpart optimization: iii. improving the quality of robust solutions. *Industrial and Engineering Chemistry Research*, 53(1):13112–13124, 2014.
- [43] J. F. Benders. Partitioning procedures for solving mixed-variables programming problems. *Numerische Mathematik*, 4(1):238–252, 1962.
- [44] A. M. Geoffrion. Generalized benders decomposition. *Journal of Optimization Theory and Applications*, 10(4):237–260, 1972.
- [45] User’s manual for cplex. *IBM ILOG CPLEX V12.1*, pages 1–314, 2015.
- [46] D. Bertsimas, D. Pachamanova, and M. Sim. Robust linear optimization under general norms. *Operation Research Letters*, 32(1):510–516, 2004.
- [47] S. Boyd and L. Vandenberghe. *Convex Optimization*. Cambridge University Press, Edinburgh, 2004.

-
- [48] L. A. Waller and C. A. Gotway. *Applied Spatial Statistics for Public Health Data*. John Willey and Sons Inc, New Jersey, 2004.
- [49] H. Anton and C. Rorrers. *Elementary Linear Algebra*. John Willey and Sons Inc, New York, 2010.
- [50] K. McLean. Novel formulation and decomposition-based optimization for strategic supply chain management under uncertainty. Master’s thesis, Queen’s University, Kingston, February 2014.
- [51] N. C. Giri. *Multivariate Statistical Inference*. Academic Press, New York, 1977.
- [52] R. E. Rosenthal. GAMS - A User’s Guide. pages 1–251, 2006.
- [53] X. Chen, M. Sim, and P. Sun. A robust optimization perspective on stochastic programming. *Operation Research*, 55(6):1058–1071, 2007.
- [54] C. Mukherjee, H. White, and M. Wyuts. *Econometrics and Data Analysis for Developing Countries*. Routledge, New York, 1998.
- [55] J. W. Blankenship and J. E. Falk. Infinitely constrained optimization problems. *Journal of Optimization Theory and Application*, 19(1):261–281, 1976.
- [56] R. Hettich and K. O. Kortanek. Semi-infinite programming: Theory, methods, and applications. *SIAM Review*, 35(3):380–429, 1993.
- [57] M. S. Lobo, L. Vandenberghe, S. Boyd, and H. Lebret. Application of second order cone programming. *Linear Algebra and its Application*, 284(6):193–228, 1998.

Appendix A

DuPont Industrial Chemical Supply Chain

From the original model developed in the literature [50], turn down limit and waste limit constraints are excluded as those constraints are redundant and has no effect in optimal solution of the optimization problem.

A.1 Nomenclature and Symbols for DuPont Supply Chain network

Related Nomenclature and Symbol for DuPont Industrial Chemical Supply Chain problem is given below.

Different sets used in the DuPont Industrial Chemical Supply Chain problem is given below.

$i \in I = \{1, \dots, 5\}$ - Plants

$j \in J = \{1, \dots, 5\}$ - Regional warehouses

$k \in K = \{1, 5\}$ - Regional markets

$s \in \omega$ Scenarios

$u \in U = \{1, \dots, 55\}$ - PRM grades

$v \in V = \{1, \dots, 23\}$ - FP grades

$w \in W = \{1, \dots, 41\}$ Impurities

$(i, j) \in \omega$ - FP shipment routes for plants to regional warehouses

$(i, k) \in \Theta$ - FP shipment routes for plants to regional markets

$(i, v) \in \Psi$ - FP grades available for production at plant i

$(j, k) \in \Pi$ - FP shipment routes for regional warehouses to regional markets

Different parameters for the DuPont Supply Chain network is given below

$a_i^{avg,FP}$ - Average additive factor for plant i

b_i^{td} - Intercept related to minimum turn down for plant i

b_i^{wl} - Intercept related to waste limit for plant i

C^{pen} - Penalty cost for not meeting demand requirements, $\$/t$

C^{cap} - Capacity cost, $\$/t$

C_i^{fix} - Fixed cost for plant i , $\$MM$

C_I^{var} - Other variable costs for plant i , $\$/t$

$C_{i,k}^{fr,FP,PD}$ - Freight cost of FP from plant i to market k , $\$/t$

$C_{i,j}^{fr,FP,PW}$ - Freight cost of FP from plant i to regional warehouse j , $\$/t$

$C_{j,k}^{fr,FP,WD}$ - Freight cost of FP from regional warehouse j to market k , $\$/t$

C_i^{PI} - Plant i on-site inventory cost, $\$/t$

C_j^{WI} - Regional warehouse j inventory cost, $\$/t$

$C_{i,u}^{PRM}$ - Cost of PRM grade u for plant i , $\$/t$

C_i^{RM2} - Cost of RM2 for plant i , $\$/t$

C_i^{RM3} - Cost of RM3 for plant i , $\$/t$

C_i^{waste} - Cost of waste for plant i, \$/t

$D_{i,v}^{FP}$ - Demand of FP grade v at plant i, t

$D_{j,v}^{FP}$ - Demand of FP grade v at regional warehouse j, t

$D_{v,k}^{min}$ - Minimum demand of FP grade v from at

$P_{k,v}^{FP}$ - Price of FP grade v for market k, \$/t

$P_{j,v}^{FP}$ - Estimated price of FP grade v for regional warehouse j, \$/t

$q_{i,u}^{RM2}$ - RM2 to PRM grade u ratio for plant i, QPU

$q_{i,u}^{RM3}$ - RM3 to PRM grade u ratio for plant i, QPU

q_u^{waste} - Impurity w content in PRM grade u, %

$q_{i,j}^{fr,PW}$ - Proportion of FP shipped from plant i to the regional warehouse j, %

$Q_{i,w}^{imp}$ - Maximum impurity w limit for PRM at plant i, % or PPM

Q_i^{imp} - Maximum limit for total blend at plant i, %

r_i^{inc} - Income tax rate for plant i, %

$r_{i,k}^{du}$ - Duty rate for shipments from plant i to market k, %

$r_{i,j}^{du}$ - Estimated duty rate for shipments from plant i to regional warehouse j, %

r^{tp} - Transfer price rate, %

$R_{i,v}^{FP}$ - Target inventory day supply of FP grade v for plant i, day

$R_{j,v}^{FP}$ - Target inventory day supply of FP grade v for regional warehouse j, day

$R_{i,u}^{PRM,P}$ - Target inventory of PRM grade u for plant i, t

$R_u^{PRM,W}$ - Target inventory of PRM grade u for the market k, t

$E_u^{PRM,W}$ - Effective percentage in PRM grade u, for generating FP, %

m_i^{td} - Slope related to minimum turndown for plant i

m_i^{wl} - Slope related to waste limit for plant i

M_u^{PRM} - PRM grade u availability, t

O_i - Scheduled outage at plant i, d/y

U_i - Uptime for plant i, %

$X_{i,v}^{FP}$ - Beginning inventory of FP grade v at plant i, t

$X_{j,v}^{FP}$ - Beginning inventory of FP grade v at regional warehouse j, t

$X_{i,u}^{PRM,P}$ - Beginning inventory of PRM grade u at plant i, t

$X_u^{PRM,W}$ - Beginning inventory of PRM grade u at the PRM warehouse, t

Y_i^{FP} - Yield of FP at plant i, %

Z_i^{max} - Maximum allowable capacity at plant i, t

Different variables for the DuPont Supply Chain network is given below

c_i^{fr} - Freight cost for plant i, \$

c_i^{du} - Duty cost for plant i, \$

c_i^I - Inventory cost for plant i, \$

c_i^{PRM} - PRM cost for plant i, \$

c_i^{RM2} - RM2 cost for plant i, \$

c_i^{RM3} - RM3 cost for plant i, \$

c_i^{waste} - Waste cost for plant i, \$

c_i^{OPVC} - Other plant i variable costs, \$

c_i^{cap} - Capacity cost for plant i, \$

$f_{i,k,v}^{FP,PD}$ - Shipment of FP grade v from plant i to market k, t

$f_{i,j,v}^{FP,PW}$ - Shipment of FP grade v from plant i to regional warehouse j, t

$f_{j,k,v}^{FP,WD}$ - Shipment of FP grade v from regional warehouse j to market k, t

$f_{i,u}^{PRM,c}$ - PRM grade u consumed at plant i, t

$f_u^{PRM,W}$ - PRM grade u purchased and sent to plant i, t

$f_{i,u}^{PRM,WP}$ - PRM grade u purchased and sent to the PRM warehouse, t

$f_{i,k,v}^{FP,PD}$ - Shipments of PRM grade u from the PRM warehouse to plant i, t

$f_{i,v}^{FP,p}$ - Amount of FP grade v produced from plant i, t

z_i - Capacity of plant i, t

Here first stage decision variable is capacity of each plant, z_i and second stage decision variables are all the flows, $f_{i,k,v}^{FP,PD}$, $f_{i,j,v}^{FP,PW}$, $f_{j,k,v}^{FP,WD}$, $f_{i,u}^{PRM,c}$, $f_u^{PRM,W}$, $f_{i,u}^{PRM,WP}$, $f_{i,k,v}^{FP,PD}$ and $f_{i,v}^{FP,p}$.

A.2 Deterministic Model for DuPont Supply Chain Network

The objective function that needs to be maximized is

$$Objective = \sum_{i \in I} (Revenue_i - TC_i)(1 - r_i^{inc}) \quad (A.1)$$

Here revenue indicates the revenue of each of the plant which is calculated from the following equation

$$Revenue_i = \sum_{(i,k) \in \Theta} \sum_{v \in V} (f_{i,k,v}^{FP,PD} \cdot P_{k,v}^{FP} + \sum_{(i,j) \in \omega} \sum_{v \in V} (f_{i,j,v}^{FP,PW} \cdot P_{j,v}^{FP}), i \in I \quad (A.2)$$

TC denotes the total cost of each of the plant and calculated as below

$$TC_i = c_i^{fix} + c_i^{cap} + c_i^{fr} + c_i^{du} + c_i^I + c_i^{PRM} + c_i^{RM2} + c_i^{RM3} + c_i^{waste} + c_i^{OPVC}, i \in I \quad (A.3)$$

Capacity costs are considered at each of the plants

$$c_i^{cap} = z_i \cdot C_i^{cap}, i \in I \quad (A.4)$$

Freight costs are calculated based off of the FP flow rates

$$c_i^{fr} = \sum_{(i,k) \in \Theta} \sum_{v \in V} (f_{(i,k,v)}^{FP,PD} \cdot C_{i,k}^{fr,FP,PD}) + \sum_{(i,j) \in \omega} \sum_{v \in V} (f_{(i,j,v)}^{FP,PW} \cdot C_{(i,j)}^{fr,FP,PW}) + \sum_{(i,j) \in \omega} \sum_{(j,k) \in Pi} \sum_{v \in V} (f_{(j,k,v)}^{FP,WD} \cdot C_{(j,k)}^{fr,FP,WD} \cdot q_{(i,j)}^{fr,PW}), i \in I \quad (A.5)$$

Duty costs are calculated from the amount of products produced

$$c_i^{du} = r^{tp} \cdot \left[\sum_{(i,k) \in \Theta} \sum_{v \in V} (f_{i,k,v}^{FP,PD} \cdot P_{k,v}^{FP} \cdot r_{i,k}^{du}) + \sum_{(i,j) \in \omega} \sum_{v \in V} (f_{j,k,v}^{FP,PW} \cdot P_{j,v}^{FP} \cdot r_{i,j}^{du}) \right], i \in I \quad (A.6)$$

Inventory costs are equated at the raw material warehouse and the regional warehouses

$$C_i^I = \sum_{(i,v) \in Psi} (f_{i,v}^{FP,p} \cdot C_i^P I) + \sum_{(i,j) \in \omega} \sum_{v \in V} (f_{i,j,v}^{FP,PW} \cdot C_j^W I), i \in I \quad (A.7)$$

The costs of PRM, the other two major raw material denoted by RM2 and RM3, waster and other plant variable costs are caluted according to the following equations respectively

$$C_i^{PRM} = \sum_{u \in U} (f_{i,u}^{PRM,c} \cdot C_{i,u}^{PRM}), i \in I \quad (A.8)$$

$$C_i^{RM2} = \sum_{u \in U} (f_{i,u}^{PRM,c} \cdot q_{i,u}^{RM2}) \cdot C_i^{RM2}, i \in I \quad (A.9)$$

$$C_i^{RM3} = \sum_{u \in U} (f_{i,u}^{PRM,c} \cdot q_{i,u}^{RM3}) \cdot C_i^{RM2}, i \in I \quad (A.10)$$

$$C_i^{waste} = \sum_{u \in U} (f_{i,u}^{PRM,c} \cdot q_u^{RM3}) \cdot C_i^{waste}, i \in I \quad (A.11)$$

$$C_i^{OPVC} = C_i^{var} \cdot \left(\sum_{(i,v) \in \Psi} f_{i,v}^{FP,p} \right), i \in I \quad (A.12)$$

The material consumed and the products produced in the manufacturing plants is limited by the following equation

$$\sum_{(i,v) \in \Psi} f_{i,v}^{FP,p} \leq z_i, i \in I \quad (\text{A.13})$$

The capacity of each plant can not exceed the following constraint

$$z_i \leq Z_i^{max}, i \in I \quad (\text{A.14})$$

$$z_i \geq 0, i \in I \quad (\text{A.15})$$

The following equation relates the amount of PRM consumed and the amount of FP produced at the plant

$$\sum_{u \in U} (f_{i,u}^{PRM,c} \cdot E_u^{PRM}) \cdot a_i^{avg,FP} \cdot Y_i^{FP} = \sum_{(i,v) \in \Psi} f_{i,v}^{FP,p}, i \in I \quad (\text{A.16})$$

The material and product flows in the supply chain system also need to satisfy a set of constraints from mass balances, inventory limits, material availability and customer demand. Specially PRM consumed can not fall below the target inventory at the PRM warehouse

$$\sum_{i \in I} f_{i,u}^{PRM,c} + f_u^{PRM,W} \leq M_u^{PRM}, u \in U \quad (\text{A.17})$$

The PRM ending inventory can not fall below the target inventory at PRM warehouse

$$X_u^{PRM,W} + f_u^{PRM,W} - \sum_{i \in I} f_{i,u}^{PRM,WP} \geq R_u^{PRM,W}, u \in U \quad (\text{A.18})$$

and at each of the plant

$$X_{i,u}^{PRM,P} + f_{i,u}^{PRM,P} + f_{i,u}^{PRM,WP} - f_{i,u}^{PRM,c} \geq R_{i,u}^{PRM,P}, i \in I, u \in U \quad (\text{A.19})$$

The ending FP inventory can not be less than the the target inventory at the plants

$$X_{i,v}^{FP,P} + f_{i,v}^{FP,p} - \sum_{(i,j) \in \omega} f_{i,j,v}^{FP,WD} \geq D_{j,v}^{FP} \cdot R_{j,v}^{FP} / 365, (i, v) \in \Psi \quad (\text{A.20})$$

At the regional warehouses

$$X_{j,v}^{FP,W} + \sum_{i \in I} f_{i,j,v}^{FP,PW} - \sum_{(j,k) \in \Pi} f_{j,k,v}^{FP,WD} \geq D_{j,v}^{FP} \cdot R_{j,v}^{FP} / 365, j \in J, v \in V \quad (\text{A.21})$$

The FP shipped to the regional market must meet the minimum demand requirement

$$\sum_{(i,k) \in \Theta} f_{i,k,v}^{FP,PD} + \sum_{(j,k) \in Pi} f_{i,j,v}^{FP,WD} \geq D_{v,k}^{min}, k \in Kv \in V \quad (\text{A.22})$$

Finally, the PRM flows purchased from different sources have different impurity contents and these flows are blended before converted into different grades of FP. In order to ensure the quality of FP, the PRM blends have to satisfy certain impurity specifications, as follows

$$\sum_{u \in U} (f_{i,u}^{PRM,c} \cdot q_{u,w}^{imp}) \leq \sum_{u \in U} (f_{i,u}^{PRM,c} \cdot Q_{i,w}^{imp}), i \in I, w \in W \quad (\text{A.23})$$

In addition, the ratio of total effective parts of the PRM blends has to be below a threshold,

$$\sum_{u \in U} (f_{i,u}^{PRM,c} \cdot E_u^{PRM}) \leq \sum_{u \in U} (f_{i,u}^{PRM,c} \cdot Q_i^{max}), i \in I \quad (\text{A.24})$$

A.3 Robust Scenario Formulation Model for DuPont Supply Chain Network

In Robust Scenario Formulation of DuPont Industrial Chemical Supply Chain Network, the second stage variables are replaced by affine functions of uncertain parameters. Here, $f_{i,k,v,\omega}^{FP,PD}$ is replaced by $\Phi_{i,k,v,\omega}^{FP,PD} \cdot (\bar{\xi} + M^{-1} \Delta \bar{\xi}_\omega) + \phi_{i,k,v,\omega}^{FP,PD}$, $f_{i,j,v,\omega}^{FP,PW}$ is replaced

by $\Phi_{i,j,v,\omega}^{FP,PW} \cdot (\bar{\xi} + M^{-1}\Delta\bar{\xi}_\omega) + \phi_{i,j,v,\omega}^{FP,PW}, f_{j,k,v,\omega}^{FP,WD}$ is replaced by $\Phi_{j,k,v,\omega}^{FP,WD} \cdot (\bar{\xi} + M^{-1}\Delta\bar{\xi}_\omega) + \phi_{j,k,v,\omega}^{FP,WD}, f_{i,u,\omega}^{PRM,C}$ is replaced by $\Phi_{i,u,\omega}^{PRM,C} \cdot (\bar{\xi} + M^{-1}\Delta\bar{\xi}_\omega) + \phi_{i,u,\omega}^{PRM,C}, f_{i,u,\omega}^{PRM,P}$ is replaced by $\Phi_{i,u,\omega}^{PRM,P} \cdot (\bar{\xi} + M^{-1}\Delta\bar{\xi}_\omega) + \phi_{i,u,\omega}^{PRM,P}, f_{u,\omega}^{PRM,W}$ is replaced by $\Phi_{u,\omega}^{PRM,W} \cdot (\bar{\xi} + M^{-1}\Delta\bar{\xi}_\omega) + \phi_{u,\omega}^{PRM,W}, f_{i,u,\omega}^{PRM,WP}$ is replaced by $\Phi_{i,u,\omega}^{PRM,WP} \cdot (\bar{\xi} + M^{-1}\Delta\bar{\xi}_\omega) + \phi_{i,u,\omega}^{PRM,WP}$ and $f_{i,v,\omega}^{FP,p}$ is replaced by $\Phi_{i,v,\omega}^{FP,p} \cdot (\bar{\xi} + M^{-1}\Delta\bar{\xi}_\omega) + \phi_{i,v,\omega}^{FP,p}$.

Robust Scenario Formulation for the DuPont Supply Chain network is given below. For overestimation of normalized uncertainty region, $\bigcup_{\omega=1}^s \Xi_\omega^{OE} \supset \Xi^{OE}$ where Ξ^{OE} indicates the uncertainty region after overestimation of normalized uncertainty region. For underestimation of normalized uncertainty region, $\bigcup_{\omega=1}^s \Xi_\omega^{UE} \supset \Xi^{UE}$ where Ξ^{UE} indicates the uncertainty region after underestimation of normalized uncertainty region.

Objective function,

$$\text{Objective} = \max_{\omega=1}^s p_\omega \left[\sum_{i=1}^S (\text{Revenue}_{i,\omega} - TC_{i,\omega})(1 - r_i^{inc}) \right] \quad (\text{A.25})$$

Subject to,

$$\begin{aligned}
 \text{Revenue}_{i,\omega} = & \sum_{(i,k) \in \Theta} \sum_{v \in V} ((\Phi_{i,k,v,\omega}^{FP,PD} \cdot (\bar{\xi} + M^{-1}\Delta\bar{\xi}_\omega) + \phi_{i,k,v,\omega}^{FP,PD}) \cdot P_{k,v}^{FP}) + \\
 & \sum_{(i,j) \in \Omega} \sum_{v \in V} ((\Phi_{i,j,v,\omega}^{FP,PW} \cdot (\bar{\xi} + M^{-1}\Delta\bar{\xi}_\omega) + \phi_{i,j,v,\omega}^{FP,PW}) \cdot P_{j,v}^{FP}), i \in I, \omega = 1, \dots, s
 \end{aligned} \quad (\text{A.26})$$

$$TC_i = c_i^{fix} + c_i^{cap} + c_i^{fr} + c_i^{du} + c_i^I + c_i^{PRM} + c_i^{RM2} + c_i^{RM3} + c_i^{waste} + c_i^{OPVC}, i \in I \quad (\text{A.27})$$

$$c_i^{cap} = z_i \cdot C_i^{cap}, i \in I \quad (\text{A.28})$$

$$\begin{aligned} \bar{c}_{i,\omega}^{fr} = & \sum_{(i,k) \in \omega} \sum_{v \in V} ((\Phi_{i,k,v,\omega}^{FP,PD} \cdot (\bar{\xi} + M^{-1} \Delta \bar{\xi}_\omega) + \phi_{i,k,v,\omega}^{FP,PD}) \cdot C_{i,k}^{fr,FP,PD}) + \\ & \sum_{(i,j) \in \omega} \sum_{v \in V} ((\Phi_{i,j,v,\omega}^{FP,PW} \cdot (\bar{\xi} + M^{-1} \Delta \bar{\xi}_\omega) + \phi_{i,j,v,\omega}^{FP,PW}) \cdot C_{i,j}^{fr,FP,PW}) + \\ & \sum_{(i,j) \in \omega} \sum_{(j,k) \in \Pi} \sum_{v \in V} ((\Phi_{j,k,v,\omega}^{FP,WD} \cdot (\bar{\xi} + M^{-1} \Delta \bar{\xi}_\omega) + \phi_{j,k,v,\omega}^{FP,WD}) \cdot C_{j,k}^{fr,FP,WD} \cdot q_{i,j}^{fr,PW}), \\ & i \in I, \omega = 1, \dots, s \end{aligned} \quad (\text{A.29})$$

$$\begin{aligned} \bar{c}_{i,\omega}^{du} = & \sum_{(i,v) \in \Psi} ((\Phi_{i,k,v,\omega}^{FP,PD} \cdot (\bar{\xi} + M^{-1} \Delta \bar{\xi}_\omega) + \phi_{i,k,v,\omega}^{FP,PD}) \cdot P_{k,v}^{FP} \cdot r_{i,k}^{du}) \cdot r^{tp} + \\ & \sum_{(i,j) \in \Omega} ((\Phi_{i,j,v,\omega}^{FP,PW} \cdot (\bar{\xi} + M^{-1} \Delta \bar{\xi}_\omega) + \phi_{i,j,v,\omega}^{FP,PW}) \cdot P_{j,v}^{FP} \cdot r_{i,j}^{du}) \cdot r^{tp}, i \in I, \omega = 1, \dots, s \end{aligned} \quad (\text{A.30})$$

$$\begin{aligned} \bar{c}_{i,\omega}^I = & \sum_{(i,v) \in \Psi} ((\Phi_{i,v,\omega}^{FP,p} \cdot (\bar{\xi} + M^{-1} \Delta \bar{\xi}_\omega) + \phi_{i,v,\omega}^{FP,p}) \cdot C_i^{PI}) + \sum_{(i,j) \in \omega} \sum_{v \in V} ((\Phi_{i,j,v,\omega}^{FP,PW} \cdot (\bar{\xi} + M^{-1} \Delta \bar{\xi}_\omega) \\ & + \phi_{i,j,v,\omega}^{FP,PW}) \cdot C_i^{WI}), i \in I, \omega = 1, \dots, s \end{aligned} \quad (\text{A.31})$$

$$\bar{c}_{i,\omega}^{PRM} = \sum_{u \in U} ((\Phi_{i,u,\omega}^{PRM,c} \cdot (\bar{\xi} + M^{-1} \Delta \bar{\xi}_\omega) + \phi_{i,u,\omega}^{PRM,c}) \cdot C_{i,u}^{PRM}), i \in I, \omega = 1, \dots, s \quad (\text{A.32})$$

$$\bar{c}_{i,\omega}^{RM2} = \sum_{u \in U} ((\Phi_{i,u,\omega}^{PRM,c} \cdot (\bar{\xi} + M^{-1} \Delta \bar{\xi}_\omega) + \phi_{i,u,\omega}^{PRM,c}) \cdot q_{i,u}^{RM2}) \cdot C_i^{RM2}, i \in I, \omega = 1, \dots, s \quad (\text{A.33})$$

$$\bar{c}_{i,\omega}^{RM3} = \sum_{u \in U} ((\Phi_{i,u,\omega}^{PRM,c} \cdot (\bar{\xi} + M^{-1} \Delta \bar{\xi}_\omega) + \phi_{i,u,\omega}^{PRM,c}) \cdot q_{i,u}^{RM3}) \cdot C_i^{RM3}, i \in I, \omega = 1, \dots, s \quad (\text{A.34})$$

$$\bar{c}_{i,\omega}^{waste} = \sum_{u \in U} ((\Phi_{i,u,\omega}^{PRM,c} \cdot (\bar{\xi} + M^{-1} \Delta \bar{\xi}_\omega) + \phi_{i,u,\omega}^{PRM,c}) \cdot q_u^{waste}) \cdot C_i^{waste}, i \in I, \omega = 1, \dots, s \quad (\text{A.35})$$

$$c_{i,\omega}^{OPVC} = \sum_{(i,v) \in \Psi} (\Phi_{i,v,\omega}^{FP,p} \cdot (\bar{\xi} + M^{-1} \Delta \bar{\xi}_\omega) + \phi_{i,v,\omega}^{FP,p}) \cdot C_i^{var}, i \in I, \omega = 1, \dots, s \quad (\text{A.36})$$

$$\begin{aligned} & \left(\sum_{(i,v) \in \Psi} \Phi_{i,v,\omega} \right) \cdot (\bar{\xi} + M^{-1} \Delta \bar{\xi}_\omega) + \delta_\omega \cdot \left\| \left(\sum_{(i,v) \in \Psi} \Phi_{i,v,\omega}^{FP,p} \right) M^{-1} \right\|_* + \left(\sum_{(i,v) \in \Psi} \psi_{i,v,\omega}^{FP,p} \right) \\ & \leq z_i, i \in I, \omega = 1, \dots, s \end{aligned} \quad (\text{A.37})$$

$$z_i \leq Z_i^{max}, i \in I \quad (\text{A.38})$$

$$\sum_{u \in U} (\Phi_{i,u,\omega} \cdot E_u^{PRM}) \cdot a_i^{avg,FP} \cdot Y_i^{FP} = \sum_{(i,v) \in \Psi} \Phi_{i,v,\omega}^{FP,p}, i \in I, \omega = 1, \dots, s \quad (\text{A.39})$$

$$\sum_{u \in U} (\Phi_{i,u,\omega} \cdot E_u^{PRM}) \cdot a_i^{avg,FP} \cdot Y_i^{FP} = \sum_{(i,v) \in \Psi} \Phi_{i,v,\omega}^{FP,p}, i \in I, \omega = 1, \dots, s \quad (\text{A.40})$$

$$\begin{aligned} & \left(\sum_{i \in I} (\Phi_{i,u,\omega}^{PRM,P}) + \Phi_{u,\omega}^{PRM,W} \right) \cdot (\bar{\xi} + M^{-1} \Delta \bar{\xi}_\omega) + \delta_\omega \cdot \left\| \left(\sum_{i \in I} (\Phi_{i,u,\omega}^{PRM,P}) + \Phi_{u,\omega}^{PRM,W} \right) M^{-1} \right\|_* \\ & + \sum_{i \in I} (\phi_{i,u,\omega}^{PRM,P}) + \phi_{u,\omega}^{PRM,W} \leq M_u^{PRM}, u \in U, \omega = 1, \dots, s \end{aligned} \quad (\text{A.41})$$

$$\begin{aligned}
& (\Phi_{u,\omega}^{PRM,W} - \sum_{i \in I} (\Phi_{i,u,\omega}^{PRM,WP})).(\bar{\xi} + M^{-1} \Delta \bar{\xi}_\omega) - \delta_\omega \| (\Phi_{u,\omega}^{PRM,W} - \sum_{i \in I} (\Phi_{i,u,\omega})) M^{-1} \|_* \\
& + \phi_{u,\omega}^{PRM,W} - \sum_{i \in I} (\phi_{i,u,\omega}^{PRM,WP}) \\
& \geq R_u^{PRM,W} - X_u^{PRM,W}, u \in U, \omega = 1, \dots, s
\end{aligned} \tag{A.42}$$

$$\begin{aligned}
& (\Phi_{i,u,\omega}^{PRM,P} + \Phi_{i,u,\omega}^{PRM,WP} - \Phi_{i,u,\omega}^{PRM,c}).(\bar{\xi} + M^{-1} \Delta \bar{\xi}_\omega) - \delta_\omega \| (\Phi_{i,u,\omega}^{PRM,P} + \Phi_{i,u,\omega}^{PRM,WP} - \Phi_{i,u,\omega}^{PRM,c}) M^{-1} \|_* \\
& + (\phi_{i,u,\omega}^{PRM,P} + \phi_{i,u,\omega}^{PRM,WP} - \phi_{i,u,\omega}^{PRM,c}) \\
& \geq R_{i,u}^{PRM,P} - X_{i,u}^{PRM,P}, i \in I, u \in U, \omega = 1, \dots, s
\end{aligned} \tag{A.43}$$

$$\begin{aligned}
& ((\Phi_{i,v,\omega}^{FP,p} - \sum_{(i,j) \in \omega} (\Phi_{i,j,v,\omega}^{FP,PW}) - \sum_{(i,k) \in \Theta} (\Phi_{i,k,v,\omega}^{FP,PD}))).(\bar{\xi} + M^{-1} \Delta \bar{\xi}_\omega) + \phi_{i,v,\omega}^{FP,p} - \sum_{(i,j) \in \omega} (\phi_{i,j,v,\omega}^{FP,PW}) - \\
& \sum_{(i,k) \in \Theta} (\phi_{i,k,v,\omega}^{FP,PD}) - \delta_\omega \| (\sum_{(i,j) \in \Omega} (\Phi_{i,j,v,\omega}^{FP,PW}) + \sum_{(i,k) \in \Theta} (\Phi_{i,k,v,\omega}^{FP,PD}) - \Phi_{i,v,\omega}^{FP,p}) M^{-1} \|_* \\
& \geq D_{i,v}^F P.R_{i,v}^{FP} / 365 - X_{i,v}^{FP}, (i, v) \in \Psi, \omega = 1, \dots, s
\end{aligned} \tag{A.44}$$

$$\begin{aligned}
& \left(\sum_{(i,u) \in \omega} (\Phi_{i,j,v,\omega}^{FP,PW}) - \sum_{(j,k) \in \Pi} (\Phi_{j,k,v,\omega}^{FP,WD}) \right) \cdot (\bar{\xi} + M^{-1} \Delta \bar{\xi}_\omega) + \sum_{(i,j) \in \omega} (\phi_{i,j,v,\omega}^{FP,PW}) - \sum_{(j,k) \in \Pi} (\phi_{j,k,v,\omega}^{FP,WD}) - \\
& \delta_\omega \left\| \left(\sum_{(i,j) \in \omega} (\Phi_{i,j,v,\omega}^{FP,PW}) - \sum_{(j,k) \in \Pi} (\Phi_{j,k,v,\omega}^{FP,WD}) \right) M^{-1} \right\|_* \\
& \geq D_{j,v}^F P.R_{j,v}^{FP} / 365 - X_{j,v}^{FP}, j \in J, v \in V, \omega = 1, \dots, s
\end{aligned} \tag{A.45}$$

$$\begin{aligned}
& \sum_{(i,k) \in \Theta} \phi_{i,k,v,\omega}^{FP,PD} + \sum_{(j,k) \in \Pi} \phi_{j,k,v,\omega}^{FP,WD} + \left(\sum_{(i,k) \in \Theta} \Phi_{i,k,v,\omega}^{FP,PD} + \sum_{(i,k) \in \Theta} \Phi_{i,k,v,\omega}^{FP,PD} + D_{k,v}^{min} \cdot \gamma_k \right) \\
& \cdot (\bar{\xi} + M^{-1} \Delta \bar{\xi}_\omega) + \delta_\omega \cdot \left\| \left(\sum_{(i,k) \in \Theta} \Phi_{i,k,v,\omega}^{FP,PD} + \sum_{(j,k) \in \Pi} \Phi_{j,k,v,\omega}^{FP,WD} - D_{k,v}^{min} \cdot \gamma_k \right) M^{-1} \right\|_* \\
& \geq 0, k \in K, v \in V, \omega = 1, \dots, s
\end{aligned} \tag{A.46}$$

$$\begin{aligned}
& \left(\sum_{u \in U} (\Phi_{i,u,\omega}^{PRM,c} \cdot q_{u,w}^{imp}) - \sum_{u \in U} (\Phi_{i,u,\omega}^{PRM,c} \cdot Q_{i,w}^{imp}) \right) \cdot (\bar{\xi} + M^{-1} \Delta \bar{\xi}_\omega) + \sum_{u \in U} (\phi_{i,u,\omega} \cdot q_{u,w}^{imp}) \\
& - \sum_{u \in U} (\phi_{i,u,\omega} \cdot Q_{i,w}^{imp}) + \delta_\omega \cdot \left\| \left(\sum_{u \in U} (\Phi_{i,u,\omega}^{PRM,c} \cdot q_{u,w}^{imp}) - \sum_{u \in U} (\Phi_{i,u,\omega}^{PRM,c} \cdot Q_{i,w}^{imp}) \right) M^{-1} \right\|_* \\
& \leq 0, i \in I, w \in W, \omega = 1, \dots, s
\end{aligned} \tag{A.47}$$

$$\begin{aligned}
& \left(\sum_{u \in U} \Phi_{i,u,\omega}^{PRM,c} \cdot E_u^{PRM} \right) - \sum_{u \in U} (\Phi_{i,u,\omega}^{PRM,c} \cdot Q_i^{imp}) \cdot (\bar{\xi} + M^{-1} \Delta \bar{\xi}_\omega) + \sum_{u \in U} (\phi_{i,u,\omega} \cdot E_u^{PRM}) \\
& - \sum_{u \in U} (\phi_{i,u,\omega} \cdot Q_i^{imp}) + \delta_\omega \cdot \left\| \left(\sum_{u \in U} (\Phi_{i,u,\omega}^{PRM,c} \cdot E_u^{PRM}) - \sum_{u \in U} (\Phi_{i,u,\omega}^{PRM,c} \cdot Q_i^{imp}) \right) M^{-1} \right\|_* \\
& \leq 0, i \in I, \omega = 1, \dots, s
\end{aligned} \tag{A.48}$$

$$\begin{aligned}
& \Phi_{i,k,v,\omega}^{FP,PD} \cdot (\bar{\xi} + M^{-1} \Delta \bar{\xi}_\omega) + \phi_{i,k,v,\omega}^{FP,PD} - \delta_\omega \cdot \left\| (\Phi_{i,k,v,\omega}^{FP,PD}) M^{-1} \right\|_* \geq 0 \\
& i \in I, k \in K, v \in V, \quad \omega = 1, \dots, s
\end{aligned} \tag{A.49}$$

$$\begin{aligned}
& \Phi_{i,j,v,\omega}^{FP,PW} \cdot (\bar{\xi} + M^{-1} \Delta \bar{\xi}_\omega) + \phi_{i,j,v,\omega}^{FP,PW} - \delta_\omega \cdot \left\| (\Phi_{i,j,v,\omega}^{FP,PW}) M^{-1} \right\|_* \geq 0 \\
& i \in I, j \in J, v \in V, \quad \omega = 1, \dots, s
\end{aligned} \tag{A.50}$$

$$\begin{aligned}
& \Phi_{j,k,v,\omega}^{FP,WD} \cdot (\bar{\xi} + M^{-1} \Delta \bar{\xi}_\omega) + \phi_{j,k,v,\omega}^{FP,WD} - \delta_\omega \cdot \left\| (\Phi_{j,k,v,\omega}^{FP,WD}) M^{-1} \right\|_* \geq 0 \\
& j \in J, k \in K, v \in V, \quad \omega = 1, \dots, s
\end{aligned} \tag{A.51}$$

$$\Phi_{i,v,\omega}^{FP,p} \cdot (\bar{\xi} + M^{-1} \Delta \bar{\xi}_\omega) + \phi_{i,v,\omega}^{FP,p} - \delta_\omega \|(\Phi_{i,v,\omega}^{FP,p}) M^{-1}\|_* \geq 0$$

$$i \in I, v \in V, \quad \omega = 1, \dots, s \quad (\text{A.52})$$

$$\Phi_{i,u,\omega}^{PRM,c} \cdot (\bar{\xi} + M^{-1} \Delta \bar{\xi}_\omega) + \phi_{i,u,\omega}^{PRM,c} - \delta_\omega \|(\Phi_{i,u,\omega}^{PRM,c}) M^{-1}\|_* \geq 0$$

$$i \in I, u \in U, \quad \omega = 1, \dots, s \quad (\text{A.53})$$

$$\Phi_{i,u,\omega}^{PRM,P} \cdot (\bar{\xi} + M^{-1} \Delta \bar{\xi}_\omega) + \phi_{i,u,\omega}^{PRM,P} - \delta_\omega \|(\Phi_{i,u,\omega}^{PRM,P}) M^{-1}\|_* \geq 0$$

$$i \in I, u \in U, \quad \omega = 1, \dots, s \quad (\text{A.54})$$

$$\Phi_{u,\omega}^{PRM,W} \cdot (\bar{\xi} + M^{-1} \Delta \bar{\xi}_\omega) + \phi_{u,\omega}^{PRM,W} - \delta_\omega \|(\Phi_{u,\omega}^{PRM,W}) M^{-1}\|_* \geq 0$$

$$u \in U, \quad \omega = 1, \dots, s \quad (\text{A.55})$$

$$\Phi_{i,u,\omega}^{PRM,WP} \cdot (\bar{\xi} + M^{-1} \Delta \bar{\xi}_\omega) + \phi_{i,u,\omega}^{PRM,WP} - \delta_\omega \|(\Phi_{i,u,\omega}^{PRM,WP}) M^{-1}\|_* \geq 0$$

$$i \in I, k \in K, v \in V, \quad \omega = 1, \dots, s \quad (\text{A.56})$$

Appendix B

The Robust Scenario Formulation for Problem (1) in Chapter 3

To demonstrate the idea of solving an optimization problem with any bounded uncertainty region, the following simple example was considered in Chapter 3. There are two uncertain parameters (ξ_1 and ξ_2) and two decision variables (x_1 and x_2) in the problem. The optimization problem is given below.

Problem 1

$$\min \quad x_2^2 - \frac{1}{2}x_1 \tag{B.1}$$

$$s.t. \quad \xi_1 x_1 + \xi_2 x_2 - 1 \leq 0, \quad \forall (\xi_1, \xi_2) \in \Xi. \tag{B.2}$$

Here the uncertainty region is defined as:

$$\Xi = \{ \xi \in \mathbb{R}^2 : 3\xi_1^2 + (\xi_2 - 2)^2 \leq 3, \xi_1 + \xi_2 \leq 3 \}.$$

After normalization, $\xi = \bar{\xi} + M^{-1}\Delta\xi$, so left-hand-side of the constraint can be reformulated as:

$$\begin{aligned} & \xi^T x - 1 \\ &= \bar{\xi}^T x + \Delta\xi^T (M^{-1})^T x - 1. \end{aligned}$$

In a robust scenario formulation, the constraint is replaced by a set of constraints, each for an uncertainty subregion $\Xi_\omega = \{\Delta\xi : \|\Delta\xi_\omega - \Delta\bar{\xi}_\omega\|_\infty \leq \delta_\omega\}$. The constraints are:

$$\bar{\xi}^T x + \Delta\xi_\omega^T (M^{-1})^T x - 1 \leq 0, \quad \forall \Delta\xi_\omega \in \Xi_\omega, \quad \omega = 1, \dots, s,$$

or equivalently,

$$\bar{\xi}^T x + \max_{\Delta\xi_\omega \in \Xi_\omega} \{\Delta\xi_\omega^T (M^{-1})^T x\} \leq 1, \quad \omega = 1, \dots, s.$$

The latter one can be further rewritten as:

$$\bar{\xi}^T x + \Delta\bar{\xi}_\omega^T (M^{-1})^T x + \max_{\Delta\xi_\omega \in \Xi_\omega} \{(\Delta\xi_\omega - \Delta\bar{\xi})^T (M^{-1})^T x\} \leq 1, \quad \omega = 1, \dots, s,$$

According to [46],

$$\max_{\Delta\xi_\omega \in \Xi_\omega} \{(\Delta\xi_\omega - \Delta\bar{\xi})^T (M^{-1})^T x\} = \delta_\omega \|(M^{-1})^T x\|_1,$$

so the constraints become

$$\bar{\xi}^T x + \Delta \bar{\xi}_\omega^T ((M^{-1})^T x) + \delta_\omega \|(M^{-1})^T x\|_1 \leq 1, \quad \omega = 1, \dots, s.$$

Using the LP reformulation discussed in Section 2.3 of Chapter 2, the robust scenario formulation of Problem (1) of Chapter 3 can be written as below:

$$\min \quad x_2^2 - \frac{1}{2}x_1 \tag{B.3}$$

$$s.t. \quad \bar{\xi}^T x + \Delta \bar{\xi}_\omega^T ((M^{-1})^T x) + \delta_\omega \sum_{i=1}^{n_\xi} t_i, \quad \omega = 1, \dots, s, \tag{B.4}$$

$$-t \leq (M^{-1})^T x \leq t, \tag{B.5}$$

$$t \geq 0. \tag{B.6}$$

Here, $\Delta \bar{\xi}_\omega$ denotes the center of uncertainty subregion Ξ_ω . Note that the subregions considered in the formulation are different for the uncertainty over-estimation and under-estimation cases.

Appendix C

Generalized Benders Decomposition Sub-Problems for simplified DuPont Industrial Chemical Supply Chain Optimization Problem

C.1 Original Problem (P)

The Original problem (P) for DuPont Supply Chain case is given below. Here Equation (C.2) is the linking constraint.

Objective function,

$$\begin{aligned}
Objective = & \min \left[- \sum_{\omega 1}^s P_{\omega} \sum_{i=1} \left(\sum_{(i,k) \in \Theta} \sum_{v \in V} \left((\Phi_{i,k,v,\omega}^{FP,PD} \cdot (\bar{\xi} + M^{-1} \Delta \bar{\xi}_{\omega}) + \phi_{i,k,v,\omega}^{FP,PD}) \cdot P_{k,v}^{FP} \right) + \right. \right. \\
& \sum_{(i,j) \in \Omega} \sum_{v \in V} \left((\Phi_{i,j,v,\omega}^{FP,PW} \cdot (\bar{\xi} + M^{-1} \Delta \bar{\xi}_{\omega}) + \phi_{i,j,v,\omega}^{FP,PW}) \cdot P_{j,v}^{FP} \right) \left. \right] - [C_i^{fix} + z_i \cdot C^{cap} + \\
& \left(\sum_{(i,k) \in \Omega} \sum_{v \in V} \left((\Phi_{i,k,v,\omega}^{FP,PD} \cdot (\bar{\xi} + M^{-1} \Delta \bar{\xi}_{\omega}) + \phi_{i,k,v,\omega}^{FP,PD}) \cdot C_{i,k}^{fr,FP,PD} \right) + \right. \\
& \sum_{(i,j) \in \Omega} \sum_{v \in V} \left((\Phi_{i,j,v,\omega}^{FP,PW} \cdot (\bar{\xi} + M^{-1} \Delta \bar{\xi}_{\omega}) + \phi_{i,j,v,\omega}^{FP,PW}) \cdot C_{i,j}^{fr,FP,PW} \right) + \sum_{(i,j) \in \Omega} \sum_{(j,k) \in \Pi} \sum_{v \in V} \left((\Phi_{j,k,v,\omega}^{FP,WD} \cdot (\bar{\xi} + \right. \\
& M^{-1} \Delta \bar{\xi}_{\omega}) + \phi_{j,k,v,\omega}^{FP,WD}) \cdot C_{j,k}^{fr,FP,WD} \cdot q_{i,j}^{fr,PW} \left. \right) \left. \right) + \left(\sum_{(i,v) \in \Psi} \left((\Phi_{i,k,v,\omega}^{FP,PD} \cdot (\bar{\xi} + M^{-1} \Delta \bar{\xi}_{\omega}) + \phi_{i,k,v,\omega}^{FP,PD}) \cdot P_{k,v}^{FP} \cdot r_{i,k}^{du} \right) \cdot r^{tp} \right. \\
& + \sum_{(i,j) \in \Omega} \left((\Phi_{i,j,v,\omega}^{FP,PW} \cdot (\bar{\xi} + M^{-1} \Delta \bar{\xi}_{\omega}) + \phi_{i,j,v,\omega}^{FP,PW}) \cdot P_{j,v}^{FP} \cdot r_{i,j}^{du} \right) \cdot r^{tp} \left. \right) + \\
& \left(\sum_{(i,v) \in \Psi} \left((\Phi_{i,v,\omega}^{FP,p} \cdot (\bar{\xi} + M^{-1} \Delta \bar{\xi}_{\omega}) + \phi_{i,v,\omega}^{FP,p}) \cdot C_i^{PI} \right) + \sum_{(i,j) \in \Omega} \sum_{v \in V} \left((\Phi_{i,j,v,\omega}^{FP,PW} \cdot (\bar{\xi} + \right. \right. \\
& M^{-1} \Delta \bar{\xi}_{\omega}) + \phi_{i,j,v,\omega}^{FP,PW}) \cdot C_i^{WI} \left. \right) \left. \right) + \left(\sum_{u \in U} \left((\Phi_{i,u,\omega}^{PRM,c} \cdot (\bar{\xi} + M^{-1} \Delta \bar{\xi}_{\omega}) + \phi_{i,u,\omega}^{PRM,c}) \cdot C_{i,u}^{PRM} \right) \right) + \\
& \left(\sum_{u \in U} \left((\Phi_{i,u,\omega}^{PRM,c} \cdot (\bar{\xi} + M^{-1} \Delta \bar{\xi}_{\omega}) + \phi_{i,u,\omega}^{PRM,c}) \cdot q_{i,u}^{RM2} \right) \cdot C_i^{RM2} \right) + \left(\sum_{u \in U} \left((\Phi_{i,u,\omega}^{PRM,c} \cdot (\bar{\xi} + \right. \right. \\
& M^{-1} \Delta \bar{\xi}_{\omega}) + \phi_{i,u,\omega}^{PRM,c}) \cdot q_{i,u}^{RM3} \right) \cdot C_i^{RM3} \left. \right) + \left(\sum_{u \in U} \left((\Phi_{i,u,\omega}^{PRM,c} \cdot (\bar{\xi} + M^{-1} \Delta \bar{\xi}_{\omega}) + \right. \right. \\
& \left. \left. \phi_{i,u,\omega}^{PRM,c} \right) \cdot q_u^{waste} \right) \cdot C_i^{waste} \left. \right) + \left(\sum_{(i,v) \in \Psi} \left((\Phi_{i,v,\omega}^{FP,p} \cdot (\bar{\xi} + M^{-1} \Delta \bar{\xi}_{\omega}) + \phi_{i,v,\omega}^{FP,p}) \cdot C_i^{var} \right) \right) (1 - r_i^{inc}) \left. \right]
\end{aligned} \tag{C.1}$$

Subject to,

$$-z_i + \left(\sum_{(i,v) \in \Psi} \Phi_{i,v,\omega} \right) \cdot (\bar{\xi} + M^{-1} \Delta \bar{\xi}_\omega) + \delta_\omega \cdot \left\| \left(\sum_{(i,v) \in \Psi} \Phi_{i,v,\omega}^{FP,p} \right) M^{-1} \right\|_2 + \left(\sum_{(i,v) \in \Psi} \psi_{i,v,\omega}^{FP,p} \right) \leq 0$$

$$\omega = 1, \dots, s, i \in I \quad (C.2)$$

$$z_i \leq Z_i^{max}, i \in I \quad (C.3)$$

$$\sum_{u \in U} (\Phi_{i,u,\omega} \cdot E_u^{PRM}) \cdot a_i^{avg,FP} \cdot Y_i^{FP} = \sum_{(i,v) \in \Psi} \Phi_{i,v,\omega}^{FP,p}, \omega = 1, \dots, s, i \in I \quad (C.4)$$

$$\sum_{u \in U} (\Phi_{i,u,\omega} \cdot E_u^{PRM}) \cdot a_i^{avg,FP} \cdot Y_i^{FP} = \sum_{(i,v) \in \Psi} \Phi_{i,v,\omega}^{FP,p}, \omega = 1, \dots, s, i \in I \quad (C.5)$$

$$\left(\sum_{i \in I} (\Phi_{i,u,\omega}^{PRM,P}) + \Phi_{u,\omega}^{PRM,W} \right) \cdot (\bar{\xi} + M^{-1} \Delta \bar{\xi}_\omega) + \delta_\omega \cdot \left\| \left(\sum_{i \in I} (\Phi_{i,u,\omega}^{PRM,P}) + \Phi_{u,\omega}^{PRM,W} \right) M^{-1} \right\|_2$$

$$+ \sum_{i \in I} (\phi_{i,u,\omega}^{PRM,P}) + \phi_{u,\omega}^{PRM,W} \leq M_u^{PRM}$$

$$\omega = 1, \dots, s, u \in U \quad (C.6)$$

$$\begin{aligned}
 & (\Phi_{u,\omega}^{PRM,W} - \sum_{i \in I} (\Phi_{i,u,\omega}^{PRM,WP})).(\bar{\xi} + M^{-1} \Delta \bar{\xi}_\omega) - \delta_\omega \| (\Phi_{u,\omega}^{PRM,W} - \sum_{i \in I} (\Phi_{i,u,\omega})) M^{-1} \|_2 \\
 & + \phi_{u,\omega}^{PRM,W} - \sum_{i \in I} (\phi_{i,u,\omega}^{PRM,WP}) \geq R_u^{PRM,W} - X_u^{PRM,W}
 \end{aligned}$$

$$\omega = 1, \dots, s, u \in U \quad (C.7)$$

$$\begin{aligned}
 & (\Phi_{i,u,\omega}^{PRM,P} + \Phi_{i,u,\omega}^{PRM,WP} - \Phi_{i,u,\omega}^{PRM,c}).(\bar{\xi} + M^{-1} \Delta \bar{\xi}_\omega) - \delta_\omega \| (\Phi_{i,u,\omega}^{PRM,P} + \Phi_{i,u,\omega}^{PRM,WP} - \Phi_{i,u,\omega}^{PRM,c}) M^{-1} \|_2 \\
 & + (\phi_{i,u,\omega}^{PRM,P} + \phi_{i,u,\omega}^{PRM,WP} - \phi_{i,u,\omega}^{PRM,c}) \geq R_{i,u}^{PRM,P} - X_{i,u}^{PRM,P}
 \end{aligned}$$

$$\omega = 1, \dots, s, i \in I, u \in U \quad (C.8)$$

$$\begin{aligned}
 & ((\Phi_{i,v,\omega}^{FP,p} - \sum_{(i,j) \in \omega} (\Phi_{i,j,v,\omega}^{FP,PW}) - \sum_{(i,k) \in \Theta} (\Phi_{i,k,v,\omega}^{FP,PD}))).(\bar{\xi} + M^{-1} \Delta \bar{\xi}_\omega) + \phi_{i,v,\omega}^{FP,p} - \sum_{(i,j) \in \Omega} (\phi_{i,j,v,\omega}^{FP,PW}) - \\
 & \sum_{(i,k) \in \Theta} (\phi_{i,k,v,\omega}^{FP,PD}) - \delta_\omega \| (\sum_{(i,j) \in \Omega} (\Phi_{i,j,v,\omega}^{FP,PW}) + \sum_{(i,k) \in \Theta} (\Phi_{i,k,v,\omega}^{FP,PD}) - \Phi_{i,v,\omega}^{FP,p}) M^{-1} \|_2 \geq D_{i,v}^F P.R_{i,v}^{FP}/365 - X_{i,v}^{FP}
 \end{aligned}$$

$$\omega = 1, \dots, s, (i, v) \in \Psi \quad (C.9)$$

$$\begin{aligned}
 & \left(\sum_{(i,u) \in \Omega} (\Phi_{i,j,v,\omega}^{FP,PW}) - \sum_{(j,k) \in \Pi} (\Phi_{j,k,v,\omega}^{FP,WD}) \right) \cdot (\bar{\xi} + M^{-1} \Delta \bar{\xi}_\omega) + \sum_{(i,j) \in \Omega} (\phi_{i,j,v,\omega}^{FP,PW}) - \sum_{(j,k) \in \Pi} (\phi_{j,k,v,\omega}^{FP,WD}) - \\
 & \delta_\omega \left\| \left(\sum_{(i,j) \in \Omega} (\Phi_{i,j,v,\omega}^{FP,PW}) - \sum_{(j,k) \in \Pi} (\Phi_{j,k,v,\omega}^{FP,WD}) \right) M^{-1} \right\|_2 \geq D_{j,v}^F P \cdot R_{j,v}^{FP} / 365 - X_{j,v}^{FP} \\
 & \omega = 1, \dots, s, j \in J, v \in V
 \end{aligned} \tag{C.10}$$

$$\begin{aligned}
 & \sum_{(i,k) \in \Theta} \phi_{i,k,v,\omega}^{FP,PD} + \sum_{(j,k) \in \Pi} \phi_{j,k,v,\omega}^{FP,WD} + \left(\sum_{(i,k) \in \Theta} \Phi_{i,k,v,\omega}^{FP,PD} + \sum_{(i,k) \in \Theta} \Phi_{i,k,v,\omega}^{FP,PD} + D_{k,v}^{min} \cdot \gamma_k \right) \\
 & \cdot (\bar{\xi} + M^{-1} \Delta \bar{\xi}_\omega) + \delta_\omega \cdot \left\| \left(\sum_{(i,k) \in \Theta} \Phi_{i,k,v,\omega}^{FP,PD} + \sum_{(j,k) \in \Pi} \Phi_{j,k,v,\omega}^{FP,WD} - D_{k,v}^{min} \cdot \gamma_k \right) M^{-1} \right\|_2 \geq 0 \\
 & \omega = 1, \dots, s, k \in K, v \in V
 \end{aligned} \tag{C.11}$$

$$\begin{aligned}
 & \Phi_{i,k,v,\omega}^{FP,PD} \cdot (\bar{\xi} + M^{-1} \Delta \bar{\xi}_\omega) + \phi_{i,k,v,\omega}^{FP,PD} - \delta_\omega \left\| (\Phi_{i,k,v,\omega}^{FP,PD}) M^{-1} \right\|_2 \geq 0 \\
 & \omega = 1, \dots, s, i \in I, k \in K, v \in V
 \end{aligned} \tag{C.12}$$

$$\begin{aligned}
 & \Phi_{i,j,v,\omega}^{FP,PW} \cdot (\bar{\xi} + M^{-1} \Delta \bar{\xi}_\omega) + \phi_{i,j,v,\omega}^{FP,PW} - \delta_\omega \left\| (\Phi_{i,j,v,\omega}^{FP,PW}) M^{-1} \right\|_2 \geq 0 \\
 & \omega = 1, \dots, s, i \in I, j \in J, v \in V
 \end{aligned} \tag{C.13}$$

$$\Phi_{j,k,v,\omega}^{FP,WD} \cdot (\bar{\xi} + M^{-1} \Delta \bar{\xi}_\omega) + \phi_{j,k,v,\omega}^{FP,WD} - \delta_\omega \|(\Phi_{j,k,v,\omega}^{FP,WD})M^{-1}\|_2 \geq 0$$

$$\omega = 1, \dots, s, j \in J, k \in K, v \in V \quad (\text{C.14})$$

$$\Phi_{i,v,\omega}^{FP,p} \cdot (\bar{\xi} + M^{-1} \Delta \bar{\xi}_\omega) + \phi_{i,v,\omega}^{FP,p} - \delta_\omega \|(\Phi_{i,v,\omega}^{FP,p})M^{-1}\|_2 \geq 0$$

$$\omega = 1, \dots, s, i \in I, v \in V \quad (\text{C.15})$$

$$\Phi_{i,u,\omega}^{PRM,c} \cdot (\bar{\xi} + M^{-1} \Delta \bar{\xi}_\omega) + \phi_{i,u,\omega}^{PRM,c} - \delta_\omega \|(\Phi_{i,u,\omega}^{PRM,c})M^{-1}\|_2 \geq 0$$

$$\omega = 1, \dots, s, i \in I, u \in U \quad (\text{C.16})$$

$$\Phi_{i,u,\omega}^{PRM,P} \cdot (\bar{\xi} + M^{-1} \Delta \bar{\xi}_\omega) + \phi_{i,u,\omega}^{PRM,P} - \delta_\omega \|(\Phi_{i,u,\omega}^{PRM,P})M^{-1}\|_2 \geq 0$$

$$\omega = 1, \dots, s, i \in I, u \in U \quad (\text{C.17})$$

$$\Phi_{u,\omega}^{PRM,W} \cdot (\bar{\xi} + M^{-1} \Delta \bar{\xi}_\omega) + \phi_{u,\omega}^{PRM,W} - \delta_\omega \|(\Phi_{u,\omega}^{PRM,W})M^{-1}\|_2 \geq 0$$

$$\omega = 1, \dots, s, u \in U \quad (\text{C.18})$$

$$\Phi_{i,u,\omega}^{PRM,WP} \cdot (\bar{\xi} + M^{-1} \Delta \bar{\xi}_\omega) + \phi_{i,u,\omega}^{PRM,WP} - \delta_\omega \|(\Phi_{i,u,\omega}^{PRM,WP}) M^{-1}\|_2 \geq 0$$

$$\omega = 1, \dots, s, i \in I, k \in K, v \in V \quad (\text{C.19})$$

$$z_i \in \{z \in Z : z \geq 0\}, i \in I \quad (\text{C.20})$$

Here, Z is the set of all integer numbers.

C.2 Primal Problem (PP_ω^k)

In (PP_ω^k), first stage decision variables are fixed as a result the problem can be decomposed to s sub-problems. Hence the objective of (PP_ω^k) does not require summation over scenarios. The modified objective is (PP.1). In (C.2), the first stage decision variables are fixed to a constant. Hence (C.2) is changed to (PP.2) and (C.3) is excluded from (PP_ω^k) problem. The first stage decision variable is replaced with the initial guess, z_i^k . The original problem, along with the changes described in this section will be solved for each individual scenarios and the summation of all the objective will be the upper bound of the original problem. Also all the sub problems will be solved for individual scenarios.

Objective function,

$$Objective = \min[-P_\omega \sum_{i=1} (\sum_{(i,k) \in \Theta} \sum_{v \in V} ((\Phi_{i,k,v,\omega}^{FP,PD} \cdot (\bar{\xi} + M^{-1} \Delta \bar{\xi}_\omega) + \phi_{i,k,v,\omega}^{FP,PD}) \cdot P_{k,v}^{FP})) + \quad (PP.1)$$

$$\begin{aligned} & \sum_{(i,j) \in \Omega} \sum_{v \in V} ((\Phi_{i,j,v,\omega}^{FP,PW} \cdot (\bar{\xi} + M^{-1} \Delta \bar{\xi}_\omega) + \phi_{i,j,v,\omega}^{FP,PW}) \cdot P_{j,v}^{FP})] - [C_i^{fix} + z_i \cdot C^{cap} + \\ & (\sum_{(i,k) \in \Omega} \sum_{v \in V} ((\Phi_{i,k,v,\omega}^{FP,PD} \cdot (\bar{\xi} + M^{-1} \Delta \bar{\xi}_\omega) + \phi_{i,k,v,\omega}^{FP,PD}) \cdot C_{i,k}^{fr,FP,PD}) + \\ & \sum_{(i,j) \in \Omega} \sum_{v \in V} ((\Phi_{i,j,v,\omega}^{FP,PW} \cdot (\bar{\xi} + M^{-1} \Delta \bar{\xi}_\omega) + \phi_{i,j,v,\omega}^{FP,PW}) \cdot C_{i,j}^{fr,FP,PW}) + \sum_{(i,j) \in \Omega} \sum_{(j,k) \in \Pi} \sum_{v \in V} ((\Phi_{j,k,v,\omega}^{FP,WD} \cdot (\bar{\xi} + \\ & M^{-1} \Delta \bar{\xi}_\omega) + \phi_{j,k,v,\omega}^{FP,WD}) \cdot C_{j,k}^{fr,FP,WD} \cdot q_{i,j}^{fr,PW})) + (\sum_{(i,v) \in \Psi} ((\Phi_{i,k,v,\omega}^{FP,PD} \cdot (\bar{\xi} + M^{-1} \Delta \bar{\xi}_\omega) + \phi_{i,k,v,\omega}^{FP,PD}) \cdot P_{k,v}^{FP} \cdot r_{i,k}^{du} \cdot r^{tp} + \\ & \sum_{(i,j) \in \Omega} ((\Phi_{i,j,v,\omega}^{FP,PW} \cdot (\bar{\xi} + M^{-1} \Delta \bar{\xi}_\omega) + \phi_{i,j,v,\omega}^{FP,PW}) \cdot P_{j,v}^{FP} \cdot r_{i,j}^{du} \cdot r^{tp}) + \\ & (\sum_{(i,v) \in \Psi} ((\Phi_{i,v,\omega}^{FP,p} \cdot (\bar{\xi} + M^{-1} \Delta \bar{\xi}_\omega) + \phi_{i,v,\omega}^{FP,p}) \cdot C_i^{PI}) + \sum_{(i,j) \in \Omega} \sum_{v \in V} ((\Phi_{i,j,v,\omega}^{FP,PW} \cdot (\bar{\xi} + \\ & M^{-1} \Delta \bar{\xi}_\omega) + \phi_{i,j,v,\omega}^{FP,PW}) \cdot C_i^{WI})) + (\sum_{u \in U} ((\Phi_{i,u,\omega}^{PRM,c} \cdot (\bar{\xi} + M^{-1} \Delta \bar{\xi}_\omega) + \phi_{i,u,\omega}^{PRM,c}) \cdot C_{i,u}^{PRM})) + \\ & (\sum_{u \in U} ((\Phi_{i,u,\omega}^{PRM,c} \cdot (\bar{\xi} + M^{-1} \Delta \bar{\xi}_\omega) + \phi_{i,u,\omega}^{PRM,c}) \cdot q_{i,u}^{RM2}) \cdot C_i^{RM2}) + (\sum_{u \in U} ((\Phi_{i,u,\omega}^{PRM,c} \cdot (\bar{\xi} + \\ & M^{-1} \Delta \bar{\xi}_\omega) + \phi_{i,u,\omega}^{PRM,c}) \cdot q_{i,u}^{RM3}) \cdot C_i^{RM3}) + (\sum_{u \in U} ((\Phi_{i,u,\omega}^{PRM,c} \cdot (\bar{\xi} + M^{-1} \Delta \bar{\xi}_\omega) + \\ & \phi_{i,u,\omega}^{PRM,c}) \cdot q_u^{waste}) \cdot C_i^{waste}) + (\sum_{(i,v) \in \Psi} (\Phi_{i,v,\omega}^{FP,p} \cdot (\bar{\xi} + M^{-1} \Delta \bar{\xi}_\omega) + \phi_{i,v,\omega}^{FP,p}) \cdot C_i^{rvar})) (1 - r_i^{inc})] \end{aligned}$$

$$- z_i^k + (\sum_{(i,v) \in \Psi} \Phi_{i,v,\omega} \cdot (\bar{\xi} + M^{-1} \Delta \bar{\xi}_\omega) + \delta_\omega \cdot \|(\sum_{(i,v) \in \Psi} \Phi_{i,v,\omega}^{FP,p}) M^{-1}\|_2 + (\sum_{(i,v) \in \Psi} \psi_{i,v,\omega}^{FP,p}) \leq 0, i \in I$$

(PP.2)

C.3 Feasibility Problem (FP_ω^k)

If Primal Problem (PP) is not feasible then a feasibility problem is solved. To ensure feasibility of the problem, slack variables, G_i is minimized in this problem. Objective of (FP) problem is given in equation (FP.1). Excluding (C.3), all the constraints are as same as original problem except (C.2). (C.2) is modified as (FP.2). Equations are given below.

Objective function,

$$\min \|G_i\|_1 \tag{FP.1}$$

$$-z_i^k + \left(\sum_{(i,v) \in \Psi} \Phi_{i,v,\omega} \right) \cdot (\bar{\xi} + M^{-1} \Delta \bar{\xi}_\omega) + \delta_\omega \cdot \left\| \left(\sum_{(i,v) \in \Psi} \Phi_{i,v,\omega}^{FP,p} \right) M^{-1} \right\|_2 + \left(\sum_{(i,v) \in \Psi} \psi_{i,v,\omega}^{FP,p} \right) \leq G_i \tag{FP.2}$$

$$\omega = 1, \dots, s, i \in I$$

$$G_i \geq 0, i \in I \tag{FP.3}$$

C.4 Relaxed Master Problem (RMP^k)

Relaxed Master problem (RMP) consists of two blocks of constraints, optimality cut and feasibility cut. RMP is given below.

Objective function,

$$\min \eta \tag{RMP.1}$$

Subject to,

$$\eta \geq \sum_{\omega=1}^s \text{obj}_{PP_{\omega}^j} + \left[\sum_{\omega=1}^s (c_{x,\omega}^T + (\lambda_{\omega}^T) A_{\omega}) \right] (z_i - z_i^k), i \in I, \forall j \in T^k \tag{RMP.2}$$

$$0 \geq \sum_{\omega=1}^s \text{obj}_{FP_{\omega}^p} + \left[\sum_{\omega=1}^s (\mu_{\omega}^j) A_{\omega} \right] (z_i - z_i^k), i \in I, \forall p \in R^k \tag{RMP.3}$$

$$z_i \leq Z_i^{max}, i \in I \tag{RMP.4}$$

$$z_i \in \{z \in Z : z \geq 0\}, i \in I \tag{RMP.4}$$

Here, Z is the set of all integer numbers. The index are defined below as,

$$T^k = \{j \in \{1, \dots, k\} : \text{Problem (P) is feasible for } x = x^j\}$$

$$R^k = \{i \in \{1, \dots, k\} : \text{Problem (P) is infeasible for } x = x^i\}$$

From the objective (C.1) of the Problem (P), $c_{x,\omega}^T = (r - 1)c_i^{CAP}$. There is only

one blocks of linking constraints, Equation (C.2) and that block of linking constraint contains 5 equations. Hence A_ω will be a (5×5) matrix having the coefficient of z_i , -1 as diagonal element. A_ω is given below,

$$\begin{bmatrix} -1 & 0 & 0 & 0 & 0 \\ 0 & -1 & 0 & 0 & 0 \\ 0 & 0 & -1 & 0 & 0 \\ 0 & 0 & 0 & -1 & 0 \\ 0 & 0 & 0 & 0 & -1 \end{bmatrix}$$

C.5 Feasibility Relaxed Master Problem ($FRMP^k$)

At the beginning, there is a possibility that the RMP is infeasible, in that case, Feasibility Relaxed Master Problem (FRMP) is solved which is given below.

$$\min \|z_i\|_1 \tag{FRMP.1}$$

Subject to,

$$0 \geq \sum_{\omega=1}^s obj_{FRMP^\omega} + \left[\sum_{\omega=1}^s (\mu_\omega^j) A_\omega \right] (z_i - z_i^k), i \in I, \forall p \in R^k \tag{FRMP.3}$$

$$z_i \leq Z_i^{max}, i \in I \tag{FRMP.4}$$

$$z_i \in \{z \in Z : z \geq 0\}, i \in I \quad (\text{FRMP.5})$$

Here, Here, Z is the set of all integer numbers and A_ω is as same as in (RMP).